

Universität
Rostock



Traditio et Innovatio

Ecology of Beach Wrack

Ökologie des Strandanwurfs

Dissertation zur Erlangung des akademischen Grades
doctor rerum naturalium (Dr. rer. nat.)
der Mathematisch-Naturwissenschaftlichen Fakultät der Universität Rostock



Submitted by Philipp-Konrad Schätzle

Born on 13.01.1983 in Wiesbaden, Germany

Rostock, 15.03.2024

https://doi.org/10.18453/rosdok_id00004691

Gutachter:

Prof. Dr. Hendrik Schubert, Universität Rostock (Mecklenburg-Vorpommern, Deutschland),
Institut für Biowissenschaften, aquatische Ökologie

Prof. Dr. William Hogland, Linnæus Universität Kalmar (Småland, Schweden), Fakultät für
Gesundheitswissenschaften, Institut für biologische und Umweltwissenschaften

Jahr der Einreichung: 2024 (15.03.2024)

Jahr der Verteidigung: 2024 (12.07.2024)

For my parents

Science knows no country,
because knowledge belongs to humanity,
and is the torch which illuminates the world

Louis Pasteur

Zusammenfassung

Treibsel, an Land angeschwemmtes Strandgut in der Form von Algen, Seegras, Treibholz etc., stellt weltweit eine Beeinträchtigung für Strandbesucher dar. Die Entfernung ist ein aus ökologischer und wirtschaftlicher Sicht großer Kostenfaktor der lokalen Behörden. An atidalen Stränden wie der Ostsee ist die Dynamik des Strandanwurfs anders als an Gezeitenstränden. Dessen kontinuierliche Anhäufung kann neben immensen Mengen an Biomasse auch zu Nährstoffrückflüssen und damit zu einer Anreicherung des küstennahen Flachwassers führen.

Um aktuelle Informationen über Artenzusammensetzung und Mengen zu erhalten, wurden zwei Strände, jeweils gemanagt und ungemangt, an der südlichen Ostseeküste in Kühlungsborn und auf der Insel Poel (Mecklenburg-Vorpommern) während der Saison 2019 beprobt. In folgenden Versuchen mit Zersetzungstaschen, sogenannten Litterbags, wurden Abbaukinetik und mikrobielle Gemeinschaften unter Berücksichtigung der abiotischen Faktoren Licht, Temperatur, Leitfähigkeit und C:N Verhältnis während dieses Prozesses erfasst.

Die größten Mengen an Treibsel wurden im Sommer angespült, die geringsten im Frühjahr. Der Anteil an Seegras war ganzjährig hoch (47–98 %), wobei besonders im Frühjahr auch Rot- (4–27 %), Braun- (3–13 %) und Grünalgen (13–48 %) vorhanden waren. Standorten mit Hartsubstrat wiesen einen höheren Algenanteil auf als sandige Standorte. Die Versuche mit Zersetzungstaschen an Land zeigten eine Anreicherung von organischem Material im Sediment unter den Taschen (0,23–0,5 %). Die Zersetzung im Wasser verlief schneller (140–210 Tage) als an Land (Restbiomasse nach 365 Tagen). Versuche zur Zersetzung unter Wechselbedingungen lieferten keine eindeutigen Ergebnisse. Statistische Analysen (PCA) ergaben Licht und Temperatur als Hauptfaktoren, sowie das C:N Verhältnis und die Leitfähigkeit (nMDS und Clusteranalysen). Die mikrobielle Gemeinschaft folgte saisonalen Mustern und unterlag dem Einfluss des jeweiligen Versuchsbeginns. Die Alpha- und Beta-Diversität in der prokaryotischen 16S rDNA zeigte signifikante Unterschiede zwischen den Ansätzen mit Sommer- bzw. Winterstart, während die eukaryotische 18S rDNA (vor allem die Zusammensetzung der Pilzgemeinschaft) keine Signifikanz aufwies.

Die hier gesammelten Daten liefern Ansätze, um die aktuellen Strandmanagement Strategien in ökologischer Hinsicht und Verträglichkeit infrage zu stellen und zu überdenken. Umweltfreundlichere Bewirtschaftungsplänen für die Zukunft, insbesondere mit Blick auf die Beseitigung des Strandanwurfs, können erarbeitet werden. Weitere Analysen könnten dazu dienen, Modelle zur Vorhersage von Treibselanlandungen und entsprechenden Maßnahmen zu entwickeln.

Summary

Beach wrack affects humanity around the world in ecological, economical and recreational ways. On microtidal beaches such as the Baltic Sea, dynamics of beach wrack are different from those on tidal beaches. Continuous accumulation of wrack on microtidal coasts can, in addition to huge amounts of biomass, lead to nutrient backflows and thus an enrichment of the shallow waters close to the coast.

In order to obtain up-to-date information on species composition and quantities, two managed and unmanaged beaches were sampled during one season along the southern Baltic Sea coast in Kühlungsborn and at the Island of Poel (Mecklenburg-Western Pommerania). In additional litterbag experiments, degradation kinetics and microbial communities were recorded under consideration of the abiotic factors light, temperature, C:N ratio and conductivity during this process.

The largest quantities of beach wrack were recorded in summer, the smallest in spring. Seagrass proportions were high all year round (47–98 %), with red (4–27 %), brown (3–13 %) and green algae (13–48 %) also being detected especially in spring. There was a higher proportion of algae at sites with hard substrate than at sandy sites. Litterbag experiments on land showed an enrichment of organic matter in the sediment under the bags (0.23–0.5 %). Decomposition in water was faster (140–210 days) than on land (residual biomass after 365 days), decomposition under alternating conditions did not yield clear results. Statistical analyses (PCA) revealed light and temperature as the main factors, as well as the C:N ratio and conductivity (nMDS and cluster analyses). The microbial community followed seasonal patterns and was subject to the respective start of the experiment (summer or winter). Alpha and beta diversity in the prokaryotic 16S rDNA showed significant differences between summer- and winter start, while the eukaryotic 18S rDNA (in especially targeting the composition of fungal communities) did not show significance.

The data collected here may lead to a rethinking and adaptation of beach management strategies and contribute to more environmentally sound management plans in the future. This refers in particular to clearing beach wrack. Further analyses could be used to develop models for predicting beach wrack landings and corresponding measures.

List of abbreviations

Approx.	Approximately
ASVs	Amplicon Sequence Variants
bp	base pairs
BW	Beach wrack
CONTRA	Conversion Of a Nuisance To a Resource and Asset
coordE	Coordinates East
coordN	Coordinates North
DOC	Dissolved organic Carbon
DW	Dry weight
DWD	Deutscher Wetterdienst, German Weather Service
FAPROTAX	Functional Annotation of Prokaryotic Taxa
IRMS	Isotope-ratio mass spectrometry
NGS	Next Generation Sequencing
nMDS	non-metric Multidimensional Scaling
NW	New wrack
OM(C)	Organic matter (content)
OTUs	Operational Taxonomic Units
OW	Old Wrack
PCA	Principal Component Analyzes
SAu20	Seasonal autumn experiment, alternating between land and water, in 2020
SE/SD	Standard error/standard deviation
SE20	Summer experiment, starting in 2020
SSp21	Seasonal spring experiment, alternating between land and water, in 2021
SSu20	Seasonal summer experiment, alternating between land and water, in 2020
SWi21	Seasonal winter experiment, alternating between land and water, in 2021
vs.	versus; in contrast with
WE21	Winter experiment, starting in 2021

Table of contents

Zusammenfassung	I
Summary	II
List of abbreviations	III
1 Introduction	1
1.1 Beach wrack definition	1
1.2 A natural element, engineer and resource	2
1.3 The question of management	4
1.4 The fate of stranded wrack	5
1.5 Microbial processes	7
1.6 Seagrass as representative of beach wrack	7
1.7 Research hypotheses	9
2 Materials & Methods	10
2.1 Sampling sites	10
2.2 Quantifying beach wrack	11
2.3 Species composition determination	13
2.4 Decay experiments	13
2.4.1 Decay on land in Warnemünde	14
2.4.2 Decay under water	15
2.4.3 Alternating decay	18
2.5 Microbiome sample preparation	21
2.6 Statistical evaluation of microbial data	25
2.7 C:N ratio analyses	28
3 Results	30
3.1 Beach wrack amounts	30
3.2 Species composition	33
3.3 Decay on land	36
3.4 Decay under water	38
3.5 Abiotic parameters	42
	IV

3.6	Alternating decay	46
3.7	Microbial community kinetics during decomposition	50
3.7.1	Prokaryotic 16S rDNA	50
3.7.2	Eukaryotic 18S rDNA	63
3.8	C:N ratio analyses	71
4	Discussion	74
5	Conclusion & Outlook	86
6	References	88
	List of figures	VI
	List of tables	XV
	Appendix	XVI
	Acknowledgements	A
	Wissenschaftlicher Lebenslauf	B

1 Introduction

1.1 Beach wrack definition

Beaches and coastal sections do not only serve humanity for recreational purposes, these shorelines are important transition zones between aquatic and terrestrial ecosystems. This ecotone accounts for approximately 8 % of the earth's surface (Ray & Hayden, 1992). Exposed sandy beaches are regarded to as primarily recipient ecosystems (Brown & McLachlan, 2010; Liebowitz et al., 2016) as they lack permanent autochthonous primary production (McLachlan et al., 1981; Griffiths et al., 1983). Foredune vegetation may establish temporally, but will be removed by wave action during storm events or spring tide periods. Organic matter (OM), feeding the ecosystem and providing nutrients for the establishment of temporal beach vegetation, mainly comes from seaborne material washed ashore. This input can come from e.g., stranded macrophytes. The material mainly consists of marine primary producers, ripped from the ground by storm events. Depending on their buoyancy, they either drift within the water column or float on the surface waters. For some species like e.g., *Zostera marina*, this can result in long-distance dispersal with the chance of new colonization potential (Harwell & Orth, 2002). Nevertheless, most of the material is washed ashore (Suursaar et al., 2014). Here, it can become a nuisance to beach visitors, especially when starting to decompose. These deposits are called beach wrack (BW): it is defined as the accumulation of drift material, consisting primarily of seagrass and algal biomass washed up to the shore (Chubarenko et al., 2021). When it also includes life or dead animals and anthropogenic litter, but excludes pebbles, stones and sand, it is referred to as beach cast (Hofmann & Banovec, 2021). Additionally, beach wrack might also contain plant material from terrestrial sources (Heerhartz et al., 2014). Depending on the buoyancy of the detached plant material, the tidal regime and the specific geomorphology, deposition can vary amongst beaches through seasons (Plag & Tsimplis, 1999; Orr et al., 2005) and its deposition area at the beach (Gómez et al., 2013). For tidal seas, a persistent wrack line often indicates the high tide line, but temporal accumulations can be found along the eulittoral zone between high tides and after heavy storms (Colombini et al., 2009). In contrast to other oceans, the Baltic Sea has little or no tidal differences and is therefore referred to as microtidal to non-tidal (Snoeijs-Leijonmalm et al., 2017), which has an effect on the residence time of its beach wrack.

1.2 A natural element, engineer and resource

Beach wrack starts its role as an important structural organism in the ecosystem already before being washed ashore. It can function as an ecosystem engineer by stabilizing habitats, giving food, shelter and refuge to marine faunal organisms (Holmquist, 1997; Norkko et al., 2000). Detached macrophyte conglomerates host different marine organisms from a wide range of trophic levels (Dugan et al., 2003). Large mats of stranded beach wrack are a major nuisance to many shallow coasts worldwide, resulting in a disturbance to the microbenthic assemblage of the beach sand (Rossi & Underwood, 2002). Depending on local conditions, landings might be washed away with the next flood. In calm bays and microtidal seas they can stay for weeks or months and get buried in the sediments over time (Hull, 1987; Valiela & Rietsma, 1995; Ford et al., 1999). These processes influence the assessment of ecological health (Menéndez et al., 2019) by changing the chemical and physical characteristics of beaches (Raffaelli & Hawkins, 1996), and serving as an important carbon and organic matter source to the beach ecosystem (Inglis, 1989). In temperate regions macrophytes additionally promote nutrient input (Brown & McLachlan, 2010). Wrack is a primary pathway for nutrient return (Karberg et al., 2008) and nutrient producer (Suursaar et al., 2014), making nutrients available as well as other organic compounds (Colombini et al., 2003).

Rotting beach wrack offers nutrient input for growth around it, with its freshly enriched sediments at the beach, having changing effects of the physical sandy environment (Rossi & Underwood, 2002). Areas with rotting beach wrack may out-compete the usually bottom-up controlled, nutrient poor sediments nearby (Schlacher & Hartwig, 2013). Through decomposition it enriches the local sand (Van Egmond et al., 2019), promoting germination of beach plants in the adjacent area. After initial microbial and invertebrate colonization (Ince et al., 2007; Porri et al., 2011; Ruiz-Delgado et al., 2015), new and pioneer species can settle in the emerging soil (Olabarria et al., 2007). This fertilizing effect depends heavily on the introduced quality of wrack, and the stage of algal growth when it was detached (Oldham et al., 2014). Beach wrack is therefore, a hotspot of microbial breakdown, remineralization and biodiversity (Hyndes et al., 2022).

The organic part of beach wrack provides food and habitat to many species (Ince et al., 2007; Schückel & Kröncke, 2013) and intertidal consumers (Michaud et al., 2019), including terrestrial species such as e.g., insects (Hubbard et al., 2014) and birds (Kirkman & Kendrick, 1997; Dugan et al., 2003; Lafferty et al., 2013; Davis & Keppel, 2021). Zoologically, wrack supply looms for the development of amphipod crustaceans (Behbehani & Croker, 1982) and

other macroinvertebrates (Colombini et al., 2009). For example, lady-bird beetles *Coccinella septempunctata*, *Hippodamia tredecimpunctata*, and *Propylea quatuordecimpunctata*, prefer seagrass wrack as a microhabitat in coastal systems (Garbary et al., 2004).

Decomposing beach wrack also serves as an incubator to dune and beach flora by providing shelter, nutrients and retaining water (Nordstrom et al., 2011; Lastra et al., 2014; Smith et al., 2014). Wrack biomass also plays an important role in dune vegetation succession, a kind of natural coastal protection (Zhang et al., 2015). Subject to additional studies, beach wrack might serve as erosion prevention on sandy beaches (Borum et al., 2004) by reducing the erosion of embryonic dunes (Innocenti et al., 2018). Macroalgae play a vital part in sediment transport systems under water by carrying e.g., rocks and carbonate (Garden & Smith, 2015), yet deposited as wrack function as sediment trap (Nordstrom et al., 2011). This could, to a certain degree, replace fences for sediment trapping to increase dune volumes and their respective stabilization (Grafals-Soto & Nordstrom, 2009). Furthermore, beach wrack is used for dune building through re-establishment and support of increased vegetation settling (Hooton et al., 2014). Thereby the decay of beach wrack increases soil nutrients (Williams & Feagin, 2010), acts as subsidy to tidal grazers (Orr et al., 2005) and therefore, controls wrack-associated taxa bottom up (Dugan et al., 2008). Through this interaction, the accumulation of e.g., *Posidonia oceanica* increased vegetation cover to an average of 10 %, especially on foredune floral communities (Del Vecchio et al., 2017).

In contrast, beach wrack is regarded as waste at recreational beaches (Hofmann & Banovec, 2021), and consequently removed through beach management by local authorities. Being very expensive to be disposed of as biowaste, it is the aim to reuse the material as a resource. Historically wrack has been used as insulation and building material. Seagrass was used as padding and filling material for mattresses and pillows. Ships were insulated with seagrass, and e.g., in Denmark at the Island of Læsø there is an over 800 years old tradition of roofing houses with seagrass. Similar use of seagrass is known in countries like Sweden, Ireland and China (Gwóźdź & Schikan, 2022). About 100 years ago in the United States of America seagrass was utilized as construction material (Wyllie-Echeverria & Cox, 1999). In Europe, by the end of the last century, seaweed was also an important source for medical production and as food supplements: substances like phycocolloids, iodine and potash were extracted (Booth, 1964; Whitney, 1987; Jensen, 1993). Recently, beach wrack has been used as compost and fertilizer (Eyras et al., 1998; Kupczyk et al., 2019; Gibilisco et al., 2020), for sewage treatment (Cole et al., 2017) or as source of natural products with so called “bio functional properties” (Balestri et

al., 2019; Harb & Chow, 2022). These are, e.g. durability, low flammability and mold resistance of seagrass (Gwózdź & Schikan, 2022). Other options, especially for mixed material, have been tested in the EU-CONTRA-project (Möller et al., 2021): production of soil improvement material, bio char, compost material, filler for dune restoration, nutrient source for constructed wetlands and source of furcellaran extraction (Almqvist et al., 2021; Chubarenko et al., 2021).

1.3 The question of management

The fate of beach wrack at the microtidal Baltic Sea coast depends on weather conditions. Dried out, it might be blown away either back to the sea or become entangled around dune flora or artificial coastal protection structures. When stranded, the decomposition rate depends on water availability and grazers. In field and laboratory experiments, it has been proven that invertebrates inhabiting the upper beach are important for decomposition (Gómez et al., 2018). The initial stage of nutrient leaching has the highest influence to the disintegration. Subsequent stages of decay related to microbial and macrofaunal activity depend on the physicochemical, morphological and nutritional features of the rotting species (Gómez et al., 2018).

Despite intense seasonal beach management (Haller et al., 2011), little is known about the seasonality, species composition and quantities. Its long residence time and large amounts of wrack after e.g., storm events (Figure 1) require beach cleaning. Studies have been performed in the past (Zielinski et al., 2019). Highly frequented and touristy beaches with economic value are usually cleaned during the tourist season and following a fixed regime. During summertime at German coasts, an average 269 kg m^{-1} mixture of wrack and sand is removed at coastal recreational areas (Mossbauer et al., 2012). This results in a total cost of wrack removal up to e.g., 38 € per meter and year of beach (Mossbauer et al., 2012). In tidal areas beach wrack accumulates for a short time period during storm events and gets flushed away with the next high tide, not posing a problem. However, at microtidal beaches like the Baltic Sea large amounts of beach wrack may persist for longer periods. Differences between the residence time on land and in the water are still unknown. Between May and October 2010 at the German coast 4,900 t of dry beach wrack matter was collected (Mossbauer et al., 2012), creating substantial disposal problems. In some cases, when eutrophication boosts blooms of amongst others fast-growing opportunistic macroalgae (Taylor, 1999), beach wrack can turn into a sudden problem, with decaying wrack implicating strong odor. It increases the risk of possible health issues during harmful algal blooms of toxic species like e.g., *Microcystis* sp. (Wasmund, 2002) and leading to water-bound diseases and toxicity (Robbe et al., 2021).



Figure 1: Stranded beach wrack, consisting mainly of seagrass, after a storm event at the beach “Schwarzer Busch” (16.10.2020). Shown is the part of the beach without beach management activities.

Nevertheless, there are more than economic effects of beach grooming (Dugan & Hubbard, 2010). The effects of wrack supply on the physical environment were recorded and investigated (Barreiro et al., 2011). Dune volumes and beach extent have been proven to be greater in unmanaged areas, with a 35 % increase in overall species abundance. Hence, unmanaged beaches foster wider dunes with the formation of further ridges (Nordstrom et al., 2012). Human interference by beach grooming results in a lower individual abundance of e.g., marine gastropods and isopods (Deidun et al., 2009). Beach management strategies, therefore, need an agreement between recreational usage for humankind and still protecting and preserving this important and fragile ecosystem.

1.4 The fate of stranded wrack

Accumulation of beach wrack is forced by storms, algal blooms and large tidal amplitudes, causing long distances between donor habitats and receiving beaches (Piriz et al., 2003; Gómez et al., 2013; López et al., 2019). At natural beaches, beach wrack tends to accumulate and decompose. Decomposition is the physical and chemical breakdown of dead organisms involving other organisms, notably bacteria, fungi and animals (Harrison, 1989). Its decay results in negative consequences for the ecosystem: the release of phenolic compounds has been shown to affect sheltered beaches (Gómez et al., 2009). The rate of decomposition influences

net organic matter accumulation, carbon and energy transfer between trophic levels, as well as the export of organic matter and nutrients (Hodson et al., 1984). Dynamics of decomposition and accumulation of detritus depend on the quantity and composition of the detritus input. They are strongly related to environmental characteristics, e.g., water temperature, depth and hydrodynamic conditions (Walker et al., 2001; Ainley & Bishop, 2015). Depositions of wrack contributes to global greenhouse gas emissions (Liu et al., 2019), and can leak heavy metals like mercury (Graca et al., 2022).

Macrophytodebris is tightly associated with the food webs, controlling their nutrient inputs. They may be affected by global change and could therefore change within the near future in composition, deposition and tropicalization (Lepoint & Hyndes, 2022). Nevertheless, not much is known about the decay processes of beach wrack, either on land or in water. Litterbag experiments are a validated technique when trying to estimate the decay of wrack biomass. Besides attempts at land (Aerts, 1997; Karberg et al., 2008) there has been research in the aquatic environment, mostly in streams and rivers (Gessner & Chauvet, 2002; Mathuriau & Chauvet, 2002; Bärlocher, 2005). These decomposition processes have been applied to assess the ecological health of coastal lagoons (Menéndez et al., 2019). Environmental conditions are the main factors for the decomposition processes. They influence the biological responses and consumers, giving high impact to latitudinal variations (Ainley & Bishop, 2015). Abiotic parameters are reflected in large-scale decomposition in terrestrial environments (Aerts, 1997). With regards to sandy beaches they represent biogeochemical hotspots for the energy flow between terrestrial and marine ecosystems (Rodil et al., 2019). For ecosystem functioning, leaching soil carbon (C) and nitrogen (N) are essential remedies. Trophic accessibility of dissolved organic carbon (DOC) depends on leaching compounds from decaying macroalgae and seagrass (Lavery et al., 2013). Microbial communities and their respective activities are based on the natural fluctuation through which soil biota are activated to induce decomposition processes (Lammel et al., 2019). Mineralization of C and N is highly affected by soil type as a basis for the disintegrational process.

All of the above mentioned attributes justify intense beach wrack management (Mossbauer et al., 2012; Weinberger et al., 2021). In contrast, wrack accumulations favor the succession of beach macro fauna and thereby influence natural coastal protection (Olabarria et al., 2007). Additionally, as seagrass stocks are recuperating beach wrack amounts are increasing (Holden et al., 2018).

1.5 Microbial processes

Controlling factors during the decomposition of beach wrack are not fully known and understood. Abiotic factors like e.g., light, temperature and salinity are assumed to significantly influence microbial development during decomposition. Plant-microbiome and algae-microbiome interactions, including their fundamental importance for the preservation and production in algal systems, have been examined (Lian et al., 2018). A large amount of knowledge has been gained about the decay of plants, plant parts and needles in terrestrial environments, in streams and freshwater (Bärlocher, 2005; Karberg et al., 2008). It was shown that the decomposition of leaf litter in woodland streams is highly influenced by fungal communities (Das et al., 2008) whereas in river beds the upper layer of sediment and its related bacterial abundance activate decomposition processes (Huang et al., 2011). All microbial processes need organic matter, air and water (Van Loo et al., 2014). Most research was executed by so called “teabag experiments”, incubating dry mass of leaf litter at landside in decomposition-resistant bags (Karberg et al., 2008). Mesh sizes from 1 mm are regarded to reflect mass loss during decay like natural conditions, and do not have additional effects (Cummins et al., 1980). But so far, in all conscience, no research has been done in a brackish habitat. This is particularly of interest, because the richness of species and, consequently faunal and floral diversity, exhibits a pronounced slope along a salt gradient with a minimum at around 8–10 PSU (Remane, 1934; Wetzel, 2001). This pattern is well documented for benthic macro fauna. Not much is known about the implications towards the shift in species composition of microbial communities along a brackish salinity gradient (Herlemann et al., 2011). Surpassing pH and temperature (Lozupone & Knight, 2007), salinity is proposed to be the major parameter of microbiome compositions (Wu et al., 2006). In full marine habitats, e.g., Ofunato Bay, Japan, it was proven that microbial communities adapt over seasons with high diversity in autumn (September) and low diversity in winter (January; Kobiyama et al., 2021), adding a seasonal aspect to brackish systems (Reboul et al., 2021).

1.6 Seagrass as representative of beach wrack

Beach wrack investigations pose special challenges for the test material, as they are usually time-consuming and require a large amount of material. For controlled decomposition experiments, a specific species was needed to be found in order to allow detection of the impact of moisture, temperature and irradiance conditions. The chosen species should be abundant in the study area, widely available and easily accessible. Additionally, it should reflect a

significant proportion of the local beach wrack. Consequently, seagrass *Zostera marina* was chosen (Figure 2). It can grow in depths up to 8 meters, and its growth period e.g., in the Kiel area (Belt Sea) starts in June and lasts for about 210 days. It reaches its climax between August and September before growth comes to an end in March. During its growth season, shoot length varies between around 20 and 140 cm (Feldner, 1976; Reusch et al., 1994). Its dry weight can reach amounts of 200 to 800 g m⁻² of biomass (Feldner, 1976). Shoot density lies between 600 to 1,600 shoots m⁻² in soft substrate (Reusch et al., 1994). Seagrass leaves are said to decompose with a half-life of 44 – 78 days after dying off (Goulter & Allaway, 1979).

Seagrass meadows are important ecosystem engineers (sensu (Wright & Jones, 2006)) with a multitude of ecological responsibilities worldwide (Costanza et al., 1997; Hemminga & Duarte, 2000; Larkum et al., 2006). Seagrass beds occur all around the world's temperate and, depending on the species, some tropic regions. Besides functioning as a breeding ground for local fauna, supporting fisheries production (Unsworth et al., 2018) and its carbon sequestration (Duarte et al., 2013), it also stabilizes and protects the coastline (Ondiviela et al., 2014), by root penetration in the sand and therefore, promotes sedimentation (Hemminga & Duarte, 2000). Seagrass meadows have been lost worldwide within the last century due to extensive human utilization of coastal areas (Waycott et al., 2009; Jankowska et al., 2018). Since 1879, 29 % of global seagrass occurrences have been lost (Waycott et al., 2009). With increased eutrophication, seagrass abundance and depth colonization decreased due to reduced water transparency and shading (Duarte, 1990; Nielsen et al., 2002; Krause-Jensen et al., 2008). Having partly recovered from mitigated eutrophication, seagrass still suffers from temperature increase and bottom trawling in the Baltic Sea (Krause-Jensen et al., 2021). However, *Zostera marina* was also chosen because it is the main macrophyte species at the coast of the island of Poel, with large amounts during autumn and after storm events (Figure 2).



Figure 2: Seagrass accumulations around a groin in the shallow water at the island of Poel, "Schwarzer Busch" (15.07.2020). Such accumulated quantities are observed especially after storms and in the fall.

1.7 Research hypotheses

Beach wrack has been subject to extend research in the past. Nevertheless, in especially regarding brackish ecosystems not much is known so far. As management activities at the Baltic Sea in Mecklenburg-Western Pomerania are limited to the tourist season, data of amounts and species composition of beach wrack throughout the year are scarce. With its removal, not much is known on the decay characteristics, whether on land or in the water. Finally, there is a lack of insight into the factors that determine the microbial community and its development. To close the aforementioned subject-related gaps in knowledge, the following hypotheses were formulated and answered by the work conducted:

1. Beach wrack landings on the Baltic Sea coast are mainly influenced by the seasons regarding amounts and species composition.

Besides the influence of weather, which are mainly wind and waves, it is stated that the seasonality of algal and seagrass biomass are the primary drivers regarding beach wrack amounts and their respective species composition.

2. There are differences between the decay characteristics of beach wrack on land and in the water.

Having biomass rotting continuously on land will have a different decay process and therefore, speed, in contrast to beach wrack constantly disintegrating within the water column. The decay will vary in its rate of decomposition and the resulting time until complete disintegration.

3. Abiotic factors influence the quantitative and qualitative microbial community composition.

Constantly changing abiotic factors, e.g., between dry land and wet water conditions, presuppose a different microbial community development. This will mimic the dynamic of beach wrack being washed ashore and retracted to the shallow waters after e.g., storm- and high-water events.

2 Materials & Methods

2.1 Sampling sites

To investigate the seasonality of composition and amount of beach wrack, field campaigns were carried out from April 2019 until September 2021. Two sites were chosen: Kühlungsborn, being exposed to the open Baltic Sea and Poel, being located in the more sheltered Wismar Bay. Beach wrack amounts as well as species composition sampling were executed at the Island of Poel (hereafter shortened to Poel), at the beach “Schwarzer Busch” and in Kühlungsborn West (hereafter shortened to Kühlungsborn). Decomposition on land was executed at the measuring field of the DWD (Deutscher Wetterdienst (German Weather Service), Offenbach, Germany) in Warnemünde in a fenced area without public access. The decomposition experiments in the water and the alternating experiments in the water and on land were split between Poel (water) and Warnemünde (land). An overview of all experiment sites is shown in Figure 3.



Figure 3: Experiment location sites along the Western Baltic Sea coast in Germany, Mecklenburg Western-Pomerania. Beach wrack amounts and species composition were evaluated at the beach “Schwarzer Busch” (Island of Poel) and in Kühlungsborn, decay under constant water exposure at Poel, solely, and alternating experiments regarding the decay of seagrass under changing conditions were conducted at Poel and in Warnemünde. Map created with QGIS version 3.14.16-Pi (QGIS Development Team. (2023). QGIS geographic information system. QGIS Association: <https://www.qgis.org/>).

2.2 Quantifying beach wrack

To investigate the beach wrack amounts a biweekly sampling was conducted in Poel and Kühlungsborn between April 2019 and November 2019. A transect of 100 m of beach length was marked parallel to the shoreline. The complete beach width was measured three times: at the beginning of the transect, in the middle and consequently at the end. With this data the total beach size in square meters on the sampling date could be calculated. For continuous traceability GPS coordinates were taken at the distinctive corner points (Table 1). Samples for species composition and amounts were collected and classified into a seasonal system. Therefore, it was decided that the seasons are defined as given in Table 2.

Table 1: GPS coordinates of respective 100 m transects at the experiment conduction sites.

Beach	Start coordN	End coordN	Start coordE	End coordE
Poel	54.00691	54.00661	11.24912	11.24831
Kühlungsborn	54.41229	54.09230	11.41911	11.41911
Warnemünde	54.18028	54.18028	12.08087	12.08093

Within the transect, metal frames with the size 20 cmx 20 cm were randomly placed on the beach surface in two respective lines. The first line, called “new wrack” (NW) was placed next to the waterline or flushing area, and the second line, called “old wrack” (OW) was further up the beach face where no observable waves could reach the beach anymore during regular water levels. The frames were set up three times in each row (Figure 4). The enclosed wrack material was collected, transferred into freezer bags, and transported dark and cool to the laboratory for species determination. Accurate sampling was achieved by cutting out the material with a knife inside the steel frame. Only material that was laying on the sediment was collected, not the buried and sand-covered wrack. The thickness of the beach wrack was measured and the percentage of coverage within the frame as well as of the whole beach was additionally estimated for calculations of total wrack coverage at the beaches.

Table 2: Seasonal classification of sampling dates for the fieldwork in 2019.

month	sampling date	season
April	30.04.2019	Spring
May	09.05.2019, 20.05.2019	
June	03.06.2019, 19.06.2019	Summer
July	08.07.2019, 22.07.2019	
August	05.08.2019, 27.08.2019	
September	05.09.2019, 19.09.2019	Autumn
October	08.10.2019, 22.10.2019	
November	05.11.2019, 19.11.2019	

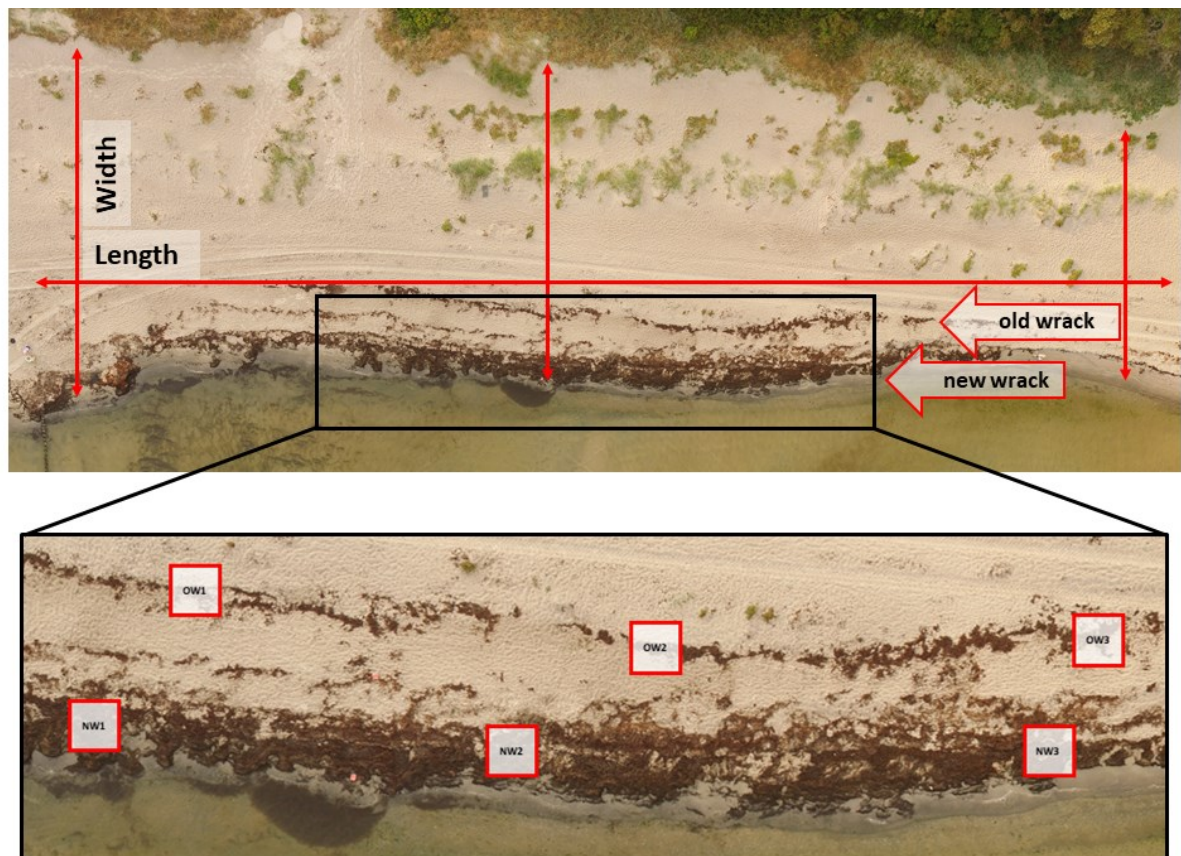


Figure 4: Beach transect and sampling frames for the different areas of old and new wrack. Length in total: 100 m, beach width depending on water level. Red arrows indicate beach length and width limitations. One square for sampling equals an area of 20 cm x 20 cm of beach wrack with three replicates per area. Replicates of new wrack are marked as NW1, NW2, NW3 and old wrack replicates as OW1, OW2 and OW3.

Samples were de-sanded in the lab by either washing in local seawater prior to further treatment or, in the case of fragile algal branches, first dried and then sieved to remove sand manually. Weights were noted wet and dry, both with and without sand as removal of sand turned out to be a variable problem within both (wet and dry) conditions. After species determination biomass was dried at 40 °C until a constant dry weight was achieved. Low temperature was chosen to avoid loss of any organic compound and to mimic temperatures close to the ground on a hot summer day at the local beaches' sand surface when drying out naturally.

2.3 Species composition determination

For species determination, collected biomass was analyzed to the lowest possible classification level. Macrophytes were cleaned from litter (human debris) and separated from fauna as it was aimed for pure algal and seagrass biomass. Then they were sorted into the groups of brown, green and red algae, angiosperms and land-originated plants. Separated fauna and litter components were kept for later analysis. Identification was done either by eyes or, where needed, with the help of a binocular (Olympus SZX16 (SZX2-ILLT T5 SN), Cam: DP26; both: Olympus Corporation, Tokyo; Japan). For identification of macroalgae, relevant literature was used (Kornmann & Sahling, 1977, 1983, 1994; Braune, 2008). Plants that could not be identified, e.g., when being too degraded or fragmented, specific morphological details or featured settings were missing, were classified as “others” in the sorting system. After species determination, wrack was sorted into the aforementioned groups, put into aluminum trays and dried at 105 °C until a constant dry weight was achieved (typically 24 h: Memmert drying oven; model: 100 – 800; Memmert GmbH & Co. KG, Schwabach, Germany).

2.4 Decay experiments

For the comparison of beach wrack decay on land and in the water, three different experiments were set up. The first experiment at the local beach in Warnemünde was carried out with mixed fresh beach wrack; the aim was to have a representative mix of local wrack. In this experiment the material was left to rot on and in the sand near the coast. In a second experiment litterbags filled with seagrass (as local main wrack species) were left to disintegrate constantly submerged in the shallow waters at Poel. In the third experiment, again seagrass was decomposing in litterbags with alternating exposure to the land at Warnemünde and in the water at Poel. For selected site information, refer to GPS coordinates given in Table 1.

2.4.1 Decay on land in Warnemünde

Fresh beach wrack was collected as found at Warnemünde beach the previous day. Wrack (approx. 2 kg) was put into a cooling box and brought to the laboratory. Species composition was determined (Kornmann & Sahling, 1977, 1983, 1994; Braune, 2008). Species were thoroughly mixed to have a homogenized wrack mass. The biomass was filled into glass fiber mesh bags (approx. 10 cm x 15 cm) with a mesh size of 10 mm x 10 mm. Each bag had a total amount of 42 ± 2.5 g fresh and wet beach wrack.

The experiment was conducted at the fenced measuring field of the DWD where it was protected from the public (Figure 5). 36 litterbags were filled for the experiment: 18 bags each were put on the surface where they were left fully exposed to weather conditions like e.g., rain, radiation and grazers. Another 18 bags were buried in the sand in approx. 10 cm depth. Every treatment was sampled six times during the course of the year to evaluate decay over time: after one, two, four, six, eight and 12 months. At each time point three replicates were retrieved. After retrieving, samples were taken into the lab and cleaned of as much sand as possible. Weighted wet samples were dried at 105 °C for 24 h until a constant dry weight was achieved. After cooling down, samples were de-sanded for a second time and weighed for their respective dry weights. The weights were measured to determine the degree of degradation of the biomass at each point in time (refer to Table A 1 for individual retrieval weights).

Sediment samples were taken with each sampling from the sand underneath each litterbag and from the bare sand approx. 1 m eastwards to determine possible nutrient leaching underneath the litterbags compared to litter-free areas. With a cut-off syringe, the sediment was taken out and transferred into individual containers. The sediments were dried until a constant dry weight was achieved (105 °C for 24 h). To determine ash free dry weights sediments were weighed and combusted at 550 °C overnight for approx. 16 h (Van Wychen & Laurens, 2013).



Figure 5: Litterbag installation at Warnemünde. On the left, the litterbags on the sediment can be seen. Covered by sand, on the right, are the buried litterbags. Installation: 10.10.2019 at the fenced measuring field of the DWD (German Weather Service) without public access.

2.4.2 Decay under water

In contrast to the decay experiment on land in this attempt solely seagrass was used. Here, the mesh size of the litterbags was reduced to 140 μm to exclude meso- and macro grazer. Special focus was given to the microbial community during decay stages. For the litterbag experiment with constant water exposure, a cage made of gabion grid was constructed. The litterbags were put in-between two layers of grid. The two layers were separated with long screws and nuts to keep enough distance (approx. 4 cm). Logger (HOBO Logger, Model U24-002; Onset Computer Corporation, Bourne, MA, USA) were put into the grid to measure abiotic factors, e.g., temperature, conductivity, light intensity and radiation.

Freshly detached seagrass of the species *Zostera marina* was collected 24 h before the start of each experiment. Collecting took place on the coast of Poel to represent its natural occurrence. Every litterbag was made of polyethylene with a mesh size of 140 μm . The measurements were approx. 10 cm x 15 cm. The collected seagrass was stored overnight in habitat water at 5 °C. The following day the start value (t_0) was recorded by wiping the microbial biofilm. Two times five

whole leaves per sample were used as subsamples. For more details on microbial handling refer to chapter 2.5. Remaining seagrass was cleaned by hand, any apparent epibiota on the leaves were removed, and leaves that were already rotting were sorted out. Each litterbag was filled with approx. 10 g of fresh seagrass biomass. On the open edges, the folded mesh was first double heat-sealed (Caso VC 100 household vacuum machine) and further sewed in-between the two seals (Silvercrest SNM 33 C1 sewing machine). This was done for two reasons: firstly, to exclude micro grazers as well as possible; secondly, to prevent any seagrass material getting lost from the litterbags. Additionally, heat-sealing protected the delicate seams from being ripped open. The opposing corners were separated from the bag with a double heat-sealing and seam for the same reasons as mentioned before. In these corners, eyelets of stainless steel were mounted. Through these loops, litterbags were connected with cable ties within the cage. In addition, these sealings were done to protect and prevent a tearing of the seams during the experiment runtime, and to further secure the litterbags from invaders like e.g., macro- and meso-grazer, and larvae who otherwise might slip through the seams. Everything was secured with pre-watered cable ties on top of a groin at Poel. The construction was put straight on the sediment surface at the time of installation. Natural fluctuations in water level had to be accepted. A complete dry-off of the installation could not be excluded. A safety steel rope was installed to prevent loss or drift of the cage when cable ties would break due to exposure to wind and wave action (Figure 6).

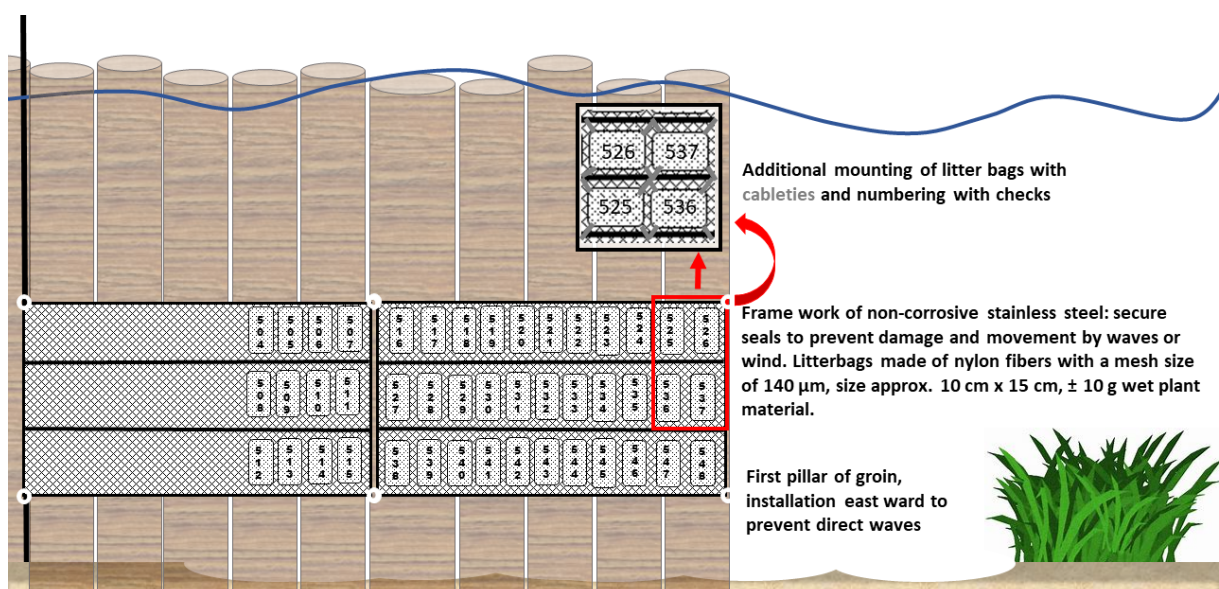


Figure 6: Litterbag cage as installed on the groin in Poel. Poles in the back represent groin poles. Black rectangle shows the two cages filled with the litterbags. Symbolical numbers are shown to represent plastic checks. Red rectangle is a close-up of some bags to show their securing against rip-off. Blue line symbolizes water level. Green bush on the right side is representative for the adjacent seagrass meadow.

Bags were consecutively numbered with large green plastic checks, and an engraved, unique number. The sight in the Baltic Sea is often below 1 m. Even under low-light conditions, in turbid water bags could therefore be identified securely. Especially in the shallow coastal waters, where lots of rotting biomass swims in the water, and water is highly turbid, depending on weather and seasonal conditions the sight can be below <10 cm. Therefore, a readable numbering even under these complicated circumstances was needed. Bags were removed with a cutter. The mesh size of the grid allowed removal without removing the grid either from the water or disassembling it for sampling. One sampling in Autumn 2020 had to be postponed due to heavy wind and waves (16.10.20 instead of 14.10.20).

The experiment was executed twice; one starting in summer 2020 (called summer experiment 2020 or SE20) and another starting in winter 2021 (called winter experiment 2021 or WE21). Each experiment was intended to last for 1 year. The first experiment had to be terminated after 210 days, as at this point the litterbags were empty. Consequently, the second experiment was directly set for 210 days. For each sampling day, three replicates were made. Experiment sampling was executed as given in Table 3. As previous research states the microbial decay is dependent on temperatures (Kirschbaum, 1995), the sampling regime was prolonged through autumn and winter.

Table 3: Sampling dates for the two litterbag experiments with constant exposure to water for 210 days. Acronyms are given in parentheses, as SE20=summer experiment, starting in summer 2020 and WE21=winter experiment, starting in winter 2021. Please note last sampling from SE20 (t_{12}) was done in January 2021.

Sampling point	Days of exposure	Starting in Summer 2020 (SE20)	Starting in Winter 2021 (WE21)
t_0	0	17.06.20	03.02.21
t_1	7	24.06.20	10.02.21
t_2	14	01.07.20	17.02.21
t_3	21	08.07.20	24.02.21
t_4	28	15.07.20	03.03.21
t_5	42	29.07.20	17.03.21
t_6	56	12.08.20	31.03.21
t_7	70	26.08.20	14.04.21
t_8	84	09.09.20	28.04.21
t_9	98	23.09.20	12.05.21
t_{10}	112	07.10.20	26.05.21
t_{11}	140	04.11.20	26.06.21
t_{12}	210	13.01.21	01.09.21

2.4.3 Alternating decay

The alternating exposure to water and land was intended to mimic the natural cycle, when beach wrack is washed ashore during storm and high-water events and dropped back into the water soon after several times over. In addition, the aim was to investigate the influence of beach wrack piling up at the beach and being stuck there with the accompanying deprivation of light when being buried. Therefore, as well as the conductivity logger, light logger were installed. There were three loggers: one being uncovered as reference. The second was wrapped into the white mesh, and the third into the black mesh to retrieve real time values for light exposure and temperature within the respective litterbags. The effects of light regarding the degradation process as well as the possible light-induced changes in the microbial community were the aim of the study. Possible short variations in light availability could be reasoned by e.g., clouds, drifting algae during water-phase or birds/mammals during land-phase or temporary settlement from especially meso- and macro-faunal organisms. It has been observed several times during sampling. On land, e.g. leaves may have been blown onto the logger by wind for a certain time period. Additionally, and to minimize measuring faults, receivers were cleaned from epibiota each sampling time. The basic setup of the litterbags was the same as described in the previous experiment (see chapter 2.4.2). Litterbags were made from the same white mesh as in the previous experiment and over and above in a black mesh. The experiment consisted of equal parts of black and white litterbags with three replicates per sampling. These were again hung into the same cage construction. Aquatic periods were executed at the groin in Poel, the terrestrial periods in Warnemünde. With the fenced area in Warnemünde it was excluded that any litterbag was removed during the experiment runtime. Acronyms for the individual experiments are: seasonal summer experiment 2020 = S_{Su}20, seasonal autumn experiment 2020 = S_{Au}20, seasonal winter experiment 2021 = S_{Wi}21 and seasonal spring experiment 2021 = S_{Sp}21. In the following, and especially in the discussion, the experiments are abbreviated with their acronyms.

Light transmission of the different mesh colors white and black was tested to identify the percentage of light absorption by the meshes. For analyzes the MACAM SR9910-PC (Macam Photometrics Ltd., Livingstone, Scotland) spectro-radiometer was used. Measurements were done in the lab and as a light source, a LED light (Jansjö LED, IKEA, Delft, Netherlands) was used. Measured spectrum ranged from 240 nm to 800 nm, it showed that the white mesh transmitted an average of 81.48 % of remaining light that was available to the microbial community. In the black mesh bags, the average transmission was down to 15.29 %. Only the longwave radiation from approx. 750 nm reaches a transmittance of 60 % (Figure 7).

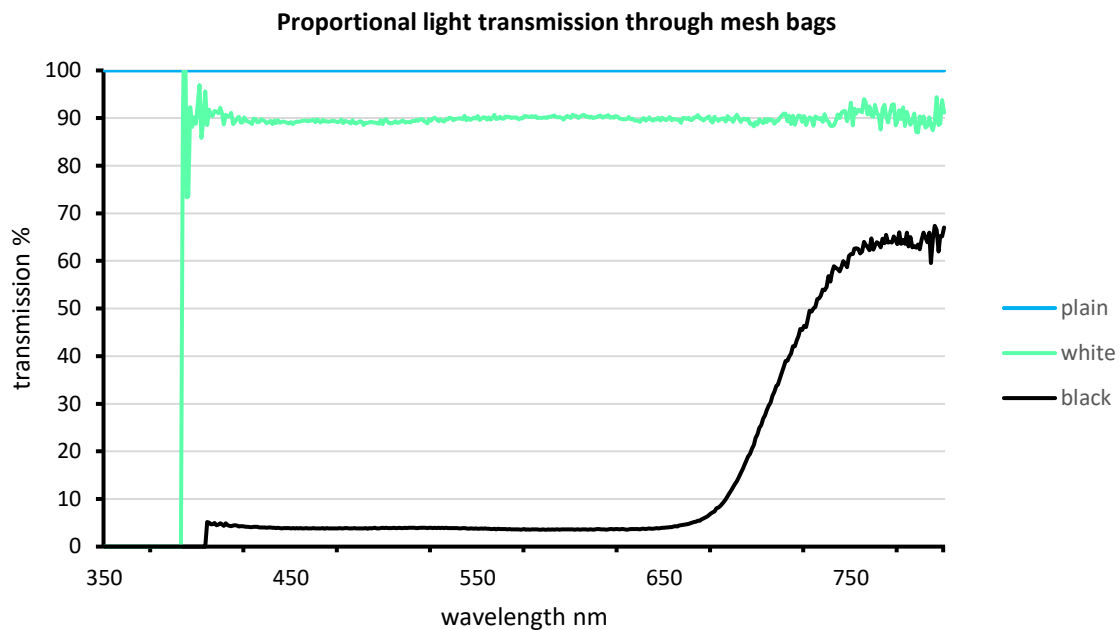


Figure 7: Transmission of light in percent of used meshes for the litterbags. Blue line representing plain light, green light representing white mesh, and black representing black mesh. X-axis is giving the spectrum in nm, y-axis is giving the percentage of transmission of individual meshes. All values were measured with a Macam SR-9910-PC (Macam Photometrics Ltd., Livingston, Scotland, UK).

In contrast to the constant exposure to water, in this case the cage was only submerged into water at the beginning of the experiment. Then, each week, the cage was transferred from Poel to Warnemünde and placed for the following week at the beach, followed by another week in the water and so on for a total period of 42 days. This experiment was conducted four times, one time for each season (Table 4). For abiotic parameters, combined light and temperature loggers were put into the same mesh as the seagrass samples, installed on the grid and ran through the whole experiment seasons. Depending whether it was on land or in the water, the light measuring logger points were turned to face towards the sun, respectively towards the sky and the main light incidence.

Evaluation and data analyses were made by Primer-e (Software Primer-e through Massey University, 5 University Avenue, Gate 1, Albany Expressway, Albany, Auckland 0632, New Zealand: Primer 7, Version 7.0.23 with add on Permanova+1 (2021)). Therefore, data was read as environmental data set, overall transformed and normalized. With this data set different analyses were run: PCA (Principal Component Analyze), nMDS (non-metric Multidimensional Scaling), and Cluster analyses (Clarke & Gorley, 2015).

Table 4: Seasonal experiments with sampling dates. Column “exposure” shows from which exposure to which alternating exposure the litterbags were transferred from and to. Acronyms are given in parentheses, as SSu20=seasonal summer experiment 2020, SAu20=seasonal autumn experiment 2020, SWi21=seasonal winter experiment 2021 and SSp21=seasonal spring experiment 2021. Please note that the spring experiment run over the meteorological spring and until June (last sampling at land in Warnemünde) in the early summer of 2021.

Sampling point	Exposure change	Summer 2020 (SSu20)	Autumn 2020 (SAu20)	Winter 2021 (SWi21)	Spring 2021 (SSp21)
t ₀	Water	05.08.20	07.10.20	13.01.21	20.04.21
t ₁	Water to Land	12.08.20	16.10.20	20.01.21	28.04.21
t ₂	Land to Water	19.08.20	21.10.20	27.01.21	05.05.21
t ₃	Water to Land	26.08.20	28.10.20	03.02.21	12.05.21
t ₄	Land to Water	02.09.20	04.11.20	10.02.21	19.05.21
t ₅	Water to Land	09.09.20	11.11.20	17.02.21	26.05.21
t ₆	Land	16.09.20	18.11.20	24.02.21	02.06.21

A decay coefficient was calculated for all experiments by the equation for exponential decay:

$$y(t) = a \cdot e^{-kt}$$

a = biomass at start; k = rate of decay; t = time; y(t) = biomass at time t (adapted from Petersen & Cummins, 1974; Bärlocher, 2005). Additionally, coefficients of determination (R²) were calculated. Hereby, an R² value that is 1 or close to 1 means that the model explains the observations perfectly. A value below 0 means that the model is worse than a random model (Prairie, 1996). R² indicates the fit of the regression model to the data, with a strong association towards characteristics when small (close to 0.2) values are shown (Renaud & Victoria-Feser, 2010). The calculated R²-values were taken for evaluation of the output.

2.5 Microbiome sample preparation

To follow up the changes within the microbial community of the decaying seagrass litter, next generation sequencing (NGS) was applied in a professional laboratory (LGC Genomics GmbH, Berlin, Germany). Whole and partial genome sequencing is readily used for the analysis of microbiomes in environmental studies. The key strengths in this method lay in being able to sequence multiple organisms in parallel, and to provide comprehensive analyses of these genomes. The microbial abundance of different environments can be detected. This can also be applied to uncultivable microorganisms and field experiments (Giovannoni et al., 1995; Lewis et al., 2021). Besides the qualitative statements regarding taxa and species occurrences, additional assertions regarding quantitative occurrences are possible with this method. Only for the seagrass-related experiments (chapters 2.4.2, 2.4.3) the microbial community was investigated. To prevent damage to a freshly retrieved sample, before any other treatment, the biofilm was scratched off the decaying seagrass. All handling materials were sterilized before work. Petri dishes, tweezers and scissors were additionally cleaned and flamed between each sample. Disinfection was done using 70 % denatured ethanol. All microbiome-related work was executed under a clean bench (BDK Luft- & Reinraumtechnik GmbH, Sonnenbühl-Genkingen, Germany). The bench was started at least 15 min prior to any practical work, and subsequently sterilized with UV light after finishing work. With gloves, one litterbag at a time was cut open. With each sample, processing an additional negative control was integrated.

From each of the three sampled litterbags per time point, five seagrass leaves were picked and transferred to a flamed petri dish. Hereby additional signaling to the pure microbiome from e.g., the seagrass itself could not be excluded anymore, which was the reason for scratching off the biofilms as much as possible in the first place. With a sterile swab with a polyester tip (CLASSIQSwabs, Model: 167KS01 by COPAN ITALIA SpA, Brescia, Italy) the complete biofilm was wiped from each leaf. One swab was used per sample, collecting the combined biofilms from all five seagrass leaves. The soaked swab-heads were cut off, individually diluted in a tube containing 10 ml of sterilized and filtered (Rotilabo -syringe filters, CME, sterile; Carl Roth GmbH & Co. KG, Karlsruhe, Germany) seawater from the sampling site (Poel), given 10 min to soak. Subsequently, they were shaken (model: Vortexer, Heathrow Scientific, Illinois, USA) at speed 1,000 rpm for 3 min. The liquid suspension was stored at 4 °C prior to centrifugation. Overall, the storage time of 10-15 min in the fridge was never exceeded. The resulting liquid suspension was pipetted into five individual 2 ml tubes per sample. The samples were centrifuged (Biofuge primo R; Heraeus GmbH, Hanau, Germany) at $21,885 \times g$ for 10 min in the centrifuge at 4 °C to form a pellet. The resulting supernatant was either poured away or

pipetted as much as possible without losing any of the pellet. The five pellets were, with the remaining water, transferred (pipet) into a sterile collecting tube. After a last centrifuging at $21,885 \times g$ for 3 min, remaining overhanging water was pipetted away and the final pellet weighed. For accuracy, each tube was pre-weighed empty and the weight difference calculated to gain pellet weight. Pellets were stored in the tube at $-80\text{ }^{\circ}\text{C}$ (CryoCube, F440h, Eppendorf AG, Hamburg, Germany) until further processing. Storage time ranged from one month up to 18 months before all experiments were conducted and samples sent to the professional laboratory.

The five seagrass leaves were measured (as well as possible) for total length and average width to be able to determine the overall leaf area being scratched off. Depending on the degree of degradation, e.g., in the final stages of the yearly experiments, scratching off the biofilm from the seagrass leaves was not possible anymore. In these cases, the remaining biomass was homogenized in a flamed glass dish, and directly pelleted as representative subsamples from the remaining biomass (median value for summer experiment: 57.85 mg; winter experiment: 104.4 mg). Volume of one subsample consisted of a spade point (approx. 25–140 mg). Resulting pellets were again weighed. Here, it needs to be noted that due to the homogenized mixture an increased amount of sediment was within each of the samples which might have falsified the result.

Three different DNA extraction kits were tested to evaluate the optimum kit for the DNA extraction of the biofilm pellets: Qiagen PowerSoilPro, Qiagen PowerBiofilm (both from Qiagen GmbH, Hilden, Germany), and Macherey-Nagel NucleoSpin Soil (Macherey-Nagel GmbH & Co KG, Düren, Germany). Evaluation has been done by executing PCR reactions with two different markers: for prokaryotic 16S rDNA primers 515f and 806r were used (Walters et al., 2016; Caporaso et al., 2018), for eukaryotic 18S rDNA F-1183mod and R-1443mod (Ray et al., 2016). Results of this PCR (Figure 8) were used as the basis for evaluation. The Macherey-Nagel kit “NucleoSpin Soil, Mini kit for DNA from soil” showed strong band intensity, especially in relation to price and performance. It was chosen for the microbial DNA extractions. After finishing all decay experiments (chapters 2.4.2 and 2.4.3), the 78 collected pellets were extracted for their total genomic DNA. With each extraction additional negative controls were run to validate results and secure cleanliness of extractions. Every obtained negative control did not show any signal, assuring clean extracts of genomic DNA.

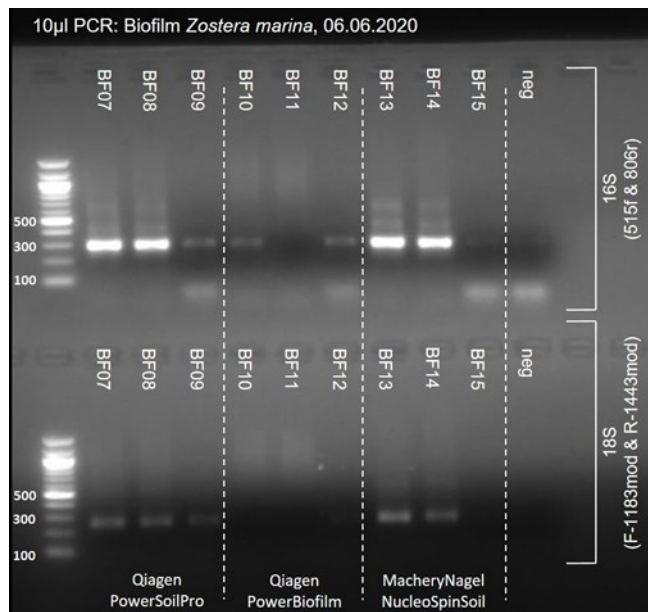


Figure 8: Gel electrophoresis picture of tested kits for DNA extraction. Marker: 100 bp DNA Ladder (New England Biolabs, Ipswich, MA; US). First row shows marker and its ladder at 100 bp, 300 bp and 500 bp. From left to right: Qiagen PowerSoil pro, Qiagen PowerBiofilm, Macherey-Nagel NucleoSpin Soil. Upper lane represents prokaryotic 16SrDNA, lower lane eukaryotic 18SrDNA. Neg is the negative control of the PCR. Used was a random seagrass test sample that was extracted for evaluating the DNA kits. These samples were not used in any following analyze

The extractions and purifications were done with the instructions from the NucleoSpin manual (March 2019 / Rev. 08). The following decisions, adaptations and verifications have been made:

- For sample preparation in step 1 SL2 buffer was used with the enhancer.
- Mixing in step 3 was done in two steps: first 20 s at 2,500 rpm with a rest on ice and another round for 20 s at 4,200 rpm.
- Mixing resulted in heavy foaming. Therefore, centrifuging was raised from $11,000 \times g$ to $21,000 \times g$ for steps 4 and 5 of the manual.
- SB buffer amount in step 6 had to be adjusted to the flow through and respectively increased.
- Before drying silica membrane in step 9, centrifuging was set from $11,000 \times g$ to $21,000 \times g$ for 2 min each.
- To elute the DNA, in step 10 the amount of SE buffer was split to two times 50 µl instead of one time 100 µl. The incubation time was increased to 2 min.
- The eluted DNA was split into a 15 µl aliquot to run a DNA verification electrophoreses with a part of the aliquot and the remaining 85 µl DNA extract for further analyses.

From each sample an agarose gel was run to yield and verify DNA quality. Agarose gels contained ethidium bromide as an intercalating agent to fluorescently tag nucleic acid. 1% agarose gels have been run in a TAE buffer at 85 V for 30–45 min. Alongside the 5 μ l of actual samples 3 μ l marker (λ / EcoRI+ Hind III; Fermentas, INFOS) were applied to each gel. Gel electrophoresis were visually inspected for their progress after 30 min, and aborted when suitable bands were seen or prolonged up to 45 min (exemplary picture shown in Figure 9).

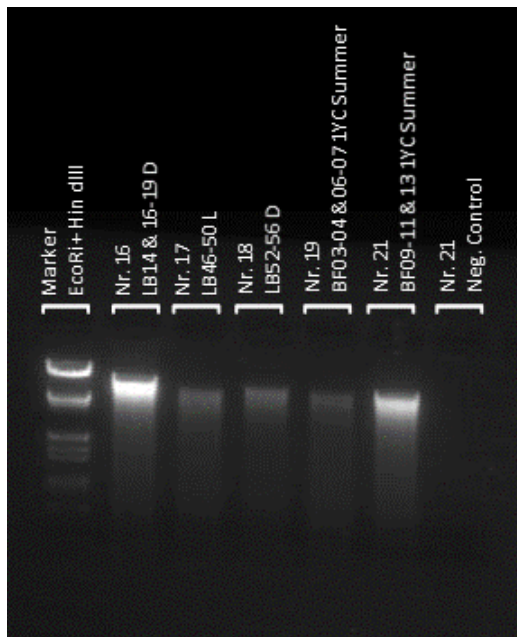


Figure 9: Gel electrophoresis of DNA extraction as run by 23.11.21. First band shows marker (λ / EcoRI+ Hind III; Fermentas), followed by the five respective samples. It can be seen that sub-samples needed to be pooled to yield enough DNA-concentration and to get a proper signal. Negative control at the end. As negative control is empty, a clean extraction is received.

Before sending in the samples, they were further measured for the respective DNA content with a fluorometer (Qubit fluorometer, by Turner BioSystems, exclusively for Invitrogen). As required by the laboratory, it was aimed for an optimal DNA concentration ranging from 1 to 10 $\text{ng } \mu\text{l}^{-1}$ of genomic DNA, dissolved in Tris/TE (5 mM, pH: 8.5); Quantity: 20–200 ng; Volume: 20 μ l. (DNA contents are shown in Table A 2 for SE20 and WE21, Table A 3 for SSu20 and SAu20, Table A 4 for SWi21 and SSp21) For insufficient samples sub-samples were pooled to raise DNA contents. Prepared DNA samples were sent to LGS laboratory.

To differentiate between prokaryotes and eukaryotes communities, both 16S rDNA and 18S rDNA were analyzed. For amplification, the following primer pairs were utilized: primers targeting the V4 region of the 16S rDNA gene (Walters et al., 2016) 515YF (5'-GTG YCA GCM GCC GCG GTA A-3') and B806R (5'-GGA CTA CNV GGG TWT CTA AT-3') and primers targeting the V7 region of the 18S rDNA gene (Ray et al., 2016) 1183F (5'-AAT TTG ACT CAA CRC GGG-3') and 1443R (5'-GRG CAT CAC AGA CCT G-3').

The chosen primers have been used in seagrass leaf surface microbiome analyzes successfully in previous research (Ray et al., 2016; Walters et al., 2016; Bengtsson et al., 2017). Processing was done by LGC (LGC Genomics GmbH Biotechnologie, Berlin, Germany) after following protocol (Carina Loose, Project Manager at LGC, 10.03.2022, personal communication): The PCRs included about 1 – 10 ng of DNA extract (total volume 1 µl), 15 pmol of each forward primer and reverse primer in 20 µL volume of 1 x MyTaq buffer containing 1.5 units MyTaq DNA polymerase (Bioline GmbH, Luckenwalde, Germany) and 2 µl of BioStabII PCR Enhancer (Sigma-Aldrich Co.). For each sample, the forward and reverse primers had the same 10-nt barcode sequence. The barcode allows you to pool tagged unique sequences into one single library (Mir et al., 2013). PCRs were carried out for 30 cycles using the following parameters: 1 min 96 °C pre-denaturation; 96 °C denaturation for 15 s, 55 °C annealing for 30 s, 70 °C extension for 90 s, and hold at 8 °C.

The DNA concentration of amplicons of interest was assessed by gel electrophoresis. About 20 ng amplicon DNA of each sample were pooled for up to 48 samples carrying different barcodes. The amplicon pools were purified with one volume Agencourt AMPure XP beads (Beckman Coulter, Inc., IN, USA) to remove primer dimer and other small mispriming products, followed by an additional purification on MiniElute columns (QIAGEN GmbH, Hilden, Germany). About 100 ng of each purified amplicon pool DNA was used to construct Illumina libraries using the Ovation Rapid DR Multiplex System 1 – 96 (NuGEN Technologies, Inc., CA, USA). Illumina libraries (Illumina, Inc., CA, USA) were pooled and size selected by preparative gel electrophoresis. Sequencing was done on an Illumina MiSeq using V3 Chemistry.

2.6 Statistical evaluation of microbial data

The retrieved data was analyzed using R (version 4.2.0) and R Studio (version 2022.12.0+353) after following procedures provided by Dr. Barrantes (21.08.2023, personal communication): With the package Bioconductor (3.16), dada2 (version 3.16; Accurate, high-resolution sample inference from amplicon sequencing data): the dada2 package infers exact amplicon sequence variants (ASVs) from high-throughput amplicon sequencing data, replacing the coarser and less accurate operational taxonomic units (OTUs) clustering approach. The dada2 pipeline takes as input demultiplexed fastq files, and outputs the sequence variants and their sample-wise abundances after removing substitution and chimera errors. Taxonomic classification is available via a native implementation of the RDP naive Bayesian classifier, and species-level

assignment to prokaryotic 16S rDNA gene fragments by exact matching (Callahan et al., 2016), decipher (version 11.17: Tools for curating, analyzing, and manipulating biological sequences): A toolset for deciphering and managing biological sequences (Wright, 2016) and phyloseq (version 1.42.0: Handling and analysis of high-throughput microbiome census data): phyloseq provides a set of classes and tools to facilitate the import, storage, analysis, and graphical display of micro-biome census data (McMurdie & Holmes, 2013).

Dada2 package in R (Callahan et al., 2016) was run with the following adjustments: After loading fastq-files from the analysis, a quality profile was done to decide on the filtered files. Besides the average quality score additionally the maximum number of “expected errors” was set to two. Visual inspection yielded a minimum length of 175 bp and a cut-off read length at 220 bp. The created amplicon sequence variant (ASV) distributed sequence length. The expected amplicon size was at 250 bp, allowing for 10 bp wiggle room either way. Therefore, sequences were cut to 240 bp or 260 bp, respectively. The amplified V4 region of the prokaryotic 16S rDNA gene did not have great length variability. The resulting track reads were put through the Silva (version r138, 2019) SSU pipeline (Pruesse et al., 2007), assigning taxonomy by using the IdTaxa classifier from the decipher package. The “not-availables” (NAs) in lower phylogenetic ranks were replaced with an entry from the next highest phylogenetic rank. Combined with the metadata, the sequence (ASV)-abundance table and the taxonomic classification table a phyloseq-object was produced.

There were few reads in the blanks, so no clean-up of the dataset with decontam package was done: it looked more like there was spilling over to the blanks from actual samples. The ASV-table was cleaned from chloroplasts, mitochondria and un-classified sequences in 16S rDNA. Hereby, 6 % of all 16S rDNA sequences were lost. Removing all samples with < 10,000 reads eliminated all blanks. Additionally, all singletons (taxa that are only present with 1 read in the whole dataset) were removed. Relative abundance was calculated, duplicated samples (dilutions) ejected, and relative abundance on class level agglomerated.

In addition, further analyses were applied exclusively with the prokaryotic 16S rDNA data: first the OTUs by bacterial phenotypes were summarized into each sample group, via the BugBase server (accessed 26.07.2023; Ward et al., 2017). To this end, OTUs were assigned against the Greengenes database version 13.5 (McDonald et al., 2012). Then, a PICRUSt analysis was carried out to predict the relative abundance of functional pathways in the microbial communities (version 2.11; Langille et al., 2013), from the OTUs assigned against Greengenes 13.5, and the obtained OTU tables were then normalized by 16S rDNA copy number to predict

functional genes and pathways from the Kyoto Encyclopedia of Genes and Genomes (KEGG) database (Kanehisa et al., 2007). The results from the PICRUSt analysis and KEGG predictions were processed with the phyloseq and DESeq2 R packages.

For further analysis of 16S rDNA data, amplicons were merged from the paired end Illumina sequencings using VSEARCH (version 2.7.0; Rognes et al., 2016). Merged fragments were then denoised with deblur (version 1.1.0; Amir et al., 2017), and OTUs were assigned to the denoised fragments with the sklearn classifier (version 0.23.1; Pedregosa et al., 2011) against prokaryotic 16S rDNAs clustered to 99 % identity from the SILVA database version 138 (Quast et al., 2012). Both deblur and sklearn were used within the QIIME2 pipeline version 2020.11 (Estaki et al., 2020). In the case of the 18S rDNA amplicons, the illumina sequencings were denoised with DADA2 (version 1.18.0; Callahan et al., 2016) and then assigned to OTUs with the sklearn classifier against the SILVA database version 138, as indicated before for the prokaryotic 16S rDNA data.

The following analyses were carried out with both 16S rDNA and 18S rDNA data: Community compositions and core microbiomes were obtained with the microbiome R package (version 1.9.96), following the instructions in the corresponding vignette (Salonen et al., 2012; Shetty et al., 2017). Shannon (α diversity) and inter-individual divergences (β diversities) were calculated with phyloseq (version 1.30.0; McMurdie & Holmes, 2013), and their significance assessed with the Wilcoxon test, as implemented in the ggpubr R package (version 0.6.0; Kassambara, 2018). Statistically- significant differences between the OTU abundances pertaining to the different sample groups (summer and winter) were calculated with the DESeq2 R package (version 1.26.0; Love et al., 2014), applying a Wald test and the Benjamin-Hochberg correction for the p-values (false discovery rate cutoff: $FDR < 0.01$). The compositions of the obtained differentially abundant OTUs were then plotted through the individual samples, to observe their dynamics over time. Afterwards, the correlation between the OTUs and the physical chemical parameters present in the sample metadata (light, temperature and conductivity) was inferred with the microbiome R package. Finally, and to observe the relationship between the sampled taxa, correlation interaction networks were built with the metagenonets web application (Nagpal et al., 2020; accessed 18.08.2023), using the following parameters: RLE transformation, Pearson correlations, p-value < 0.01 , 500 iterations, Critical-R correlation cutoff. Prevalence cutoff of 0.01 in 50 % of the samples was applied for the 16S rDNA data, and 0.001 prevalence in 5 % of the population for the 18S rDNA amplicons.

For eukaryotic 18S rDNA the following changes were made compared with prokaryotic 16S rDNA: visual inspection yielded a minimum length of 175 bp and a cut-off read length at 210 bp. Because the V4 region of the 18S rDNA gene is more variable in length, all sequences were used. "NAs" were replaced with "Unclassified". Cleaning the ASV-table by removing unclassified sequences, resulted in ~11 % loss of all eukaryotic 18S rDNA sequences. Singletons, blanks and dilutions were eliminated. Here in eukaryotic 18S rDNA, the ASV-table was not cleaned from chloroplasts, mitochondria to keep possible fragments of *Zostera marina* visible in the data set.

In order to figure out statistical importance (Clarke: User Manual/Tutorial - Google Scholar, 2001) of abiotic parameters, the top 25 abundant classes of prokaryotic 16S rDNA were evaluated in Primer (Plymouth Routines In Multivariate Ecological Research; Primer-e Version 6; Primer-e Quest Research Limited, Albany, Auckland, New Zealand). Here, data was first normalized as environmental data set for principal component analysis (PCA; Nichols, 1997). For non-metric Multi-Dimensional Scaling (nMDS), data was transformed by fourth root, samples standardized by total and after S17 Bray-Curtis similarity applied. Additionally, group averages were clustered by summer and winter, following a cluster analysis. An additional flowchart of executed procedures is given in Figure A 1 in the appendix.

2.7 C:N ratio analyses

From all samples of the experiments constantly in water (chapter 2.4.2) and alternating between land and water (chapter 2.4.3), subsamples were used for determination of total carbon (C) and nitrogen (N) contents. To test and examine the changes in C:N composition over time, from the remaining dry matter of seagrass subsamples were taken. These samples were pulverized with pestle and mortar, and homogenized for each sampling (in total: 78 samples, depending on the available amount of biomass pooling of sub-samples was executed to get enough plant material). After testing for the correct amount with pre-samples, it was decided in consultation with the executing laboratory to pack 1.5 mg for t_0 and consequently 3 mg for the remaining time points. This sample weight ensures that C and N loads are significantly higher than those given by the limit of quantification (C = 20 μ g, N = 20 μ g). The pulverized samples were weighed (Sartorius micro balance, Model: M2P Pro 11, Sartorius AG, Göttingen, Germany) and encapsulated (tin boats S22 137 48, measurements 4 mm x 4 mm x 11 mm, thin, produced by Elementar Analysesysteme GmbH, Langenselbold, Germany).

Laboratory work for analyzing the C:N ratio and stable isotopes was done by the Institute of Oceanology, Polish Academy of Sciences (IOPAN) in Sopot, Poland, in the marine biogeochemistry lab according to the procedure described by Kuliński et al., 2014 (Katarzyna Koziarowska-Makuch,, IOPAN marine biogeochemistry laboratory, 15.02.2023, personal communication):

The analyses of carbon and nitrogen concentrations and stable isotopes composition ($\delta^{13}\text{C}$ and $\delta^{15}\text{N}$) were performed in an Elemental Analyser (Flash EA 1112 series) combined with an Isotopic Ratio Mass Spectrometer Delta V Advantage (IRMS, Thermo Electron Corp., Germany). In short, dried and homogenized seagrass samples were weighed into silver capsules (about 1.5 - 3 mg; depending on the day of incubation). This sample weight ensures that C and N loads are significantly higher than those given by the limit of quantification (C = 20 μg , N = 20 μg). In an Elemental Analyser, received samples were oxidized (1020 °C) in the presence of chromium(III) oxide (Cr_2O_3) and cobalt(II,III) oxide (Co_3O_4). After catalytic oxidation, gases, including CO_2 , NO_x and H_2O , were transported to the second reactor, where NO_x was reduced to N_2 on the metallic copper (650 °C). The analysis products were dried with magnesium perchlorate (MgClO_4) and separated on a Gas Chromatographic column (45 °C). The separated gases (CO_2 and N_2) were transported to the IRMS. Quantitative measurements were calibrated against analyses of certified reference materials (Flußsediment/river sediments) provided by HEKAtech GmbH (Germany). The precision (expressed as the relative standard deviation) was better than 1.4 (n = 5) for carbon and 1.8 % (n = 5) for nitrogen measurements.

The isotopic composition of carbon and nitrogen was calculated using laboratory working pure reference gases (CO_2 and N_2) corrected against IAEA standards (CO-8 and USGS40 for $\delta^{13}\text{C}$ and N-1 and USGS40 for $\delta^{15}\text{N}$). Results of $\delta^{13}\text{C}$ and $\delta^{15}\text{N}$ were given in the conventional delta notation, i.e., versus Vienna Pee Dee Belemnite for carbon and versus atmospheric air for nitrogen as parts per thousand (‰) according to the following equation:

$$\delta X (\text{‰}) = \left[\frac{R_{\text{sample}}}{R_{\text{standard}}} - 1 \right] \times 1000$$

where: X is the stable isotope ratio of $\delta^{13}\text{C}$ and $\delta^{15}\text{N}$; R is the ratio of $^{13}\text{C}/^{12}\text{C}$ or $^{15}\text{N}/^{14}\text{N}$. The measurement precision was better than 0.20‰ for $\delta^{13}\text{C}$ and 0.18‰ for $\delta^{15}\text{N}$ (n= 5) (Kuliński et al., 2014). The isotopic composition is given as additional information in the appendix (Table A 8 to Table A 13).

3 Results

3.1 Beach wrack amounts

To gain a better insight into the variability of beach wrack landings, two beaches with contrasting exposition characteristics were sampled for a full vegetation period. Table 5 summarizes the results, showing the area sampled, beach wrack coverage and thickness as well as dry weights per area and sand contents. Both beaches had the same length of 100 m as chosen. Beach width varied. The average beach wrack coverage at Poel was 7% higher than in Kühlungsborn. The thickness in new wrack at both beaches was similar whereas in old wrack Poel exceeded Kühlungsborn tenfold. The dry weight of beach wrack in Poel was with 1.35 kg m^{-2} double the amount of Kühlungsborn with 0.66 kg m^{-2} . The weights of old wrack had minor differences, only. A comparison of the sand content of both sites showed that mostly more sand than beach wrack was found in the samples. Only in the new wrack of Poel, the average sand content per square meter was 0.02 lower than measured biomass. The highest content was observed at the old wrack in Kühlungsborn with 1.61 kg m^{-2} on average, exceeding Poel by 60 %.

Table 5: Beach and beach wrack characteristics found at Poel and Kühlungsborn. Beach length was given as 100 m for each sampling. Remaining values are given as average (avg.). Abbreviations: BW = beach wrack, NW = new wrack, OW = old wrack. Beach wrack coverage is given as percentage of total beach's surface. Please note difference in unity regarding beach wrack thickness.

	Poel	Kühlungsborn
beach length (m)	100.00	100.00
avg. width (m)	29.40	19.97
avg .BW coverage (%)	8.5	1.5
avg. thickness NW (cm)	2.4	2.2
avg. thickness OW (cm)	4.9	0.4
avg. dry weight NW (kg m^{-2})	1.35	0.66
avg. dry weight OW (kg m^{-2})	0.75	0.73
avg. sand content NW (kg m^{-2})	1.33	0.93
avg. sand content OW (kg m^{-2})	1.01	1.61

In Figure 10, detailed information about new and old wrack landings as well as the respective sand content is given for each sampling at Poel, sorted by month. Especially in months with low wrack landings sand content exceeded the overall sample weights, e.g. in the autumn samples more sand than beach wrack was found. This was particularly true for individual new wrack samples, for instance at the sampling on 05.11.2019 sand content was 2.28 kg m^{-2} compared to 0.82 kg m^{-2} beach wrack biomass which corresponded to more than 2.5 times sand. But with regard to the spring and summer samples, this ratio can also be reversed. On 03.06.2019 the biomass was more than five times higher, showing 3.02 kg m^{-2} compared to 0.6 kg m^{-2} sand. During the transition of the seasons the ratio was virtually balanced, having had 0.25 kg m^{-2} of wrack compared to 0.23 kg m^{-2} of sand on 20.05.2019. Proportions in the old wrack through the year were more balanced with similar amounts during individual samplings. This balance vanished in autumn where biomass to sand ratio changes in favor of sand. The highest amount of sand in an individual sample was found on 08.10.2019 where sand content was nearly four times the amount compared to biomass, with a value of 3.03 kg m^{-2} sand compared to 0.77 kg m^{-2} of wrack.

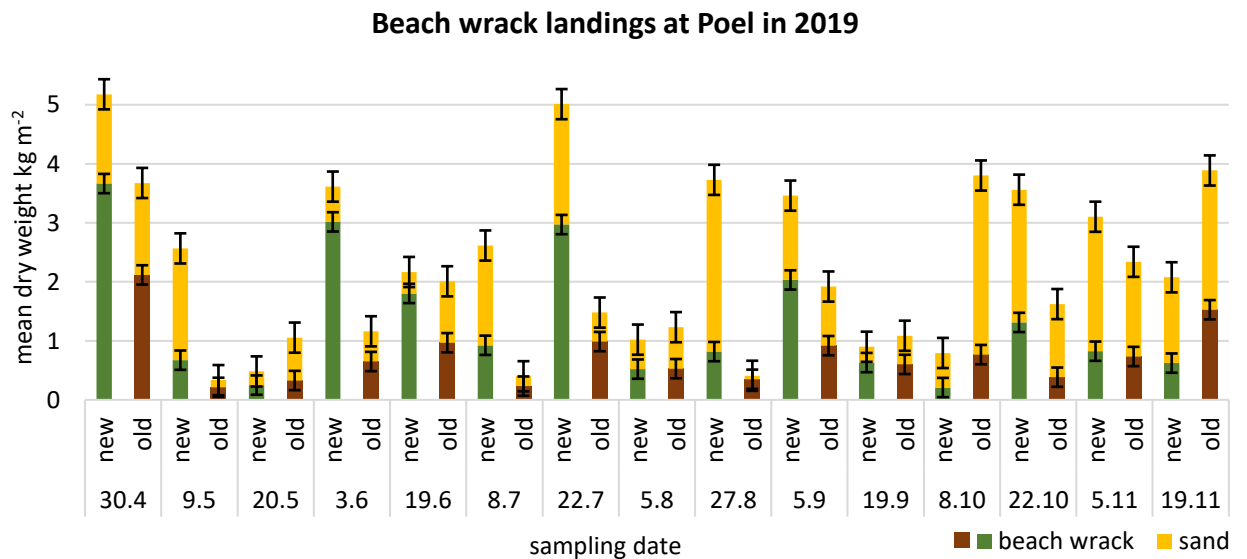


Figure 10: Beach wrack landings in 2019 at the beach "Schwarzer Busch" (Poel) with shares of new wrack (green bars) and old wrack (brown bars) with respective added sand mounts (yellow bars). All values are given in mean dry weight kg m^{-2} on y-axis, x-axis including sampling dates and wrack status (\pm SE, $n=3$).

The results showed that Poel had more beach wrack landings than Kühlungsborn. Moreover, as shown in Figure 11, distinguishing between old and new beach wrack, Kühlungsborn rarely accumulated beach wrack for long. Measurable amounts of old wrack were found only in autumn. Beach wrack landings were highest in autumn where the only old wrack occurred. In autumn old wrack had a median of 0.99 kg m^{-2} representing roughly a more than five times higher value than new wrack with 0.16 kg m^{-2} . Spring's amount of new wrack was 0.41 kg m^{-2} . In summer average amounts were double compared to spring with 0.87 kg m^{-2} . Values for Poel always exceeded the values for Kühlungsborn except for the old wrack amounts in autumn. High dynamics in both wrack amounts were seen. Starting with average 0.33 kg m^{-2} old wrack in spring it was half the amount of new wrack with 0.67 kg m^{-2} . Summer had highest amounts of beach wrack, showing a median value of 0.59 kg m^{-2} for old, and a more than double that amount of 1.36 kg m^{-2} for new wrack. Similar amounts were shown with 0.75 kg m^{-2} in old wrack and 0.73 kg m^{-2} in new wrack during autumn, respectively.

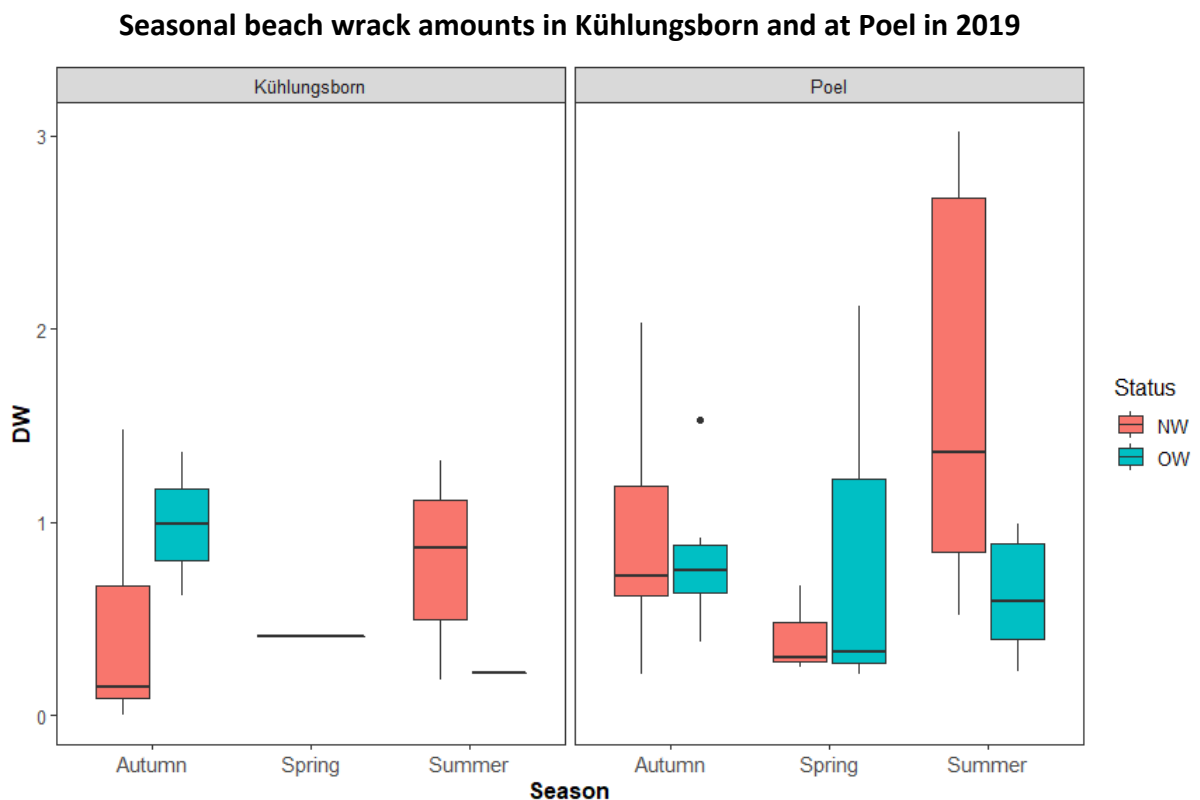


Figure 11: Beach wrack amounts between April 2019 and November 2019 in Kühlungsborn and at Poel. Amounts given cumulated for each season (x-axis), with dry weight (DW) given in kg m^{-2} (y-axis). NW = new wrack (red), OW = old wrack (turquoise, both \pm SD). For definition of seasonal time frames please refer to Table 2.

3.2 Species composition

Species composition was studied to follow up on e.g., possible seasonal patterns. As not every specimen could be identified anymore (e.g., too degraded, small fragment size, missing identification characteristics), for statistical evaluation, species were categorized into four large groups: angiosperms, chlorophytes, phaeophytes and rhodophytes. Simultaneously differences at the two beaches were traced. Between new and old wrack there are species composition differences: in spring there is no old wrack at all whereas in summer and autumn old wrack in Kühlungsborn is dominated by seagrass. In autumn a quarter of the old wrack is a mixture of red, brown and green algae. Most of old wrack were red algae. The seasonality of new beach wrack was dominated by red algae in summer, with a co-dominance of green algae in spring, reflecting the algae's vegetation periods. In autumn a proportion of red algae was still present, but new beach wrack was here, like old wrack, dominated by seagrass (Figure 12).

Compared with Kühlungsborn, in Poel seagrass was dominant throughout the whole year, with variations in the algal proportions (Figure 13). New beach wrack at Poel was composed of 73.3 % of angiosperms, 14.3 % of red, 7 % of green and 5.6 % of brown algae (Figure 13). In spring the species composition is the richest. Rhodophytes are co-dominant but still represent only half of the amount of eelgrass. Chlorophytes and Phaeophytes equal the amount of Rhodophytes. All algae combined make up about the same amount as seagrass.

Beach wrack species composition at Kühlungsborn

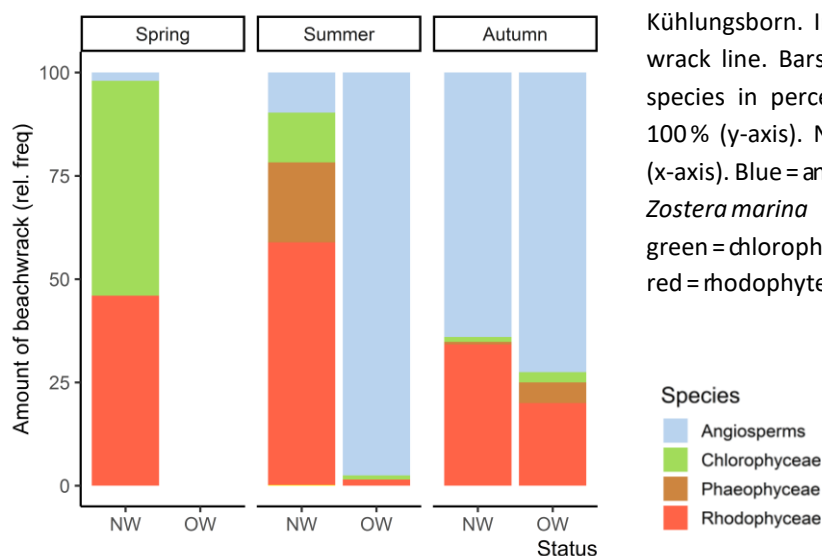


Figure 12: Beach wrack species composition at Kühlungsborn. In spring, there has been no old wrack line. Bars display relative abundance per species in percentage, calculated to a total of 100 % (y-axis). NW = new wrack, OW = old wrack (x-axis). Blue = angiosperms (consisting of seagrass *Zostera marina* only in this data collection), green = chlorophytes, brown = phaeophytes, red = rhodophytes.

The percentage of red algae varies by 2 % only between summer and autumn compared to 15 % from spring. New and old wrack show similar proportions in species composition of macrophytes. From summer onwards, seagrass takes over and remains dominant for the rest of the year. Angiosperms, namely eelgrass, has a share of 78.6 %, red algae a mean of 12 %, green algae 5 % and brown algae show 4.3 %. Old beach wrack at Poel shows similarities to the new wrack (Figure 13). New wrack in both seasons contains green and brown algae whereas in the old wrack of summer only green algae are left. Both in summer and autumn, the proportion of red algae show a similar pattern in quantity proportion.

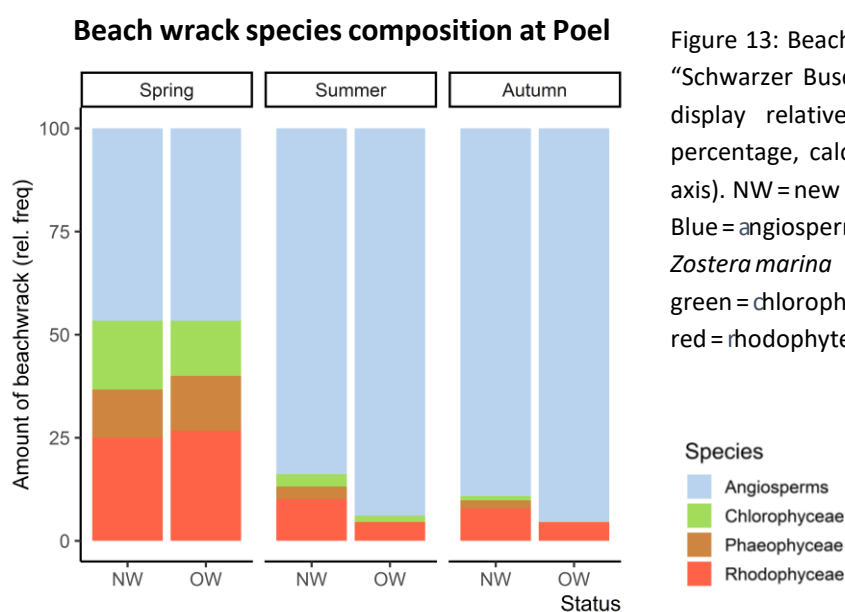


Figure 13: Beach wrack species composition at “Schwarzer Busch” at the Island of Poel. Bars display relative abundance per species in percentage, calculated to a total of 100% (y-axis). NW = new wrack, OW = old wrack (x-axis). Blue = angiosperms (consisting of seagrass *Zostera marina* only in this data collection), green = chlorophytes, brown = phaeophytes, red = rhodophytes.

Beach wrack landings in Kühlungsborn (Figure 14) are very low compared to Poel (Figure 15). This is because Poel is located in the Wismar Bay, and once trapped macrophyte biomass is enclosed in this sheltered area. Removal only happens during storm and high-water events. Kühlungsborn with the exposed coastline towards the open Baltic Sea has higher dynamics in wrack landings and ablation. Landings are lower in biomass, and species richness is more influenced by abiotic parameter like e.g., wind direction, wave flow direction and water level changes. Seagrass drifts from meadows nearby and is washed ashore with favorable wind and current conditions towards the beach.



Figure 14: Unmanaged beach of Kühlungsborn at 19.06.2019. Beach transect=100 m length, varying beach width. On the left, between the pillars, the so called “Riedenbach” and its estuary can be seen. Low beach wrack amounts lie at the beach, more macrophytes can be seen in the shallow water (bottom of picture). The shore is sandy at the beach and rockier in the shallow adjacent water.



Figure 15: Unmanaged beach of Poel, beach “Schwarzer Busch” at 19.06.2019. Beach transect = 100 m length, varying beach width. On the left the last groin separates the managed (left of groin) to the unmanaged (right of groin) beach section. Between the two wrack lines new (splash zone) and old wrack (second line, towards the dry zone of the beach) can be distinguished on the beach. Behind the old wrack line tire track of the management vehicles can be seen. Shore and shallow water are both sandy.

3.3 Decay on land

The experiment runtime of the decomposition of litterbag content on land was between 13.09.2019 and 14.09.2020 (Figure 16). Sampling was executed after 1, 2, 4, 6, 8 and 12 months. Litterbag dry weight on the surface did not change within the first month (5.73 g vs. 5.84 g, difference at 0.11 g). Buried bags gained weight (5.47 g) through sand adherence to the content. Filling of the litterbags consisted of the filamentous, fine-branched *Ceramium* spp. It was not possible to remove sand completely: due to the fragility of the algae it was not reasonable to wash the bags as too much of the remaining biomass would have been lost. Therefore, samples were first dried and afterwards de-sanded by sieving over a 1 mm sieve. This was applied for both samples, buried and surface. During the first half year till March 2020 was only weight gain in both treatments (Figure 16). They reached their respective highest weight through the run time of the experiment (surface: 16.2 g; buried: 15.1 g). After eight months, in May 2020, there was a drop in weight within the buried bags, and the initial weight (6.71 g) was regained (6.46 g). From here on the weight of the buried bags remained nearly stable (after 12 months: 7.17 g). The surface bags lost weight until the final retrieval (6.98 g). The surface bags had a stable increase for the first 6 months whereas the buried bags had constantly fluctuating weights (Figure 16 and Table A 1 in the appendix), but did not show statistically significant differences (Pearson-correlation; $p=0.46$).

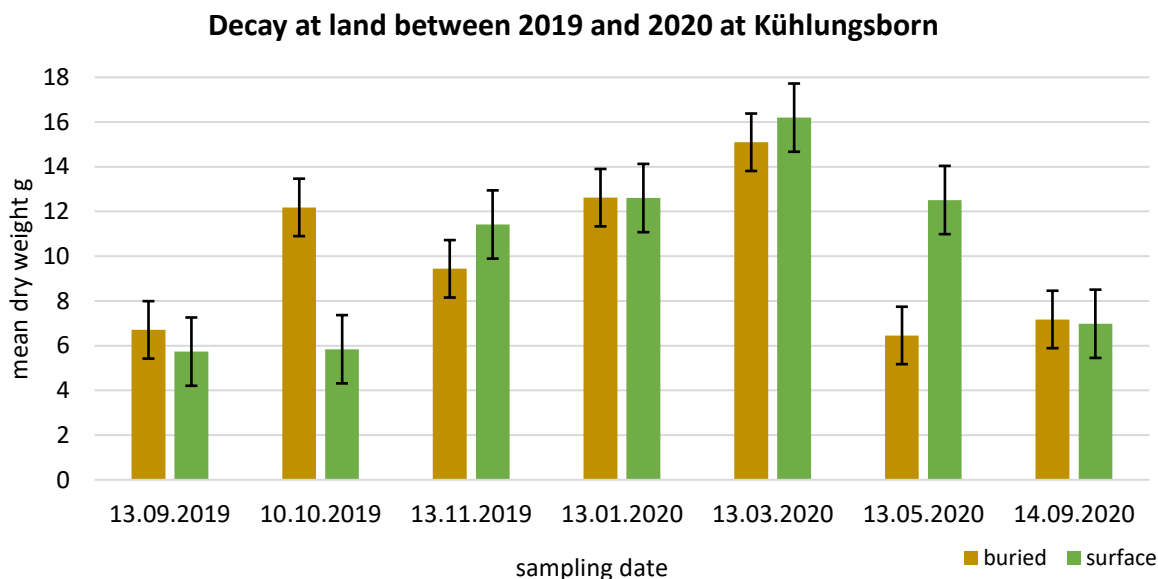


Figure 16: Decay of beach wrack in litterbags over the course of one year. Installation was done in September 2019, sampling was executed after 1, 2 and 4 months (year 2019), and after 6, 8 and 12 months (year 2020). Half of litterbags were buried in approx. 10cm depth (brown), another half laid at the surface (green). Experiment site was in Warnemünde at the back of the beach without exposure to water and waves in the measuring field from the DWD ((Deutscher Wetterdienst, German Weather Service; fenced area, Figure 5); x-axis sampling dates, y-axis mean dry weight in g; \pm SE, $n=3$).

Organic matter contents (OMC) of sediments underneath the litterbags and within the surrounding area were additionally taken (Figure 17). They did show differences over time. OMC underneath the buried bags was higher (0.504 %) than the content underneath the bags on the surface (0.304 %) at the beginning and for the retrieval (buried: 0.481 %; surface: 0.436 %). OMC is fluctuating over time. After four months contents between surface and buried bags are same (surface: 0.398 %, buried: 0.399 %), with higher amounts of organic material underneath the buried bags between month six and eight. At the final sampling after 12 months the highest content is present under the buried bags (0.481 %). Sediments from the bare sand showed low values between 0.174 % (after 6 months) and 0.375 % (after 12 months), exceeding the surface sediments only in the first (0.329 %) and second month (0.312 %).

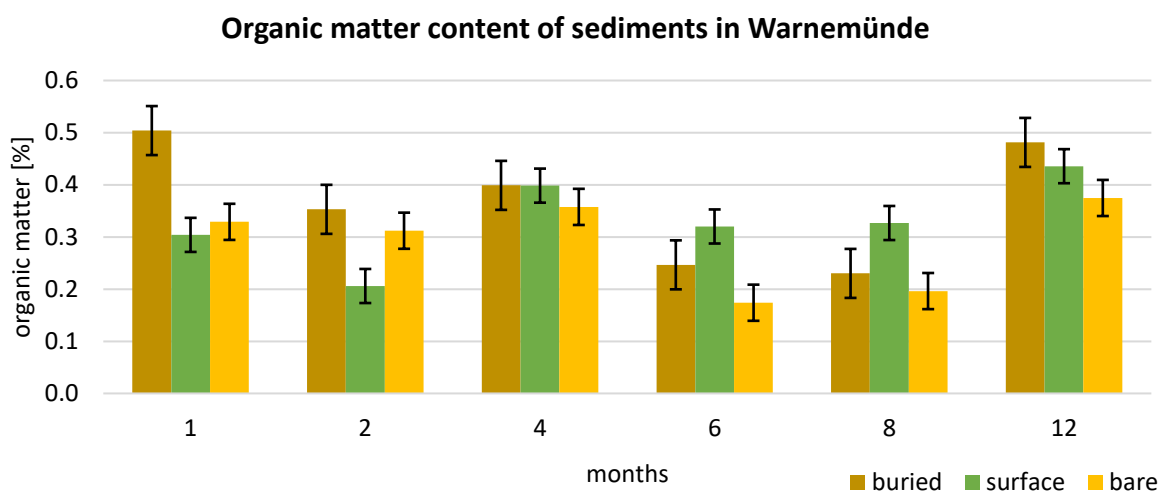


Figure 17: Organic matter content of sediment samples taken underneath and besides the litterbags in Warnemünde. Values are given in chronological order: (ranging from left to right) after 1, 2 and 4 months (year 2019), and after 6, 8 and 12 months (year 2020). Brown = organic matter content in sediment underneath buried bags, green = underneath surface bags and yellow = within bare sand aside, all in % (x-axis sampling month, y-axis organic matter of sediments in %, \pm SE, $n = 3$).

For statistical evaluation regression analyses for each treatment were done. As organic matter contents kept changing over time, a polynomial trend line was chosen. The resulting coefficient of determination (R^2) is an important component to evaluate the goodness of the prediction of the model, and denotes the degree to which a model can explain the real data. The higher the value, the better the model can explain the real observations. Lowest R^2 is present in the bare sand ($R^2 = 0.2946$), indicating a very low relationship here between organic matter in bare sand over time. Surface bags showed a R^2 of 0.4284, and buried bags a R^2 of 0.6441 which points towards a low predictive power of this model and the need to search for other variables as explanatory factors for changes in OMC.

3.4 Decay under water

The experiment starting in summer (SE20) showed an initial increase in weight, with a peak after 28 days (Figure 18). Dry weights within the replicates ranged between 3.69 g and a maximum of 6.83 g, with a mean of 4.68 g. Weights after 21 and 42 days were similar, with a mean of 2.36 g after 21 days and 2.28 g after 42 days. Between days 56 and 84 weights decreased from 0.93 g (mean value, 56 days) to a minimum of 0.14 g (84 days). From 84 days to 98 days weights almost doubled to 0.27 g, and had five times the weight (1.49 g) after 112 days. The last two samplings after 140 and 210 days did not show differences (0.22 g after 140 days vs. 0.21 g after 210 days; mean values). At the final retrieval after 210 days a lot of sand was within the litterbags which was washed out as well as possible. Nevertheless, remaining contamination with extra sand cannot be excluded. As the samples were rotten and not in leaf-form anymore, subsamples of the homogenized rest were taken, with a mean weight of 9.8 mg. The winter experiment (WE21, Figure 18) had almost stable weights for the first 42 days; mean values were 1.53 g after 7 days, 1.50 g after 14 days, 1.59 g after 21 days, 1.62 g after 28 days and 1.54 g after 42 days. After 56 days there was an increase to 1.87 g, followed by a drop to 1.24 g (70 days). With values at 1.48 g after 84 days, there was another weight gain to 1.72 g till 98 days. After 112 days, almost the same amount of seagrass was left in the bags (1.16 g) as after 70 days. In the following 28 days weights increased to 1.94 g after 140 days, reaching a higher amount than after 56 days. For the last sampling after 210 days, there was only 0.59 g of biomass left in the bags. An overview of decay coefficients $k \text{ d}^{-1}$ is given in Figure 19.

Chronological image documentation of the rotting seagrass within the litterbags in the respective experiment is given in Figure 20. In some cases, seagrass was too rotten to be sampled regularly (e.g., see Figure 20, t_{12} , 13.01.2021). The sampling method was adjusted accordingly. A full table with remaining dry weights of litterbag contents at each sampling point is given in Table A 5 in the appendix.

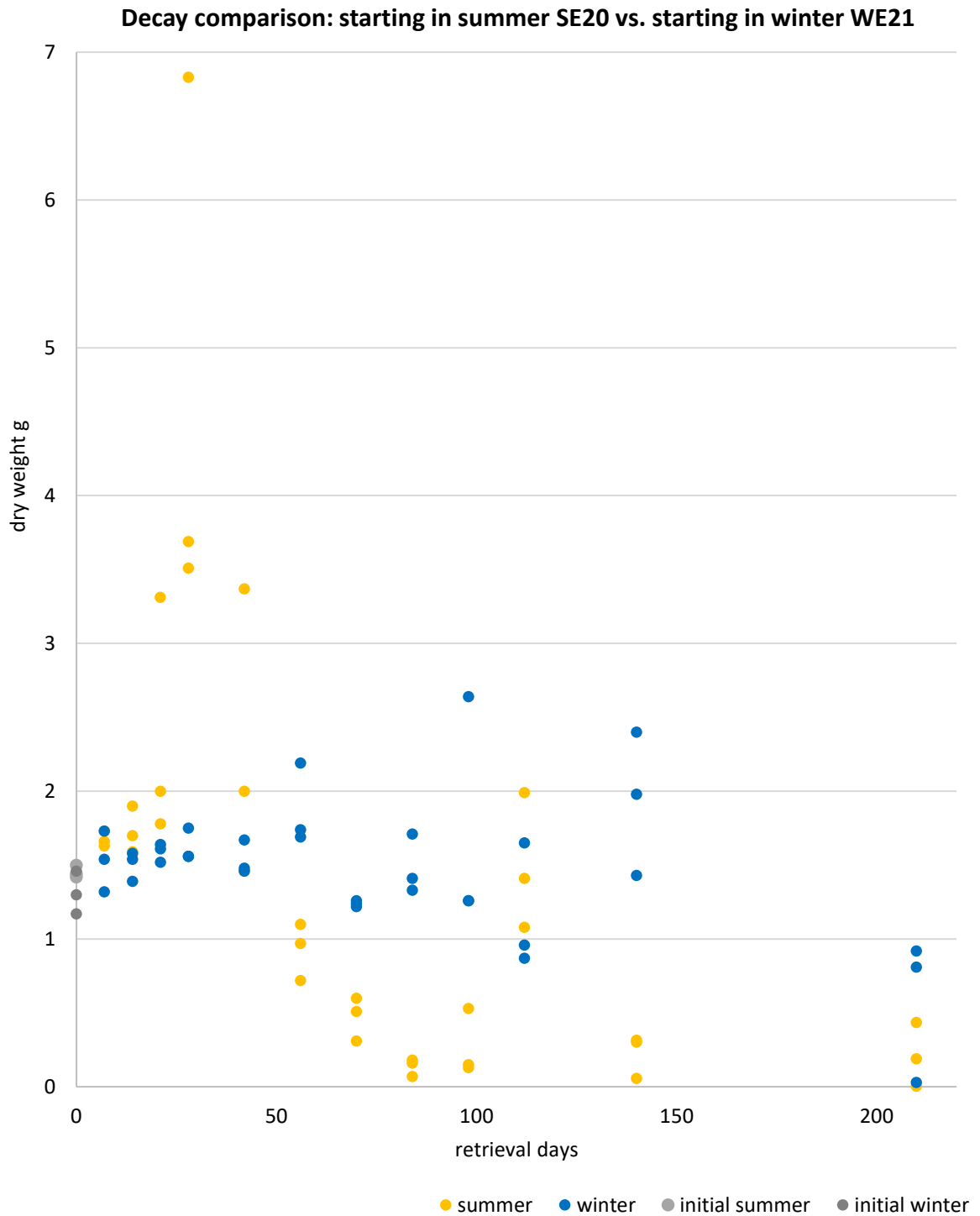


Figure 18: Decay of seagrass litterbags being constantly exposed to water. Given are remaining dry weights in grams after indicated days on x-axis. The two different approaches are labeled in yellow (starting in summer 2020, SE20) and blue (starting in winter 2021, WE21) dots. Light grey dots mark initial bag dry weight for summer, dark grey for winter experiment (x-axis retrieval days, y-axis dry weight in g, n = 3).

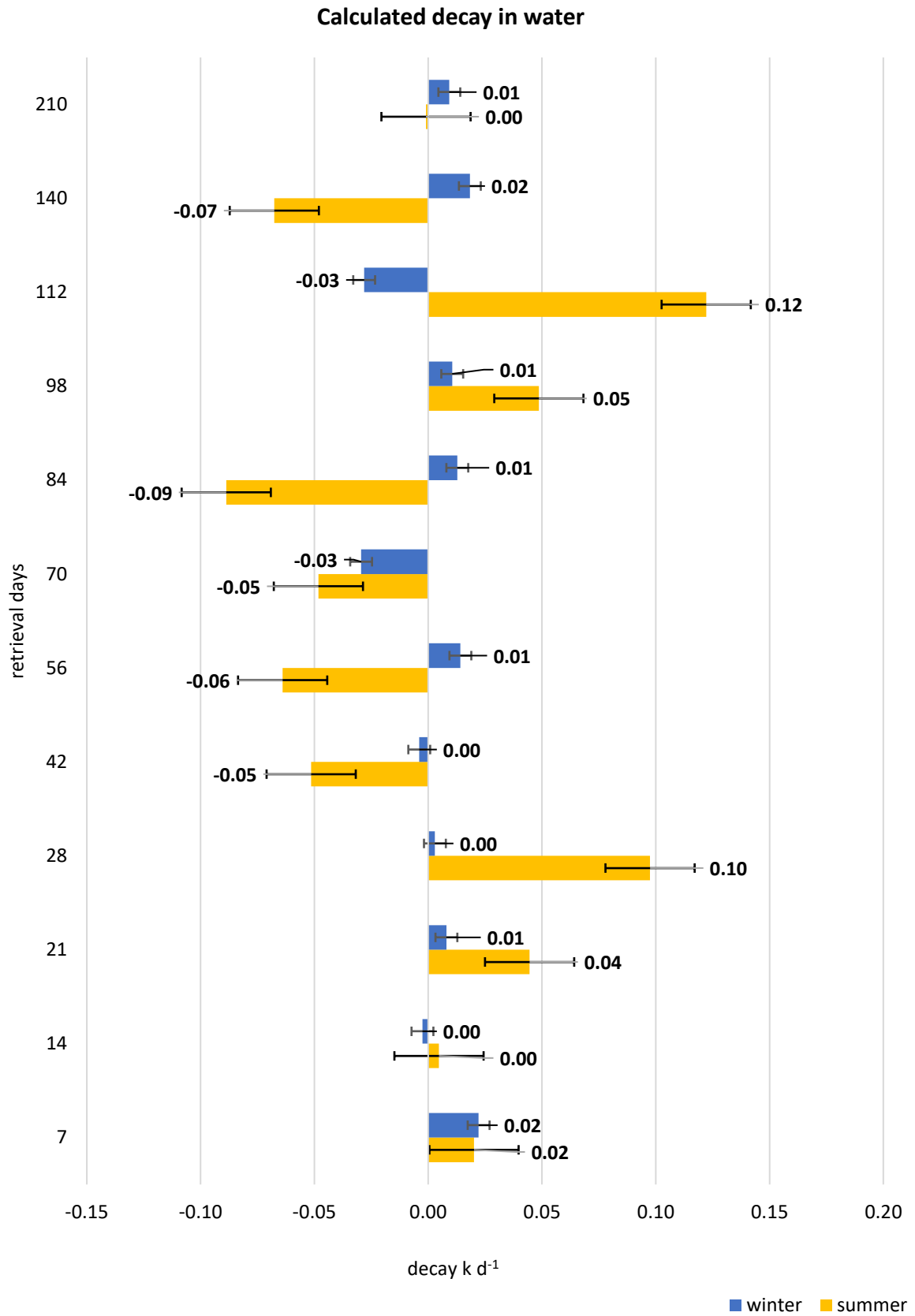


Figure 19: Weight loss given as decay: $k \text{ d}^{-1}$ in the x-axis; yellow=experiment starting in summer (SE20), blue=experiment starting in winter (WE21; y-axis retrieval days, \pm SE, $n=3$).

Summer Cycle 2020
Starting at 17.06.2020



t_1 - 7 days; 24.06.2020



t_2 - 14 days; 01.07.2020



t_3 - 21 days; 08.07.2020



t_4 - 28 days; 15.07.2020



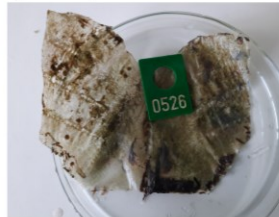
t_5 - 42 days; 29.07.2020



t_6 - 56 days; 12.08.2020



t_7 - 70 days; 26.08.2020



t_8 - 84 days; 09.09.2020



t_9 - 98 days; 23.09.2020



t_{10} - 112 days; 07.10.2020



t_{11} - 140 days; 04.11.2020



t_{12} - 210 days; 13.01.2021

Winter Cycle 2021
Starting at 03.02.2021



t_1 - 7 days; 10.02.2021



t_2 - 14 days; 17.02.2021



t_3 - 21 days; 24.02.2021



t_4 - 28 days; 03.03.2021



t_5 - 42 days; 17.03.2021



t_6 - 56 days; 31.03.2021



t_7 - 70 days; 14.04.2021



t_8 - 84 days; 28.04.2021



t_9 - 98 days; 12.05.2021



t_{10} - 112 days; 26.05.2021



t_{11} - 140 days; 23.06.2021



t_{12} - 210 days; 01.09.2021

Figure 20: Experiments with constant exposure to water. Left two columns represent decay starting in summer (17.06.2020, SE20), right two columns starting in winter (02.02.2021, WE21). Initial t_0 and final t_{13} are not shown; initial sample has not been packed in litterbags and final sample has been nearly empty with very few contents being left due to almost complete decomposition.

3.5 Abiotic parameters

In order to better understand variations in decay and microbial community, the abiotic parameters, temperature, light availability and C:N ratio and conductivity were measured continuously during all experiments. Conductivity varied during all of the experiment's runtime between approx. 10 mS cm^{-1} and 20 mS cm^{-1} (Figure 21). There are some drop-downs (approx. 0 mS cm^{-1}) during the experiment which might indicate dates where the experiment had fallen dry at low water (this was observed only one time by visual inspection at 01.07.2020), or heavy rain diluted the average salinity in the shallow waters around Poel. Additionally, the loggers had some malfunctions, where they did not record values. By running two loggers in parallel, this malfunction was reduced to a minimum. Still, some values are not available.

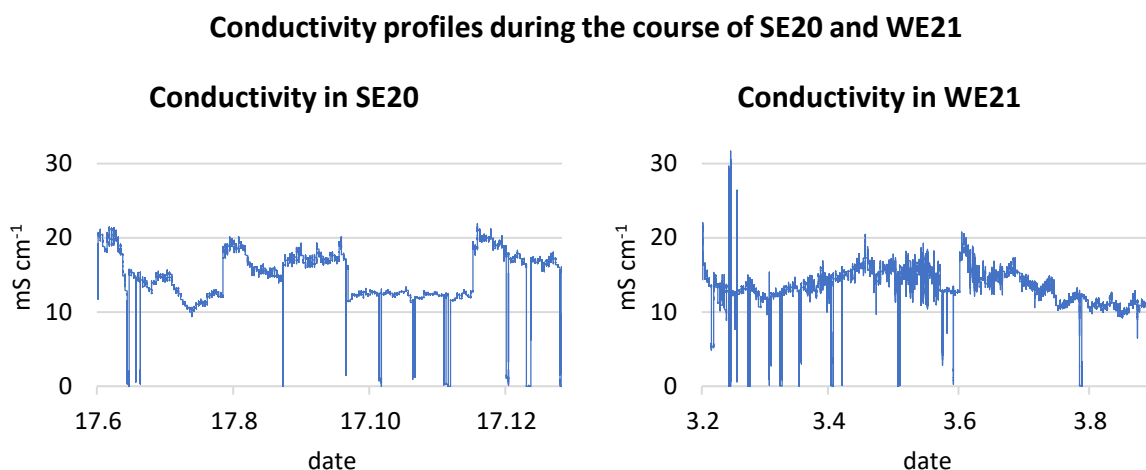


Figure 21: Conductivity profile given in mS cm^{-1} during the complete run-time of experiments. Left graphic representing values for experiment that started in summer 2020 (SE20), and right graphic showing conductivity values for experiment starting in winter 2021 (WE21). As seasonal experiments were taken out of the water every second week, this conductivity profile represents values for all experiments (x-axes respective date, y-axes conductivity in mS cm^{-1}).

In the first experiment (starting in summer 2020, SE20), minimum conductivity was at 0 mS cm^{-1} and maximum at 21.87 mS cm^{-1} . Mean conductivity was at 13.67 mS cm^{-1} . Temperatures ranged from a minimum of $1.6 \text{ }^\circ\text{C}$ to a maximum of $28.1 \text{ }^\circ\text{C}$, with a mean temperature of $14.6 \text{ }^\circ\text{C}$ through the experiment's runtime. In the second experiment (starting in winter 2021, WE21), minimum conductivity was at 0 mS cm^{-1} and maximum at 31.69 mS cm^{-1} . Mean conductivity was at 13.29 mS cm^{-1} . Temperatures ranged from a minimum of $-2.3 \text{ }^\circ\text{C}$ to a maximum of $27.4 \text{ }^\circ\text{C}$, with a mean temperature of $11.9 \text{ }^\circ\text{C}$ through the experiment's runtime. These temperature values are valid for the water only.

Table 6: Table of associated Eigenvalues and Eigenvectors of previous PCA (Figure 22) of abiotic factors.

Principal Component Analysis				
<i>Eigenvalues</i>				
PC	Eigenvalues	%Variation	Cum.%Variation	
1	2.13	53.4	53.4	
2	1.04	26.0	79.4	
3	0.518	13.0	92.3	
4	0.308	7.7	100.0	
<i>Eigenvectors</i>				
Variable	PC1	PC2	PC3	PC4
light	-0.576	0.052	0.351	0.736
conductivity	-0.220	-0.933	0.200	-0.202
temperature	-0.555	-0.040	-0.830	-0.035
C:N ratio	-0.559	0.353	0.384	-0.645

Furthermore, non-metric Multi-Dimensional Scaling (nMDS) was done to visualize the similarity level of individual samplings during the experiments (Figure 23).

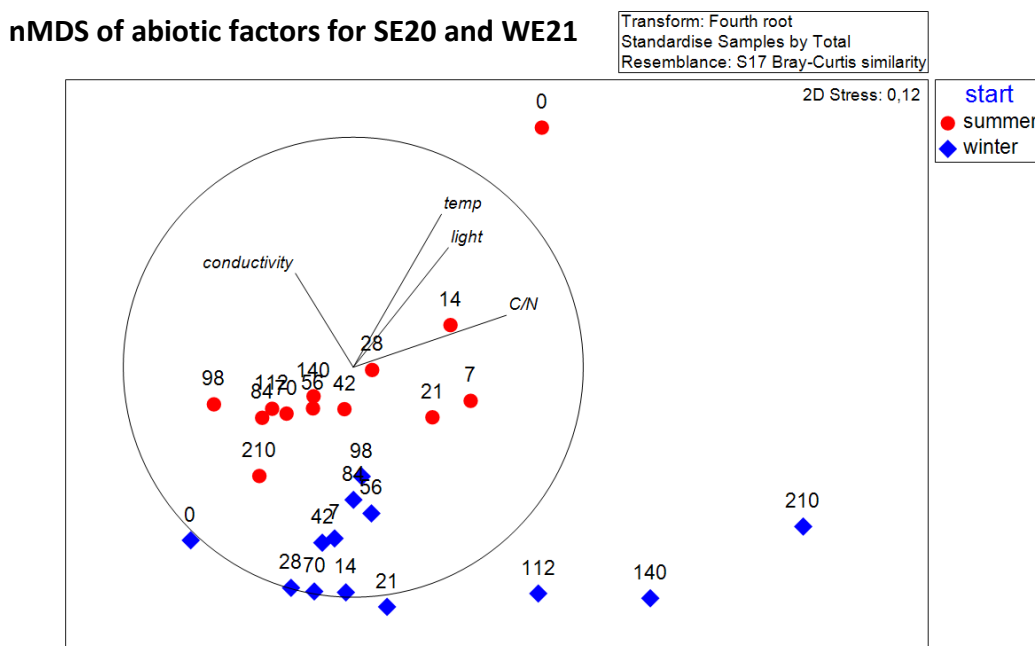


Figure 23: Non-metric multidimensional scaling of abiotic factors during the two consecutive 210 days experiments. Pretreatments: transformation to fourth root, standardizing samples by total and calculating resemblance to Bray-Curtis similarity. Red dots = start in summer (SE20), blue rhombs = start in winter (WE21). Small numbers next to the symbols indicate sampling after respective days. Parameters: light, temperature, conductivity and C:N ratio. Points closer together are more similar than those further apart.

In a nMDS, a two-dimensional configuration is calculated, grouping similar objects close to another. In contrast to PCA, the MDS plot shows a clear separation of the two experiments. Summer and winter run vice versa, as, just like in the previous analysis, e.g. sample 0 (blue) in winter was collected at 10.02.2021 and sample 210 (red) from summer at 13.01.2021. This is confirmed by the following cluster analysis (Figure 24). The C:N ratio explains the variability within the individual experiments; the axis of C:N runs through SE20 more or less horizontal and separates WE21. Samples with a collection in a similar time of the year group together, whereas samples in different seasons or times of the year spread apart. Similarities within the two experiments group around related sampling dates or time periods. The grouping in the final samplings during the winter experiments are clearer than the last samples in the summer experiments; here, the grouping is torn apart, and different time points match better than in chronological order.

A final statistic test was done, using a cluster analysis for the two experiments. In a cluster analysis similar objects are put together depending on their properties. The result of the cluster analysis is shown in Figure 24.

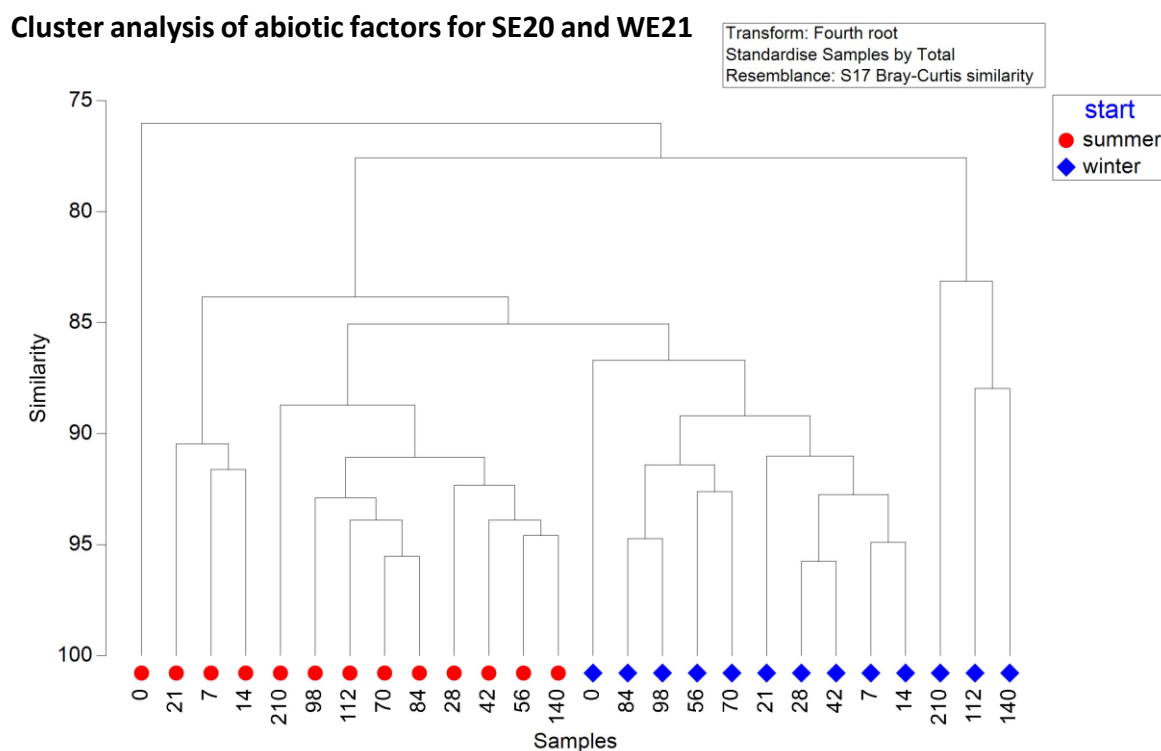


Figure 24: Cluster analysis, comparing samples with their respective similarities. Pre-treatment: transformation of fourth root, standardizing samples by total and creating resemblance matrix by S17 Bray-Curtis similarity. Red dots = samples from SE20, blue rhombs = WE21; x-axis showing samples and y-axis showing similarity in %.

The cluster analysis clearly supports the results of the PCA: the whole data collection of abiotic factors split into the two experiments: data for the experiment starting in summer group as well as data for the experiment starting in winter group, respectively. As the experiments were conducted one after the other, the last samplings from the winter experiment are in a similar time of the year as the first values from the summer experiment. The only value not assignable is the initial dataset for the summer experiment.

As the seasonal experiments were performed in different colored litterbags to identify the influence of light availability during decay, the corresponding light and temperature values were logged (Figure 25). Loggers were fixed to the litterbag cage, and moved from water to land and vice versa like the litterbags every week.

Light and temperature show seasonal variations (Figure 25). The scale for temperature and light had to be changed in the winter and spring experiment (Figure 25c and d) due to negative temperature values. Lower light conditions required an adapted scale for the light availability in the winter experiment (Figure 25c). Values represent anticipated results for annual readings. The highest light availability was given in summer, with 330,668.9 Lux on 08.08.2020 at 9:40 am for plain light, and with 99,200.7 Lux on 20.02.2021 at 11:50 am the lowest light conditions in winter. The temperature ranged between -8.4°C in winter on 09.02.2021 at 6:30 am during a land-phase and up to 48°C on 16.08.2020 at 3:20 pm in summer, again during a land-phase. Especially during land-phases the logger in black litterbags tended to heat up high through the strengthening effects of the color. Temperatures in the water were near and below 0°C on some occasions but mainly cold periods were experienced during the land-phases of the experiments.

3.6 Alternating decay

During alternating decay, litterbag weights were subject to constant fluctuations, no trends could be seen within the time frames (Table 7). In all experiments at the beginning weight was gained instead of lost. White litterbags tended to gain weight more often than black litterbags. The relatively high weight gains of the black litterbags during autumn are noticeable Decay is always very slow, and proceeds mostly during air exposure. In submerged periods, weight is gained by all litterbags. Weights decreased in general towards the end of the experiments, seemingly in need of an initial phase before decomposition started.

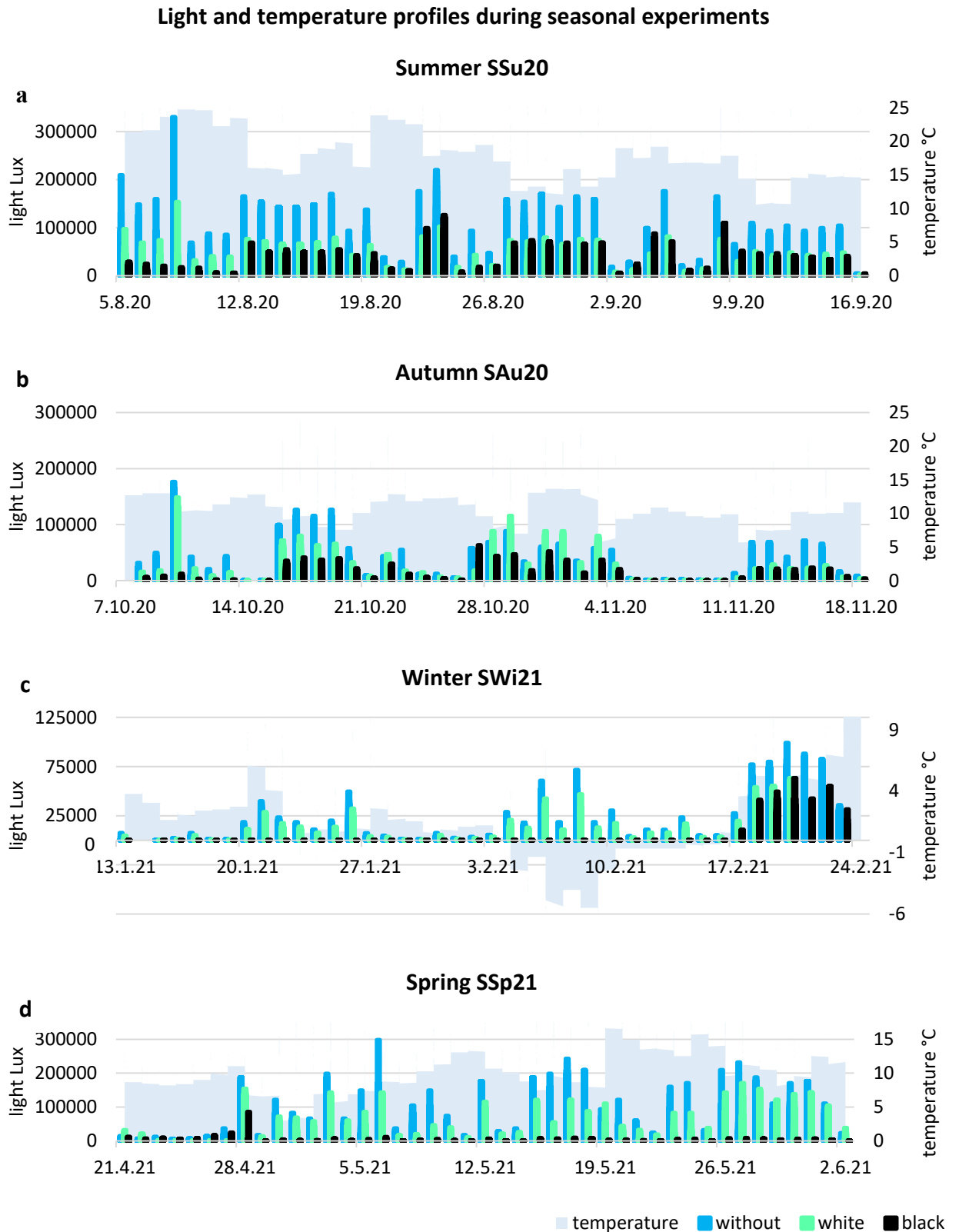


Figure 25: Seasonal values for light and temperature. Light availability is given on the first y-axis on the left in Lux. Blue columns show logged values for logger without any coverage, green columns show values in white bags and black columns in black bags (as given in Figure 7 for light transmission percentage). Light blue background displays temperature, with the scale on the second (right) y-axis, x-axis giving respective dates, a) and b) in 2020, c) and d) in 2021. Please note: due to a broad range between the seasons, it was not possible to set the same scales for the light- or temperature-axis in all graphs.

Table 7: Mean litterbag dry weights in grams through seasonal experiments, separated in white and black mesh bags respectively. Initial weight given as “start” with collected material from respective season. Start serves as reference weight for the decay during the experiment.

	Summer SSu20		Autumn SAu20		Winter SWi21		Spring SSp21	
start	1.45		1.72		1.51		1.39	
days	white	black	white	black	white	black	white	black
7	1.93	1.48	2.26	2.06	2.16	1.98	2.56	1.78
14	1.75	1.18	1.72	1.79	1.59	1.65	1.66	1.71
21	1.35	1.19	1.52	1.86	1.77	1.77	1.47	1.50
28	1.65	1.15	1.49	2.02	1.49	1.51	1.38	1.18
35	1.80	1.18	1.74	2.05	1.63	1.43	1.60	1.39
42	1.77	1.12	1.61	1.55	1.28	1.17	1.38	1.40

Litterbag decay by loss of dry weight and their respective coefficient of determination for each season are given in Figure 26. Graphs illustrate that, at the beginning of any seasonal experiment, there is weight gain before weight starts to decrease and therefore, decay sets in. The range of weight changes varies, not only between black and white and between seasons but also between the different replicates of each sampling point (data given in Table A 6 for SSu20 and SAu20, and Table A 7 for SWi21 and SSp21).

R^2 indicates that, when trying to fit a linear model, decay in black litterbags tends to follow a linear decay in summer ($R^2 = 0.42$ black vs. 0.008 white) and winter ($R^2 = 0.8$ black vs. 0.58 white), while in autumn for white litterbags ($R^2 = 0.26$ white vs. 0.08 black) no regularity can be determined. In spring there is only a minor difference ($R^2 = 0.44$ white vs. 0.39 black) so that a prediction is difficult to identify.

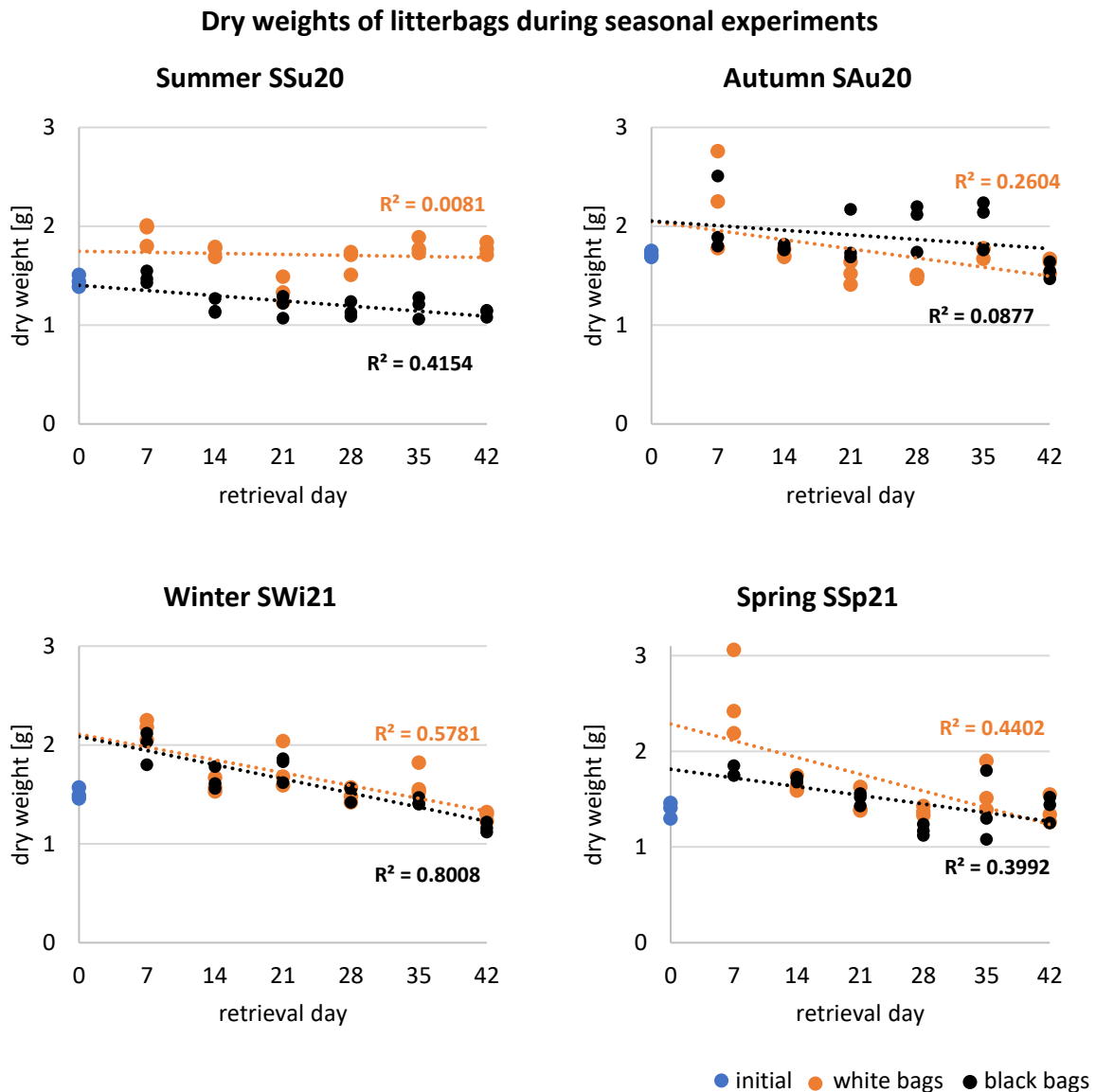


Figure 26: Seasonal decay experiments. Blue dots = initial weights, orange dots = white litterbags, black dots = black litterbags; x-axis indicating sampling points in days, and y-axis giving dry weights of litterbag contents in grams. R^2 = coefficient of determination for the respective experiment and season ($n = 3$ per treatment).

Calculating decay coefficients resulted in negative values (Table 8), indicating decay, with exception of white summer and black spring. In these experiments, weight has been gained and hence a positive coefficient is calculated. Comparing black and white litterbags proves that the decay in black litterbags was in general higher than in white litterbags. The highest decay rate is calculated for winter in black litterbags whereas in summer and white litterbags a positive decay is calculated; here, weight gain has been happening. The weight gain was high with a decay coefficient value of 0.005 d^{-1} , which is almost as high as the highest decay rate in both summer and winter within the black litterbags, having a calculated decay coefficient of -0.006 d^{-1} each.

Table 8: Decay coefficients $k \text{ d}^{-1}$ for the seasonal experiments in white and black litterbags, respectively.

	White bag $k \text{ d}^{-1}$	Black bag $k \text{ d}^{-1}$
Summer SSu20	0.005	-0.006
Autumn Sau20	-0.001	-0.002
Winter SWi21	-0.004	-0.006
Spring SSp21	-0.0001	0.0002

3.7 Microbial community kinetics during decomposition

3.7.1 Prokaryotic 16S rDNA

To gain an insight into microbial community kinetics during decomposition of litterbag content, the following different analyses were done. For better clarity graphics are split into prokaryotic 16S rDNA analysis first and followed by graphical eukaryotic 18S rDNA analyzation. In regards to seasonal analysis, microbial community is presented by phylum. To get an impression of functional microbial community kinetics next graphics are done on a class level. In a final analysis, and for species diversity determination, the microbial community is shown at genus level.

Figure 27 shows the two experiments separated by a) samples and b) seasons. The development over time runs in a similar vice versa scheme between summer and winter, with an increased proportion of *Cellulophaga*, *Maribacter* and *Methylothera* in winter. All of the aforementioned genera live primarily aerobically. In summer especially towards the end of the experiment the proportion of the Sva0996 marine group of bacteria increases, which are able to utilize organic matter (OM). In part b) of the figure it becomes clear that the proportion of *Sphingorhabdus* is higher in winter. This genus is known to contain sphingosine, known to have antifungal and antibacterial properties. The last representative genus is *Granulosicoccus*. The vast majority of microbial communities in both experiments consists of uncultured, unclassified and other bacteria, consisting of reads that do not show sufficient matches with the data base.

In Figure 28 the functional diversity is outlined. On the left, the summer experiment is shown, with Alpha- and Gamma Proteobacteria being dominant together with Bacteroidia. Planctomycetia are cooccurring with Verrucomicrobiota. In the collected material for the

experiment setup and during the initial phase Cyanobacteria are dominant, and *Campylobacter*. Towards the end of the summer experiment Acidimicrobiia start to get an increased abundance. The winter experiment shows a similar composition, only towards the end of this experiment the percentage of Desulfobulbia, Clostridia increases, with *Campylobacter* and Fibrobacteres appearing at the very end. Hence, the percentage of Acidimicrobiia and unclassified Actinobacteria run vice versa to the summer experiment.

Figure 29 shows seasonal microbial community kinetics. It can be seen that at the beginning, in summer, Alpha- and Gamma Proteobacteria are dominant in both treatments, whether black or white, with a tendency towards a more abundant expression in black litterbags. Bacteroidia develop vice versa when being exposed to aquatic or land conditions: in black litterbags they develop better under aquatic conditions whereas on land, under dry conditions, they develop better in the white litterbags. Bacilli and Cyanobacteria are present only in summer, with a preference towards white litterbags. It appears that Alpha Proteobacteria reduce by the end of the autumn experiment, giving way to and being replaced by Gamma Proteobacteria, during winter and spring. Bacteroidia are omnipresent, with a lower abundance in summer. Verrucomicrobiae show highest amounts in summer, especially in white litterbags.

For seasonal diversity Figure 30a is outlining the phylum composition by sample, while Figure 30b is showing the phylum composition by season. Proteobacteria are most abundant, with shares of Bacteroidota and Actinobacteriota through all seasons, validating the previous results. Planctomycetota are mainly present in summer, together with Cyanobacteria and Myxococcota. In winter the amount of Desulfobacterota is higher which can be explained by the fact that the litterbags towards the end of the winter experiment silted up and got buried within the sediment, most likely causing anoxic conditions.

In Figure 31 the core microbiomes both for summer (a, left) and winter (b, right) are described in heat maps. Heat maps are a form of presentation where the genera are shown in different colors, depending on their specific abundance. In this case: the darker the blue the lower the respective share, and the higher the proportion the more yellow the representation. There are differences but in both experiments the Rhodobacteraceae and Flavobacteriaceae are the most abundant.

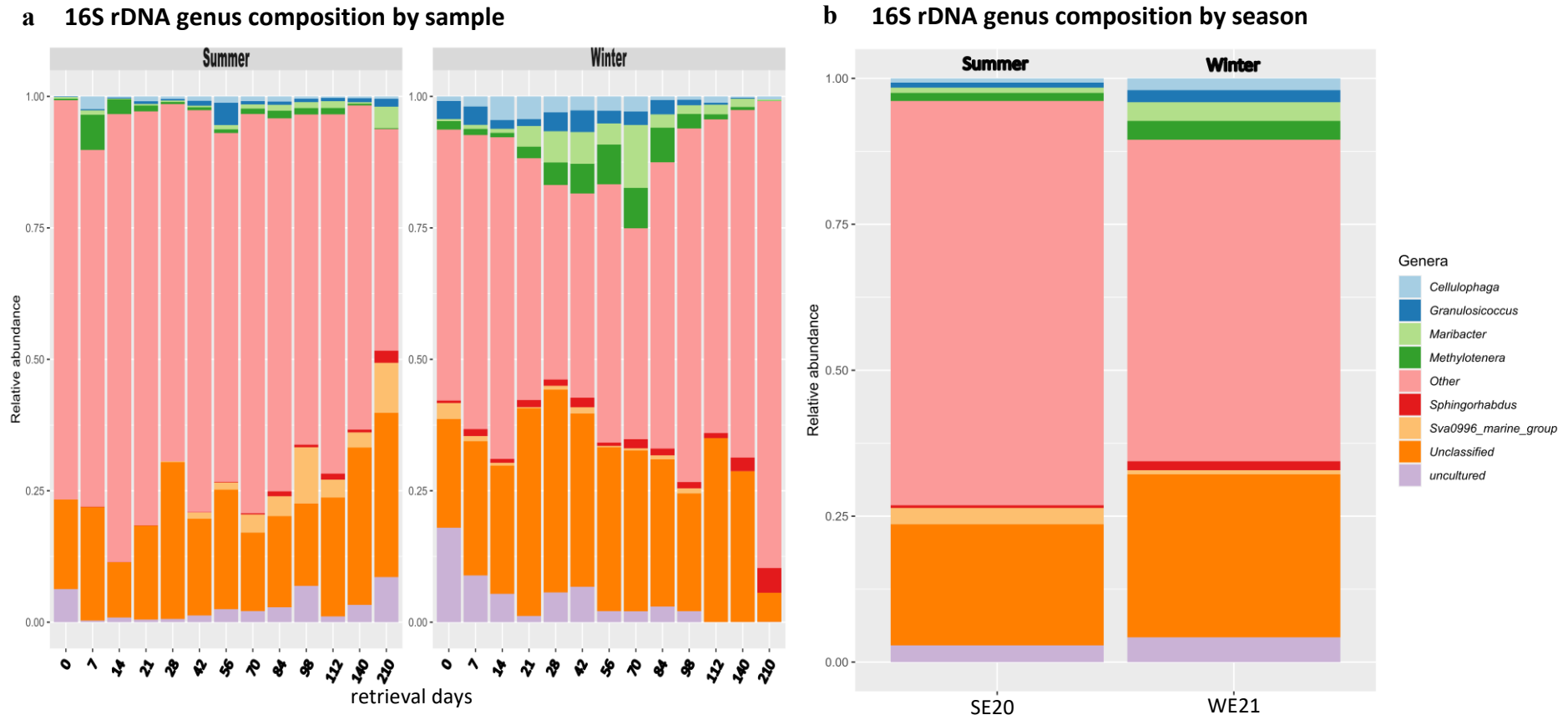


Figure 27: 16S rDNA genus composition by a) samples and b) experiment for SE20 (left) and WE21 (right). Stack bars show genus composition in relative abundance, extrapolated to a total of 1.00 equaling 100%. On the x-axis in Figure a), time points of collection of samples is shown, in Figure b) respective experiment starting point. In both graphics the two blocks are divided by experiment. A prevalence cutoff of 0.01 in 50% of the samples was used, and a detection limit of 0.6% as a classifier for the lowest possible abundant species within the samples (Graphics created by I. Barrantes, adapted).

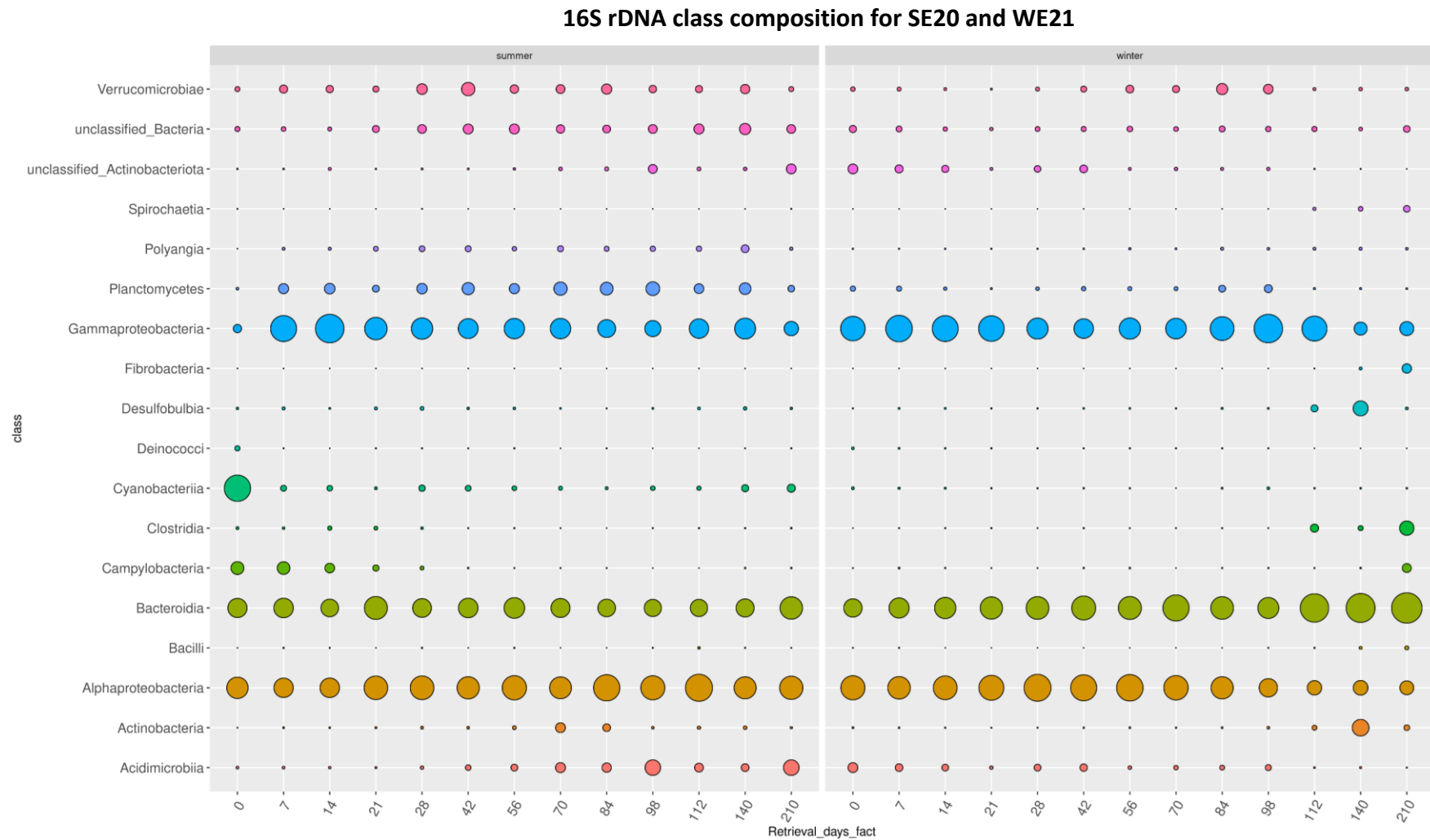


Figure 28: 16S rDNA class composition for SE20 (left half of graphic) and WE21 (right half of graphic). Bubbles represent abundance of classes, with increasing abundance along with increasing bubble size; x-axis is time line, with retrieval days given for both experiments, y-axis representing individual classes (Graphic created by K. Keszy).

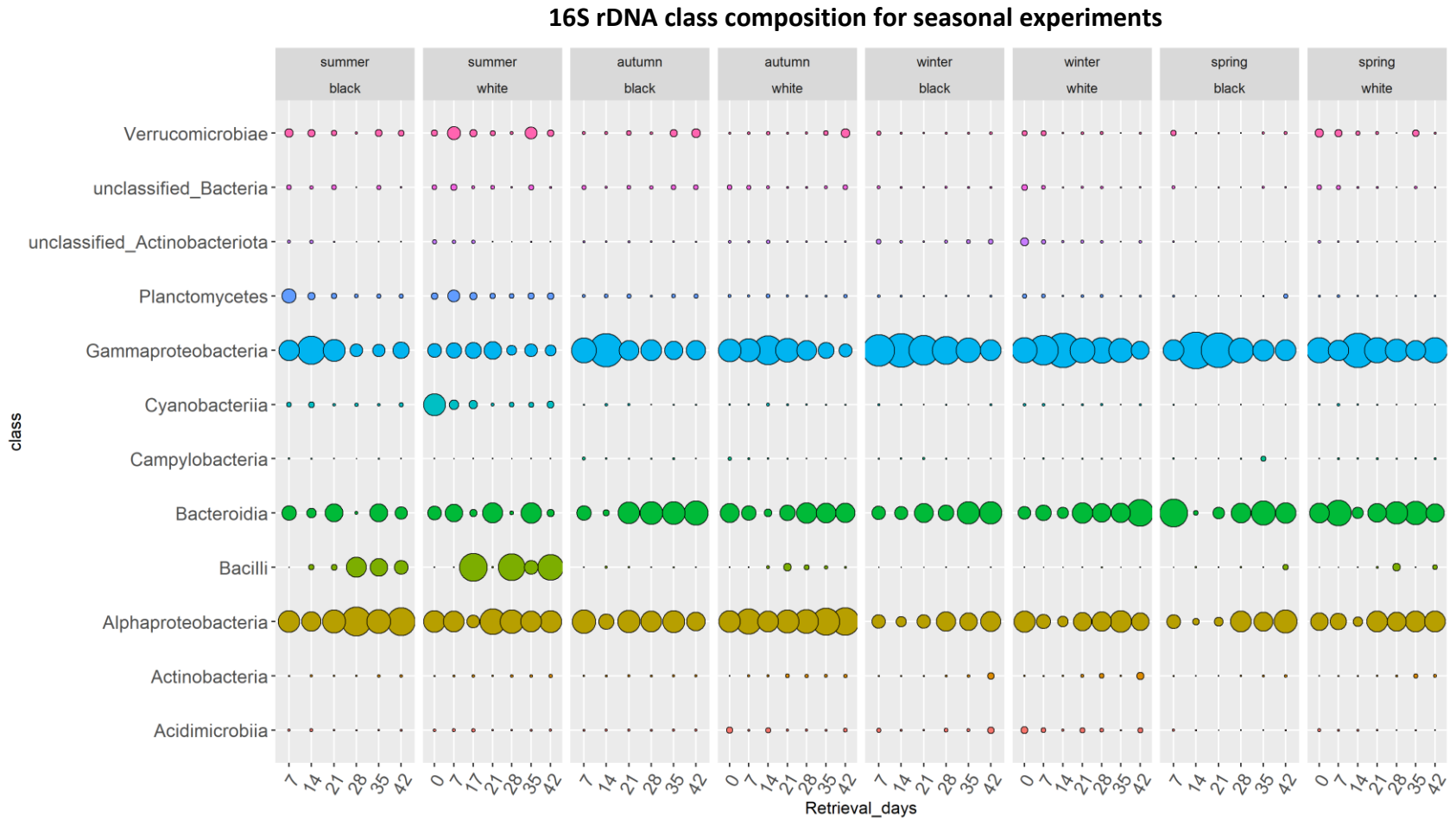


Figure 29: 16S rDNA class composition for the seasonal experiments under changing conditions (SSu20, SAu20, SWi21, SSp21, each split into black or white mesh treatment). Exposure to water and land changed weekly, starting in water (0 days) and finishing at land (42 days). Bubbles represent abundance of classes, with increasing bubble size; x-axis shows retrieval days for each seasonal experiment, y-axis representing individual classes. Additionally, results are split into black or white litterbags, respectively; please refer to headlines in each plot to distinguish. Note: initial samples have only been taken once, and are therefore, listed together with the graphs for the white litterbags – although being fresh from nature and hence not having any pre-treatment regarding light availability (Graphic created by K. Keszy).

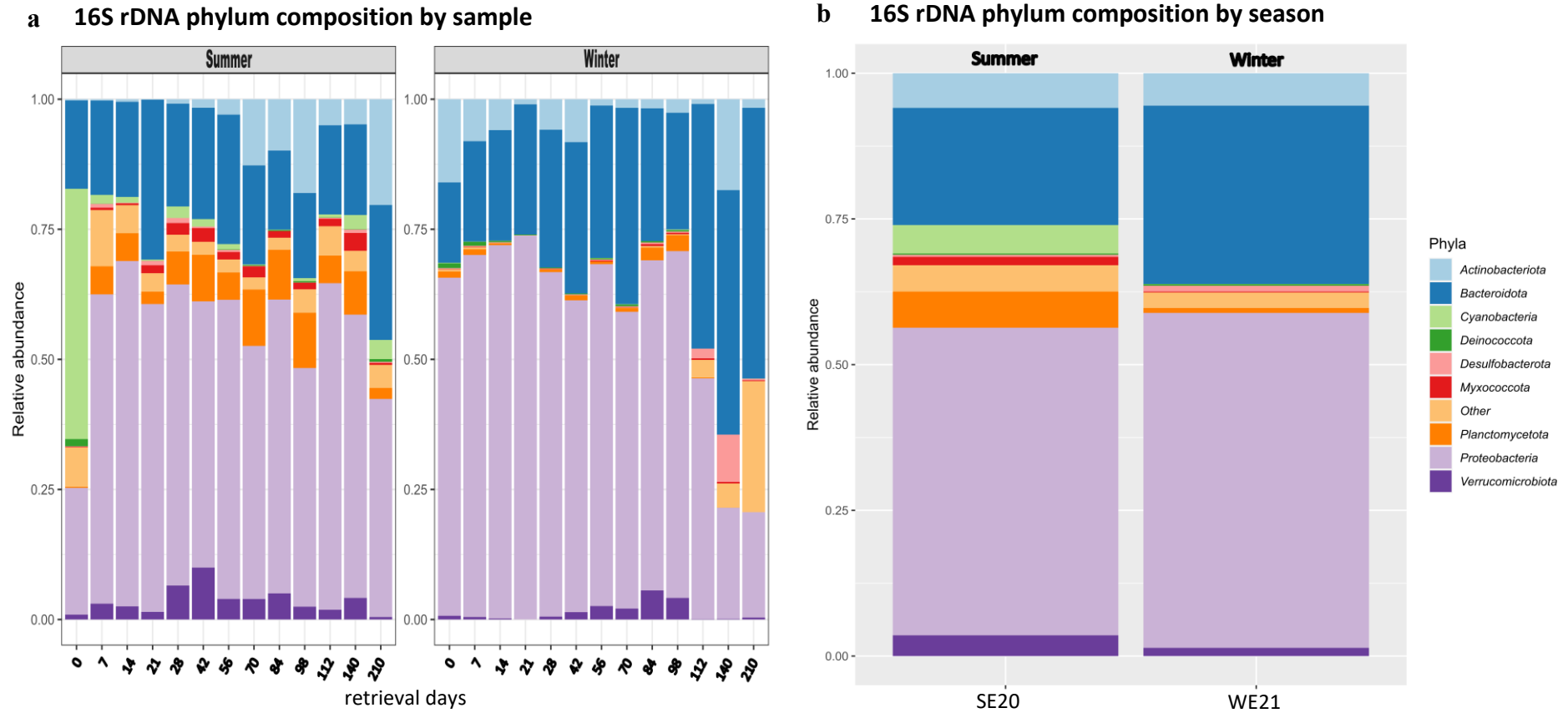


Figure 30: 16S rDNA phylum composition by a) samples and b) experiment for SE20 (left) and WE21 (right). Stack bars show genus composition in relative abundance, extrapolated to a total of 1.00 equaling 100%. On the x-axis in Figure a), time points of collection of samples is shown, in Figure b) respective experiment starting point. In both graphics the two blocks are divided by experiment. A prevalence cutoff of 0.01 in 50% of the samples was used, and a detection limit of 0.1% as a classifier for the lowest possible abundant species within the samples (Graphics created by I. Barrantes, adapted).

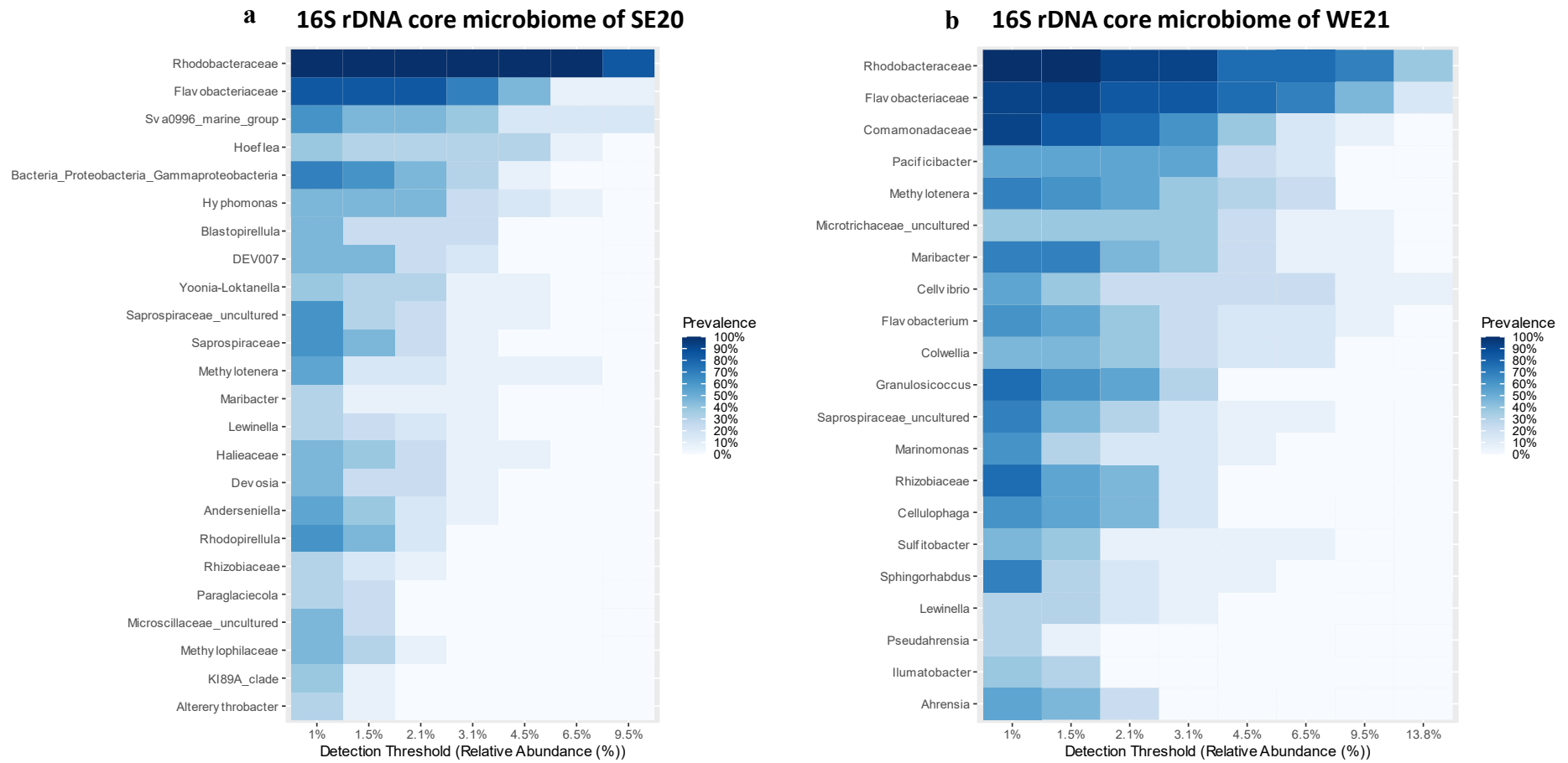


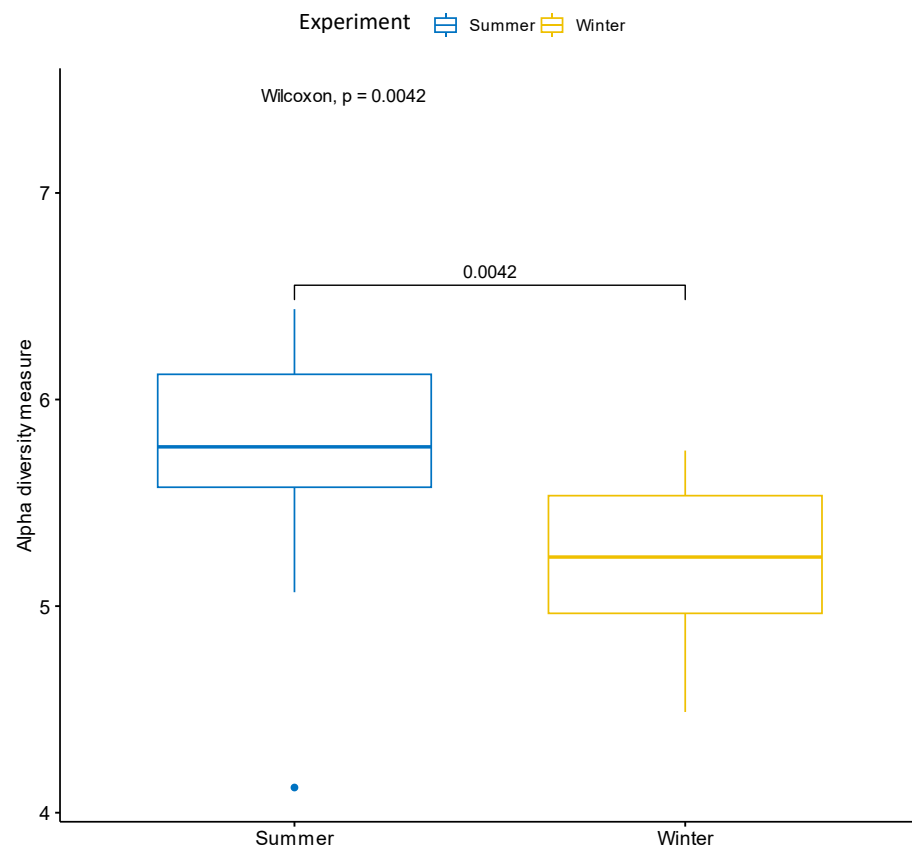
Figure 31: 16SrDNA core microbiome in the first experiment, starting in a) summer (SE20) and the second experiment starting in b) winter (WE21). On the x-axis the relative abundance of genera is given in percent, on the y-axis respective genera are listed. Least abundant genus white/light blue, and getting darker and changing color from white/light blue towards blue, abundance of genus is increasing. Most abundant genera are marked dark blue. A prevalence cutoff of 0.3 in 80% of the samples was used, and a detection limit of 0.1% as a classifier for the lowest possible abundant species within the samples. Please note the difference on the x-axis' extent, with the summer core microbiome ranging from 1% to 9.5% and the winter microbiome ranging from 1% to 13.8% relative abundance (Graphics created by I. Barrantes).

The Shannon diversity and Bray divergence are shown in Figure 32a (α diversity) and Figure 32b (β diversity). The α diversity is the mean species diversity in a site at a local scale, whereas β diversity is the ratio between regional and local species diversity. Both diversities are represented by season, with box-plots for summer on the left in blue and winter in yellow on the right. Horizontal lines indicate the median. In these box-plots there has been only one outlier within the α diversity in summer, below the box-plot. The Wilcoxon test checks whether two dependent samples differ significantly from each other. The p-value is a probability measure for the indications against the acceptance of the null hypothesis with a p-value < 0.05 providing stronger evidence to decline the null hypothesis. This applies, in this test, to both α and β diversity and hereby showing significant differences between the diversities in the two experiments.

Correlation analyses are shown in Figure 33 for differential abundant genera (a) and differential abundant pathways (b). Different genera are only present in specific experiments. *Bacteroides*, *Acrobacter*, *Rhodopirellula* and *Hypomonas* are related to the summer experiment, whereas *Shewanella*, Rhodobacteraceae, Flavobacteraceae are omnipresent in both experiments. In general, during winter differential abundant genera are higher than in summer. Differential abundant pathways are more evenly split between the two experiments. In summer degradational processes are dominant, while in winter the main focus lies on different metabolisms, e.g., amino acid (summer) or Tyrosine and D-Glutamine (winter). In both experiments pathways of biosynthesis are represented.

To compare the experiments in respect of ecological and metabolic functions a FAPROTAX (Functional Annotation of Prokaryotic Taxa) was done (Figure 34). Chemoheterotrophy is omnipresent through the experiments, with a slight dominance towards aerobic chemoheterotrophy in winter. Respiration, (dark) oxidation, reduction and fermentation are more related to the winter experiment. In summer oxygenic photoautotrophic processes and chloroplast related functions and cyanobacteria are favored. Nitrogen fixation, ureolysis and fumarate respiration happen in summer, only. Intracellular parasites occur to a comparable degree in both experiments, with a slightly higher consistency in winter.

a 16S rDNA Shannon diversity by experiment



b 16S rDNA Bray divergence by experiment

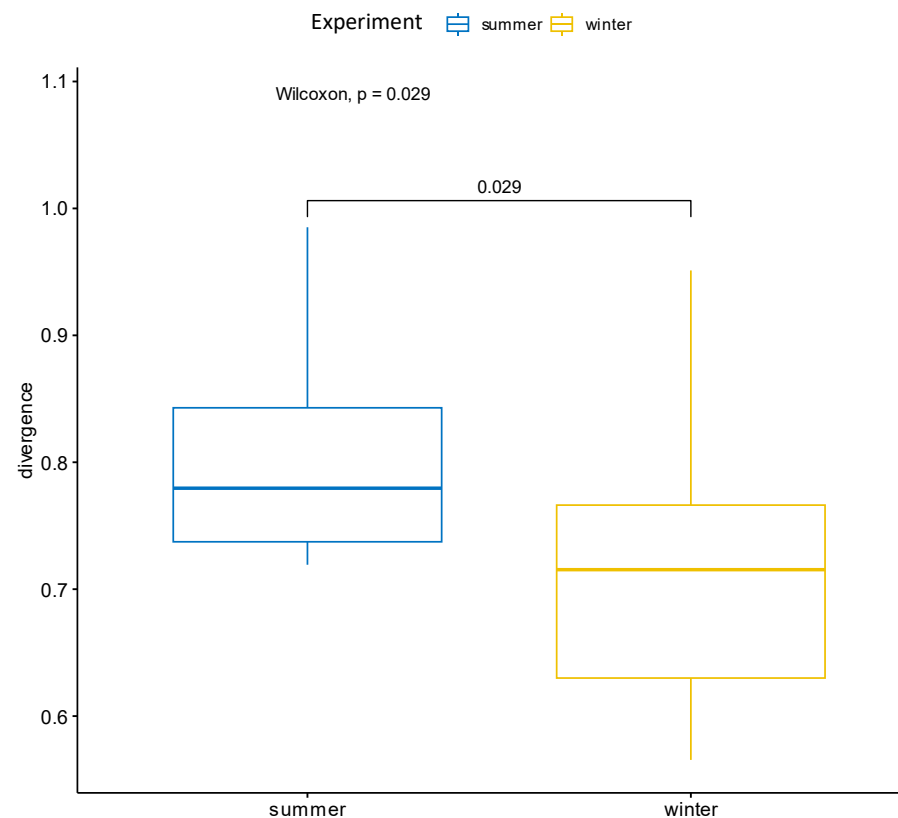


Figure 32: 16S rDNA a) α (Shannon) diversity and b) β diversity (Bray divergence). Both diversities are represented by experiment, with boxplots for SE20 on the left in blue and WE21 in yellow on the right in each graphic. Horizontal lines indicate the median, with upper and lower quartile, vertical lines show upper and lower whisker. In these box-plots there has been only one outlier within the α diversity in summer, below the boxplot. The α diversity is the mean species diversity in a site at a local scale, whereas β diversity is the Bray divergence, the ratio between regional and local species diversity. The Wilcoxon test checks whether two dependent samples differ significantly from each other. The p-value is a probability measure for the indications against the acceptance of the null hypothesis with a p-value < 0.05 providing stronger evidence to decline the null hypothesis. This applies, in this test, to both α and β diversity (\pm SD, graphics created by I. Barrantes, adapted).

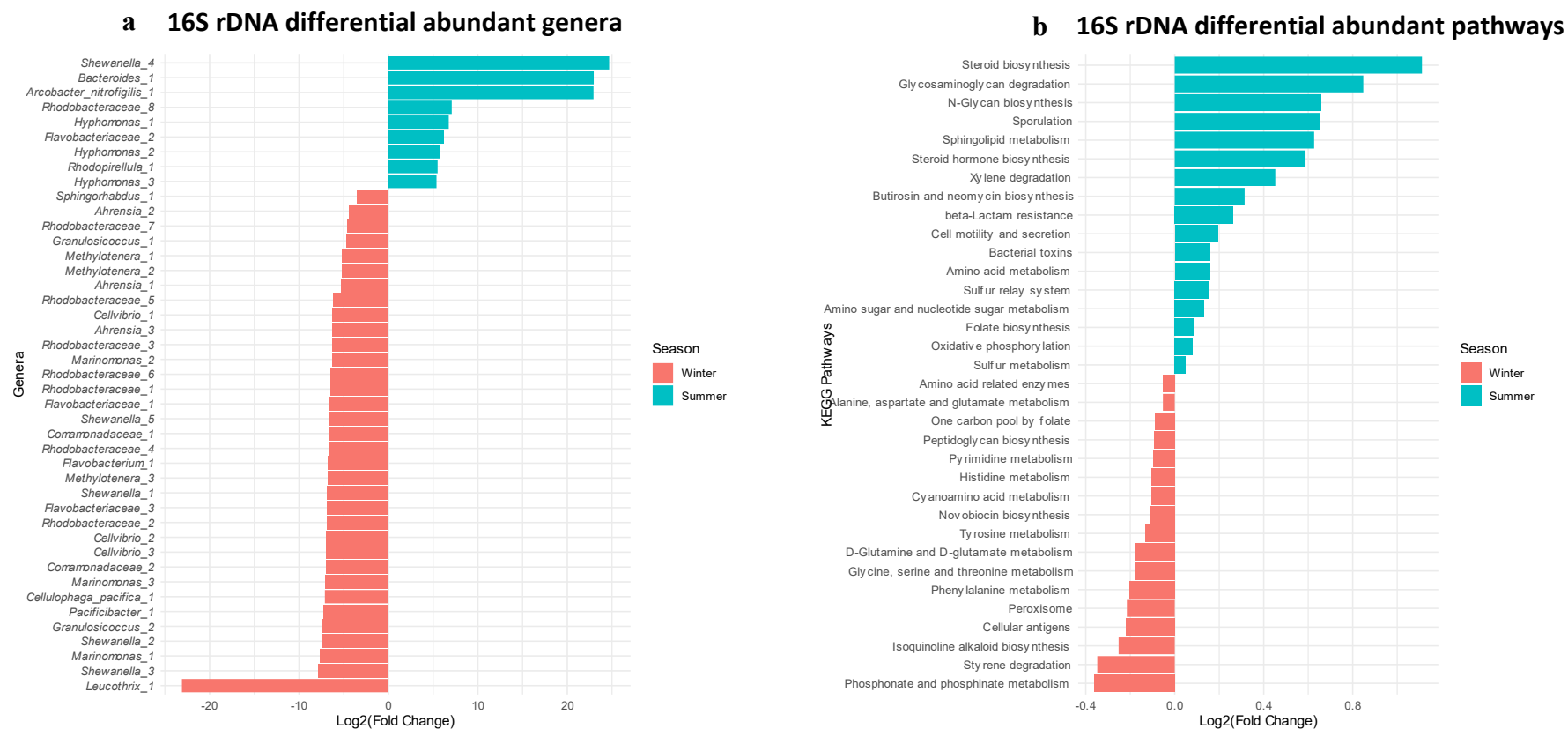


Figure 33: Correlation analysis of differential abundant a) genera and b) pathways in 16S rDNA for SE20 (turquoise) and WE21 (red). Used method: DESeq2, which is automatically performing data normalization and adjusts the p-value. With the Wald test the null hypothesis is kept while the distribution of a suitable test statistic is performed. Please note that the fit-type for genera in a) is local (numerical integration for dispersion), whereas in b) for pathways parametric (closed-form expression for the variance stabilizing transformation of dispersion), and x-axis have different measuring units. FDR (False Discovery Rate) has been set to < 0.01 for both analyses. X-axis is the log₂ transformed fold change and y-axis for a) genera and b) KEGG (Kyoto Encyclopedia of Genes and Genomes) pathways (Graphics created by I. Barrantes).

16S rDNA FAPROTAX for SE20 and WE21

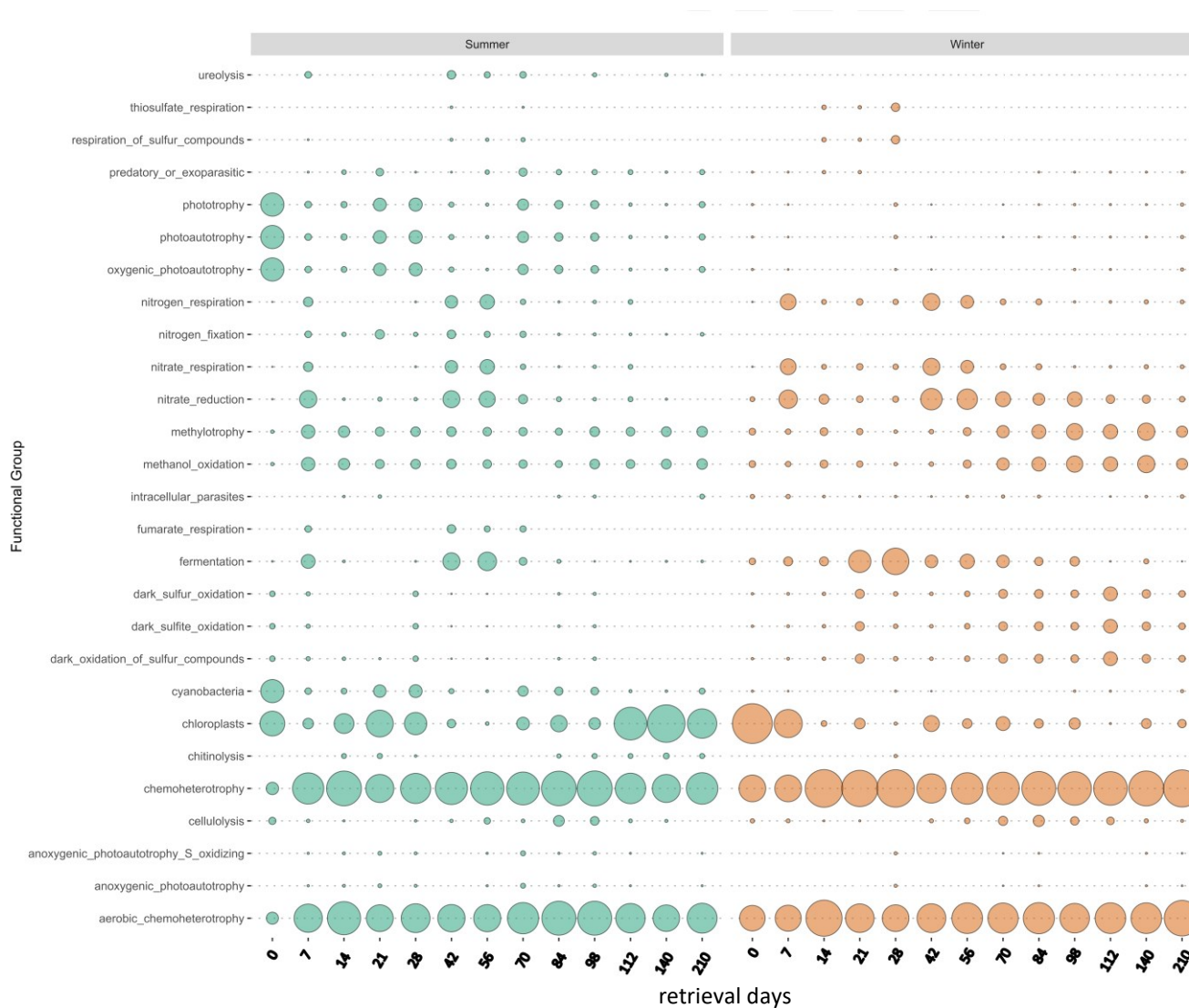


Figure 34: Results of a FAPROTAX (Functional Annotation of Prokaryotic Taxa) plotted as bubble chart, comparing SE20 (left, green) and WE21 (right, red) cycles. It predicts bacterial or archaeal taxa and their respective ecological and metabolic relevant functions. X-axis shows retrieval days for the two experiments, and y-axis the annotation, according to the ecological or metabolic function. The size of bubbles shows its percentage weight; the larger the bubble the more relevant is its respective function (Graphic created by I. Barrantes, adapted).

With the results of the differential abundant genera analysis in Figure 33 and the resulting conclusion of omnipresent genera further analyses were done. Time trajectories of *Shewanella*, Flavobacteriaceae and Rhodobacteraceae were created as shown in Figure 35:

16S rDNA differential abundant genera trajectories: Omnipresent

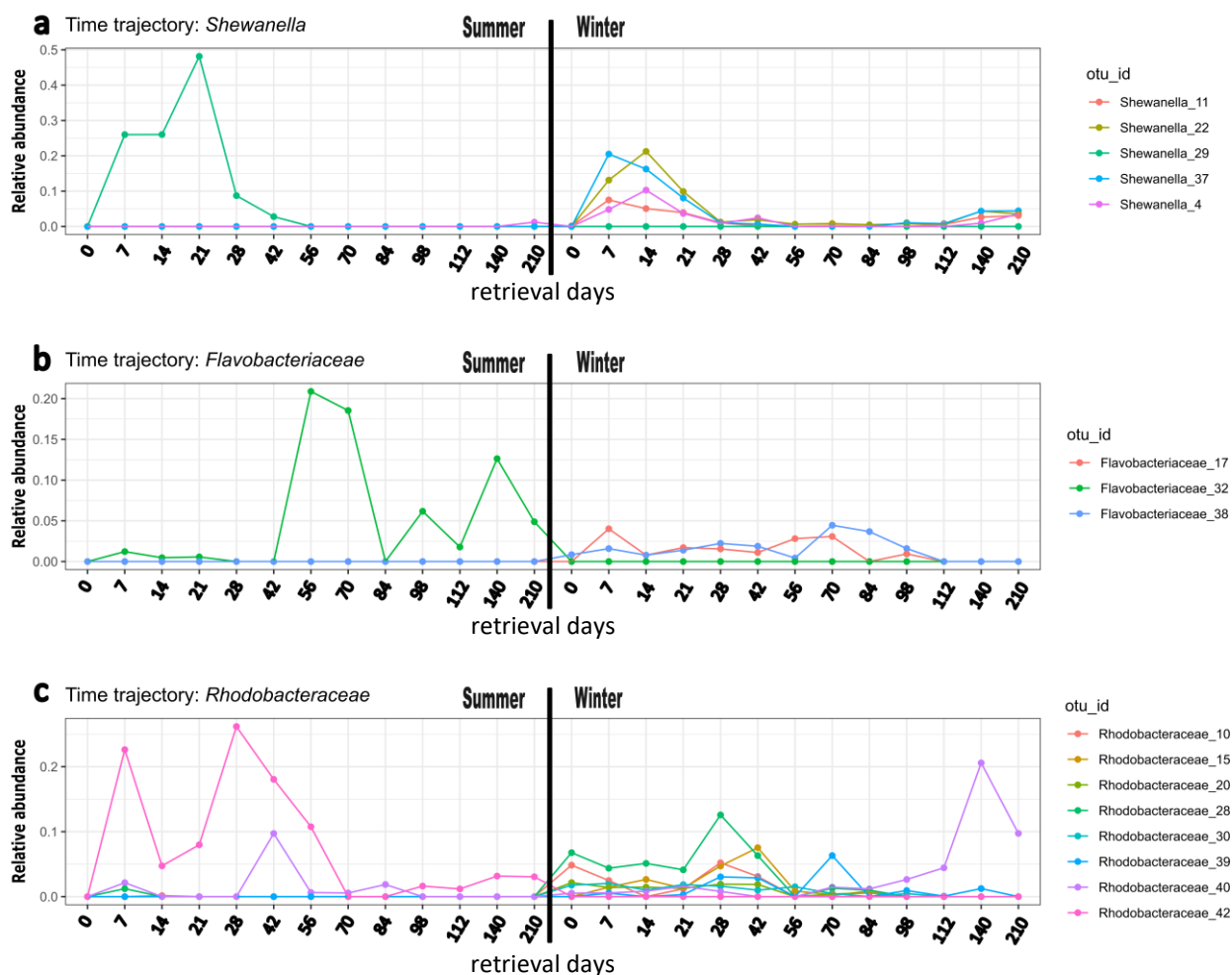


Figure 35: Time trajectory for omnipresent prokaryotic 16S rDNA genera, a) *Shewanella*, b) Flavobacteriaceae, c) Rhodobacteraceae; x-axis representing timeline, with the two experiments divided by the black bar: SE20 on the left, WE21 on the right. Both ranging from 0 to 210 days runtime. Y-axis showing relative abundance per genus in percent; out_id=operational taxonomic unit-identifier, that is used to classify groups of closely related individuals, given as additional number behind the id (Graphic created by I. Barrantes, adapted).

Shewanella is more present at the beginning of each experiment, Flavobacteriaceae in summer with high abundances from sampling point t₅ and in winter constant. Rhodobacteraceae do not follow a specific pattern, being always present.

To assign abiotic factors to the respective OTUs, correlations between those and the physicochemical factors were calculated (Figure 36). All OTUs are negatively correlated with the temperature except for Hyphomonadaceae_6 which is negatively correlated with light. Conductivity was also included in the analysis, but did not show any correlation with OTUs.

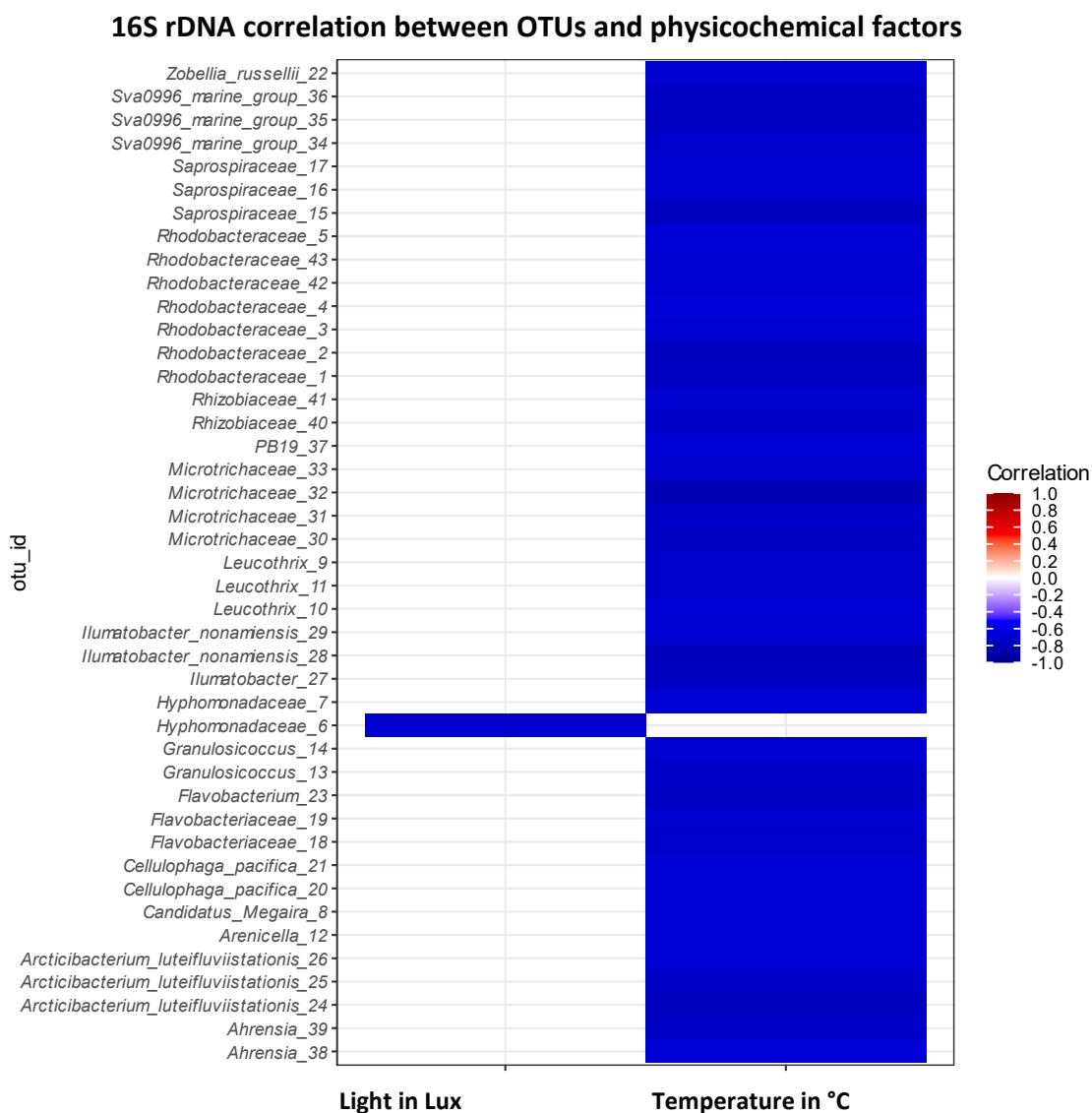


Figure 36: Analysis of correlations between OTU (Operational Taxonomic Unit) and physicochemical factors. Here, abiotic factors of both experiments (SE20 and WE21) are combined for analysis. Correlation is color coded: red shows positive correlation, and blue negative correlation. X-axis is representing the factors light in lux and temperature in degree Celsius, y-axis shows the respective out_id (operational taxonomic unit-identifier) (Graphic created by I. Barrantes).

3.7.2 Eukaryotic 18S rDNA

Microbial community kinetics for eukaryotic 18S rDNA are described below. The results are less than in the previous prokaryotic analysis. This is due to the fact that 18S rDNA had fewer genera, classes and phyla in each experiment compared to 16S rDNA. Therefore, not all analyses could be executed the same way as before. Some of the procedures could not be performed due to the lack of data, rDNA content or replicates for a better database.

The first Figure 37 shows the genus composition by a) samples and b) season. In both experiments a lot of unidentifiable/other genera are present. Additionally, in summer the relative abundance of Magnoliophyta is high. Here, fragments of the seagrass from the litterbags themselves could have been detected within the analysis. *Navicula* (a boat-shaped genus of diatom algae) are present mainly during the cold periods of the experiments, with a higher abundance in winter. In the summer experiment, their occurrence is restricted mainly to the last samplings that took place between autumn and turn of the year. *Diplonema* (biflagellated unicellular protists) are only present during the winter experiment.

Proceeding to Figure 38 the class composition of the microbiome is shown. Phaeophyceae, Nematoda and Bacillariophyta are omnipresent through both experiments. Ulvophyceae peak at the last sampling of the summer experiment, but do not occur to such an extent in the winter experiment at any time. Ascomycota occur early in the summer, but only during the last samplings in the winter experiment. The two peaks in Annelida can be explained by the discovery of a *Nereis diversicolor* at both time points within the litterbags retrieved. Unclassified Stramenopiles in winter vanish with continued decomposition. Labyrinthulomycetes peak after 70 days into the winter experiment, and Cnidaria after 98 days. Although having a higher abundance in winter, Bacillariophyta remain omnipresent.

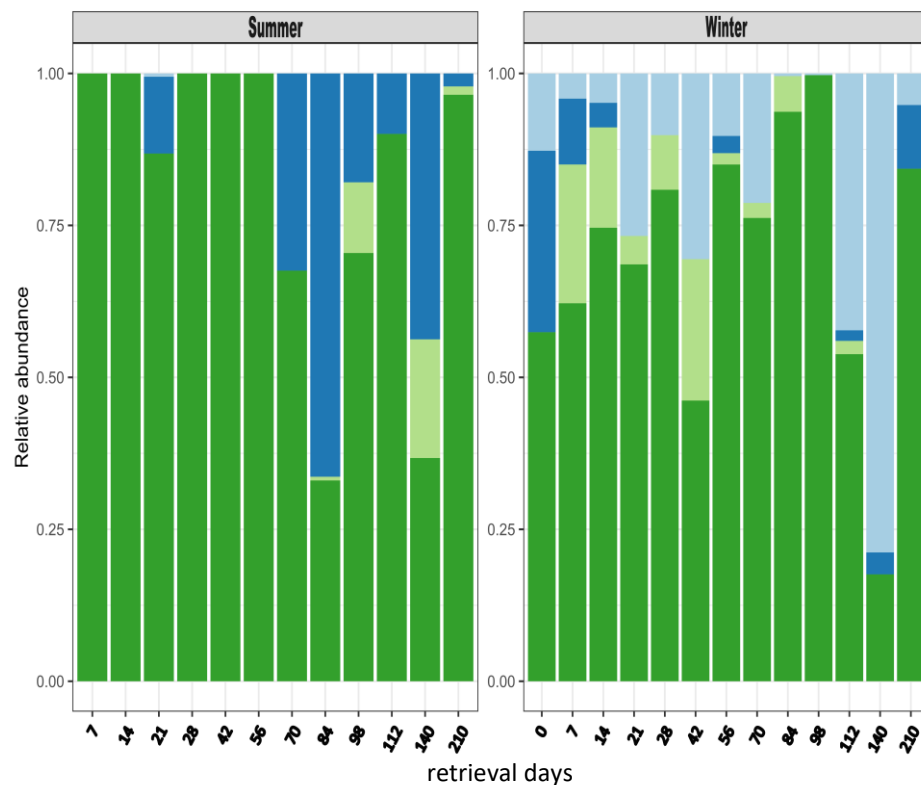
In the seasonal class composition during the seasonal experiments (Figure 39) no pattern can be predicted or observed. Unclassified Stramenopiles occur predominantly in winter, and here especially during aquatic periods of the experiment. Particularly in the white litterbags their abundance is higher. Unclassified Archaeplastida can be found in spring, no matter which treatment (black/white), and Spirotrichea in autumn under dark (black) conditions. Dinophyceae vanish after a start within the white litterbags in summer, whereas Chlorodendrophyceae and Cercozoa do the same in the black litterbags in that season. Phaeophyceae dominate both treatments in winter and spring, Labyrinthulomycetes remain omnipresent through both treatments and all seasons. After initially high abundances in summer, Ascomycetes vanish through autumn and are replaced by Bacillariophyta, mainly

within the white litterbags. Annelida can be found in autumn's first two samplings; this points towards an introduction of larvae while preparing the litterbags during the initial phase.

The phylum composition (Figure 40), both by sample (a) and season (b), demonstrates the development of the microbial community in the two long-time experiments. Other phyla are dominant in both seasons. Phragmoplastophyta appear later in summer but stay till the second to last sampling point. In the winter experiment they occur during the initial phase, vanish and come back towards the end of the respective experiment. The relative abundance of Ochrophyta and Nematozoa are similar. Hereby Ochrophyta are present during the start of the experiments and are replaced by Nematozoa later in the experiments. Diatoms are omnipresent in both experiments, with a higher abundance in the winter experiment. Euglenozoa are more dominant in winter, as well. Cercozoa and Centrohelida occur in both experiments, with higher abundances in winter. The same accounts for Ascomycota and Arthropoda, but these two phyla dominate the summer experiment.

The core microbiome of the two experiments is outlined in Figure 41, with the summer being displayed in a and winter in b. The omnipresent genus in both experiments are Magnoliophyta with a higher abundance in summer. This was already observed in Figure 37. Still, the most abundant genus in summer is represented by *Chromadorida*, and in winter by *Diplonema*. Otherwise there is no clear pattern apparent in the development of the core microbiome.

a 18S rDNA genus composition by sample



b 18S rDNA genus composition by season

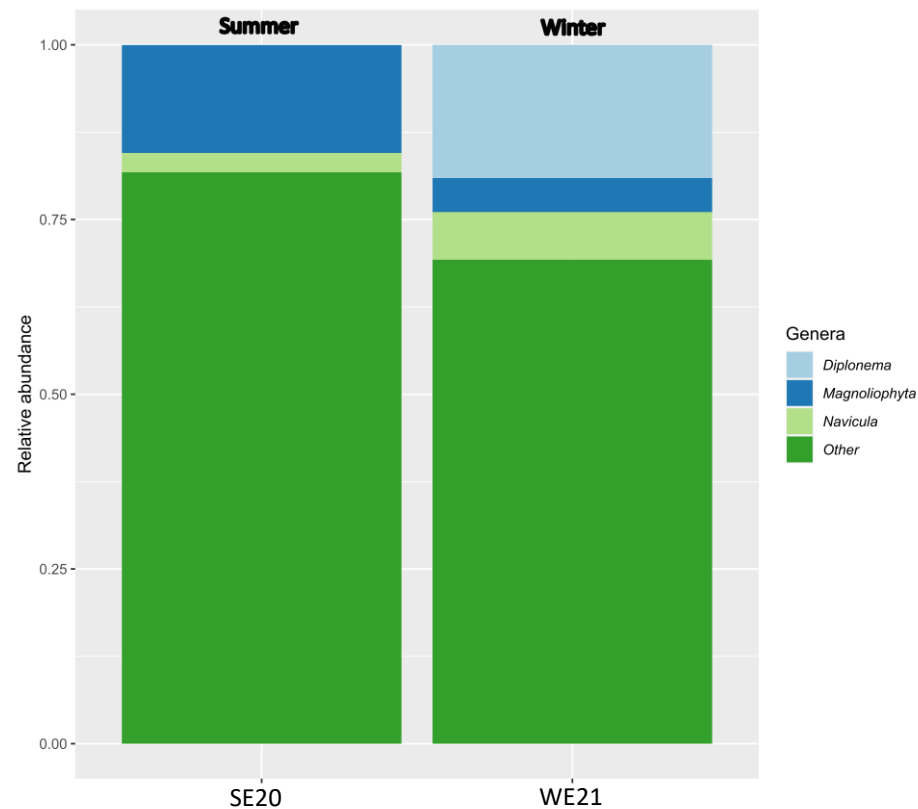


Figure 37: 18S rDNA genus composition by a) samples and b) experiment for SE20 (left) and WE21 (right). Stack bars show genus composition in relative abundance, extrapolated to a total of 1.00 equaling 100%. On the x-axis in Figure a), time points of collection of samples is shown, in Figure b) respective experiment starting point. In both graphics the two blocks are divided by experiment. A prevalence cutoff of 0.01 in 50% of the samples was used, and a detection limit of 0.1% as a classifier for the lowest possible abundant species within the samples (Graphics created by I. Barrantes, adapted).

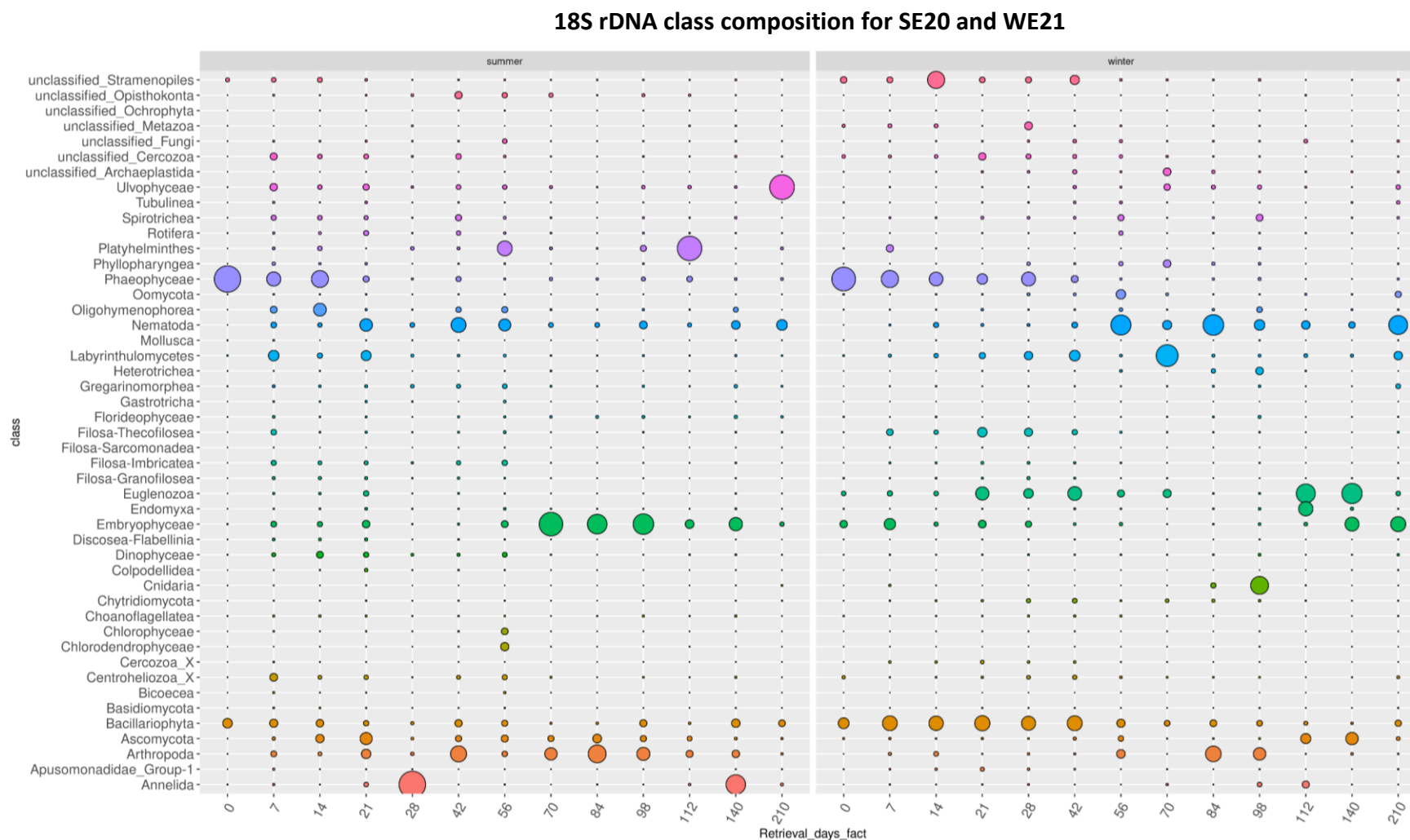


Figure 38: 18S rDNA class composition for SE20 (left half of graphic) and WE21 (right half of graphic). Bubbles represent abundance of classes, with increasing abundance along with increasing bubble size; x-axis is time line, with retrieval days given for both experiments, y-axis representing individual classes (Graphic created by K. Kesý).

18S rDNA class composition for seasonal experiments

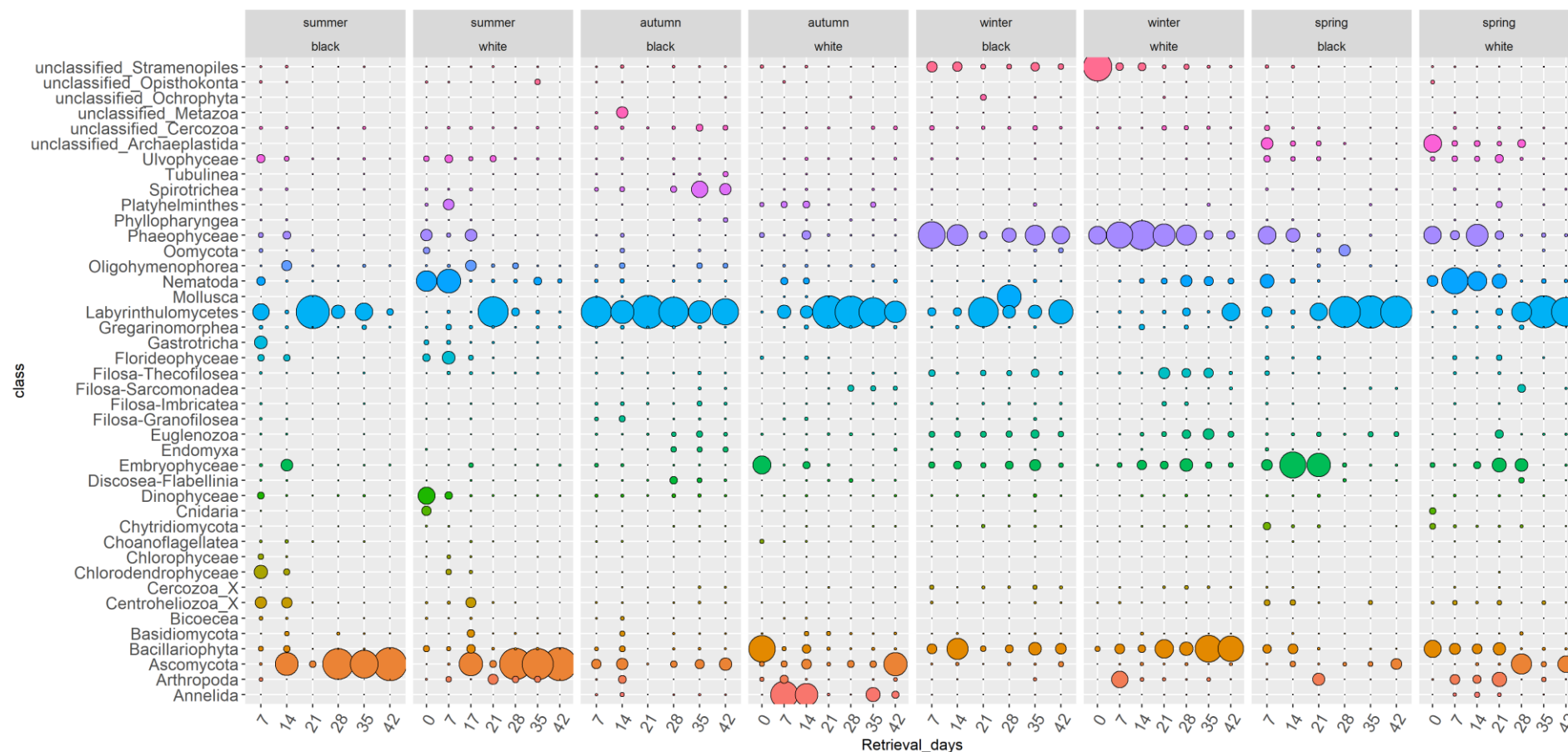


Figure 39: 18S rDNA class composition for the seasonal experiments under changing conditions (SSu20, SAu20, SWi21, SSp21, each split into black or white mesh treatment). Exposure to water and land changed weekly, starting in water (0 days) and finishing at land (42 days). Bubbles represent abundance of classes, with increasing abundance along with increasing bubble size; x-axis shows retrieval days for each seasonal experiment, y-axis representing individual classes. Additionally, results are split into black or white litterbags, respectively; please refer to headlines in each plot to distinguish. Note: initial samples have only been taken once, and are therefore, listed together with the graphs for the white litterbags – although being fresh from nature and hence not having any pre-treatment regarding light availability (Graphic created by K. Kesý).

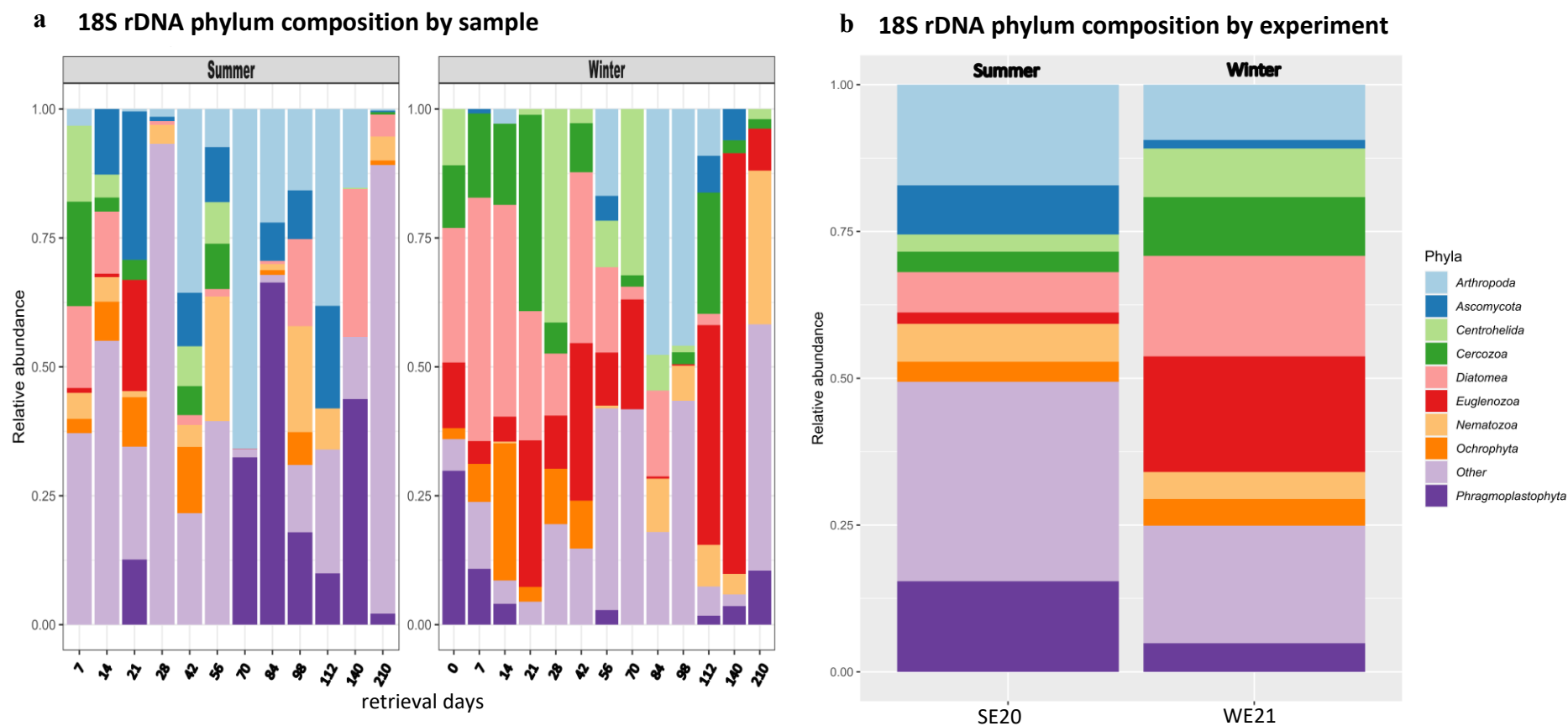


Figure 40: 18S rDNA phylum composition by a) samples and b) experiment for SE20 (left) and WE21 (right). Stack bars show genus composition in relative abundance, extrapolated to a total of 1.00 equaling 100%. On the x-axis in Figure a, time points of collection of samples is shown, in Figure b) respective experiment starting point. In both graphics the two blocks are divided by experiment. A prevalence cutoff of 0.01 in 50% of the samples was used, and a detection limit of 0.1% as a classifier for the lowest possible abundant species within the samples (Graphics created by I. Barrantes, adapted).

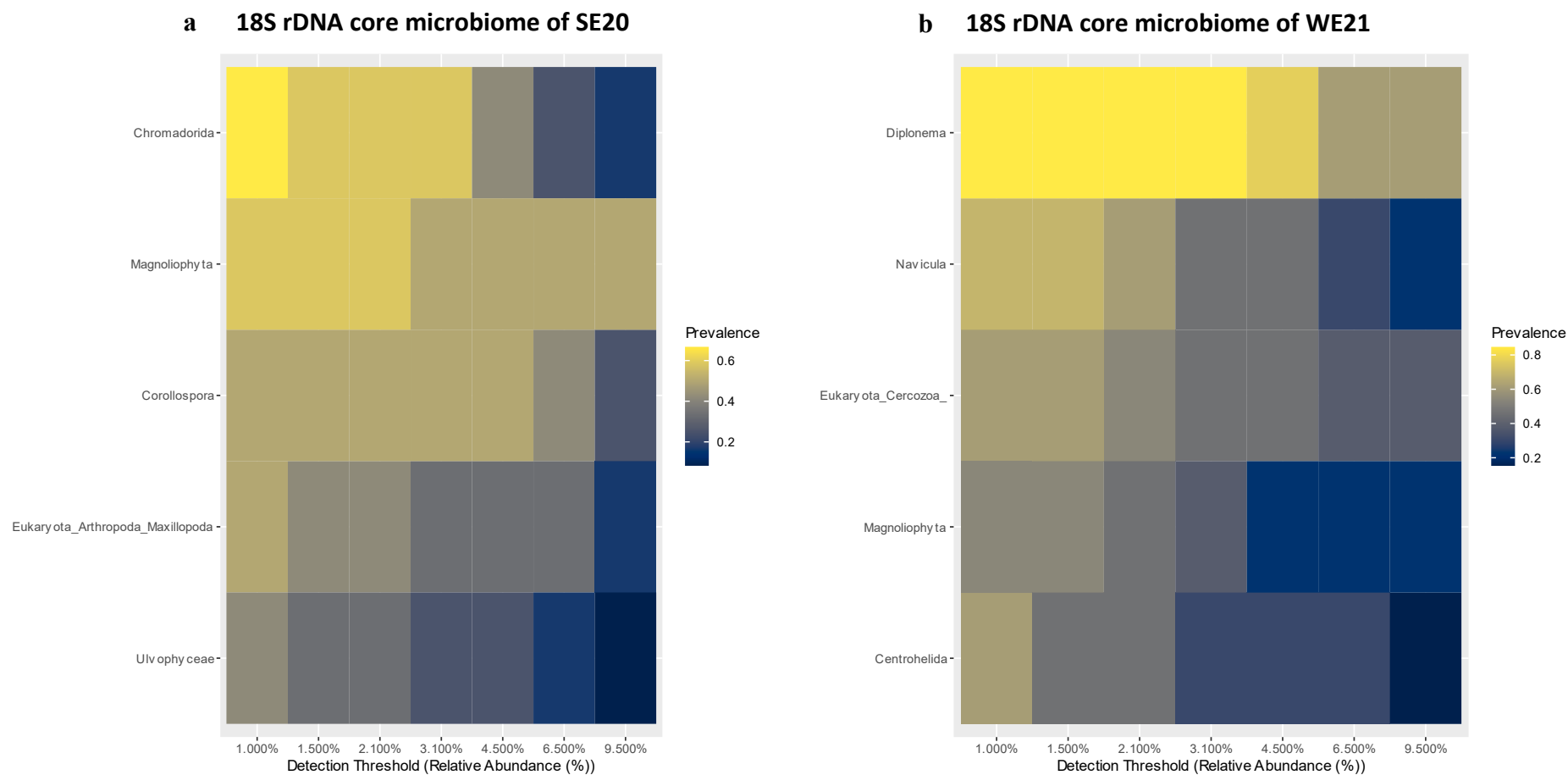


Figure 41: 18S rDNA core microbiome in the first experiment, starting in a) summer (SE20) and the second experiment starting in b) winter (WE21). On the x-axis the relative abundance of genera is given in percent, on the y-axis respective genera are listed. Least abundant genus dark blue, and getting lighter and changing color from blue towards yellow, abundance of genus is increasing. Most abundant genera are marked bright yellow. A prevalence cutoff of 0.4 in 50% of the samples was used in summer, and a prevalence cutoff of 0.5 in 50% in winter. Detection limit was set to 0.1% as a classifier for the lowest possible abundant species within the samples. Please note the difference on the y-axis' prevalence extent, with the core microbiome ranging from 0.2 to 0.6 in summer and the microbiome ranging from 0.2 to 0.8 in winter (Graphics created by I. Barrantes).

In another test α and β diversity were calculated; β diversity did not show any result, and α diversity is shown in Figure 42. Comparing the two boxplots it is obvious that the α diversity in summer is higher (median \cong 2.6) than in winter (median \cong 2.45). With a Wilcoxon test and a resulting p-value of 0.29, and therefore > 0.05 , it is statistically proven that there are no significant differences between the two experiments.

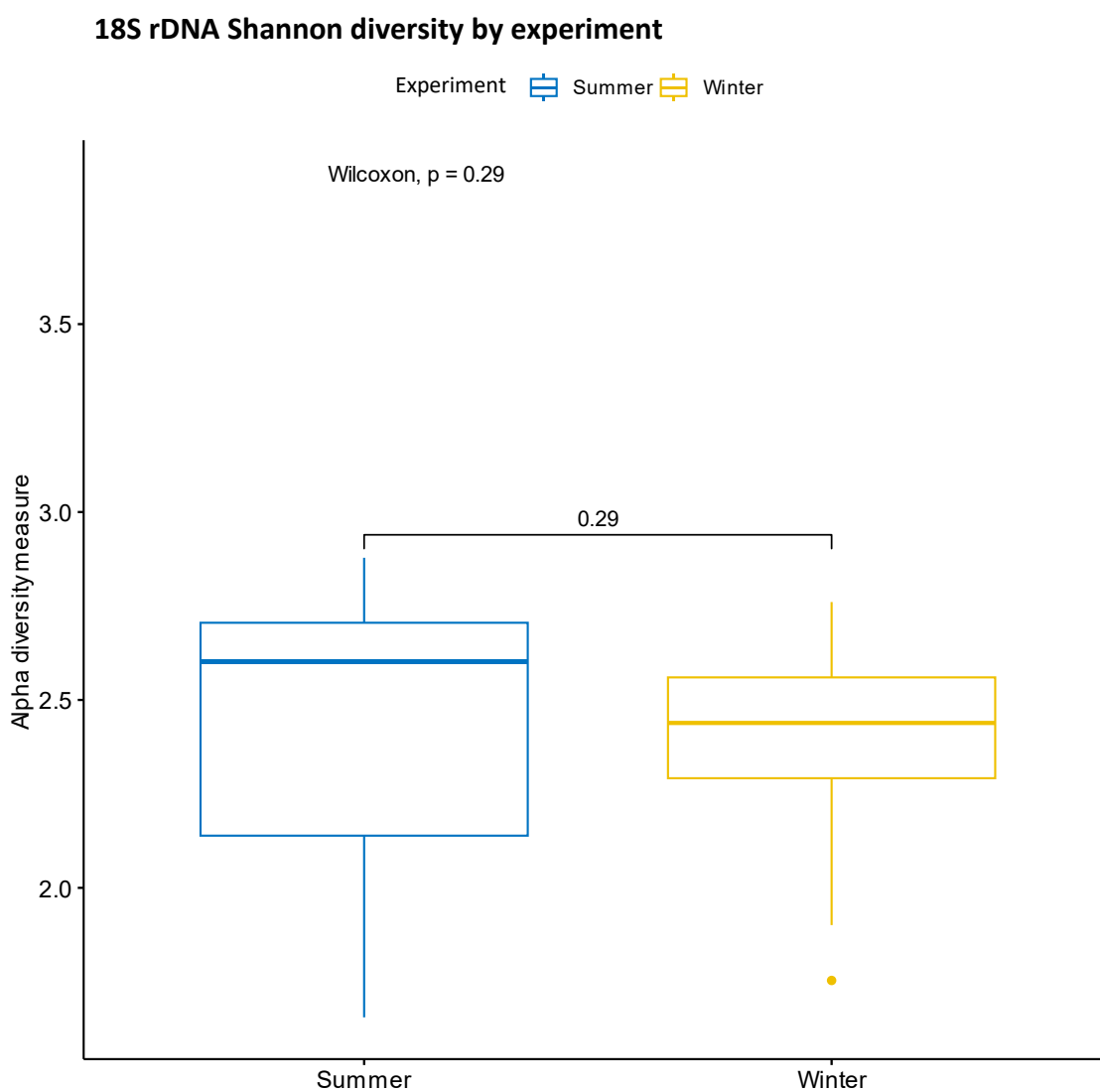


Figure 42: 18S rDNA α diversity. Diversity is represented by experiment, with boxplots for summer (SE20) on the left in blue and winter (WE21) in yellow on the right. Horizontal lines indicate the median, with upper and lower quartile, vertical lines show upper and lower Whisker. In these box-plots there has been only one outlier within the α diversity in winter, below the boxplot. The α diversity is the mean species diversity in a site at a local scale. The Wilcoxon test checks whether two dependent samples differ significantly from each other. The p-value is a probability measure for the indications against the acceptance of the null hypothesis with a p-value < 0.05 providing stronger evidence to decline the null hypothesis. In this test, α diversity is > 0.05 with a value of 0.29 meaning that there is evidence to reject the null hypothesis, and therefore, having no different diversities between the two experiments (\pm SD, graphic created by I. Barrantes).

3.8 C:N ratio analyses

The C:N ratio reflects the fertility of an organic environment. Therefore, carbon (C) and nitrogen (N) are measured. Both elements are present, organically bound, in the humus, or in this case within the litterbags, and are mineralized by microorganisms (mineralization), in especially converted into inorganic compounds; N thus becomes available to plants. Soils with a narrow C:N ratio (high N content) are nutrient-rich and fertile. A wide C:N ratio is evidence of low biological activity and vegetation with nitrogen-poor litter. Results for the two long-term experiments are shown in Figure 43.

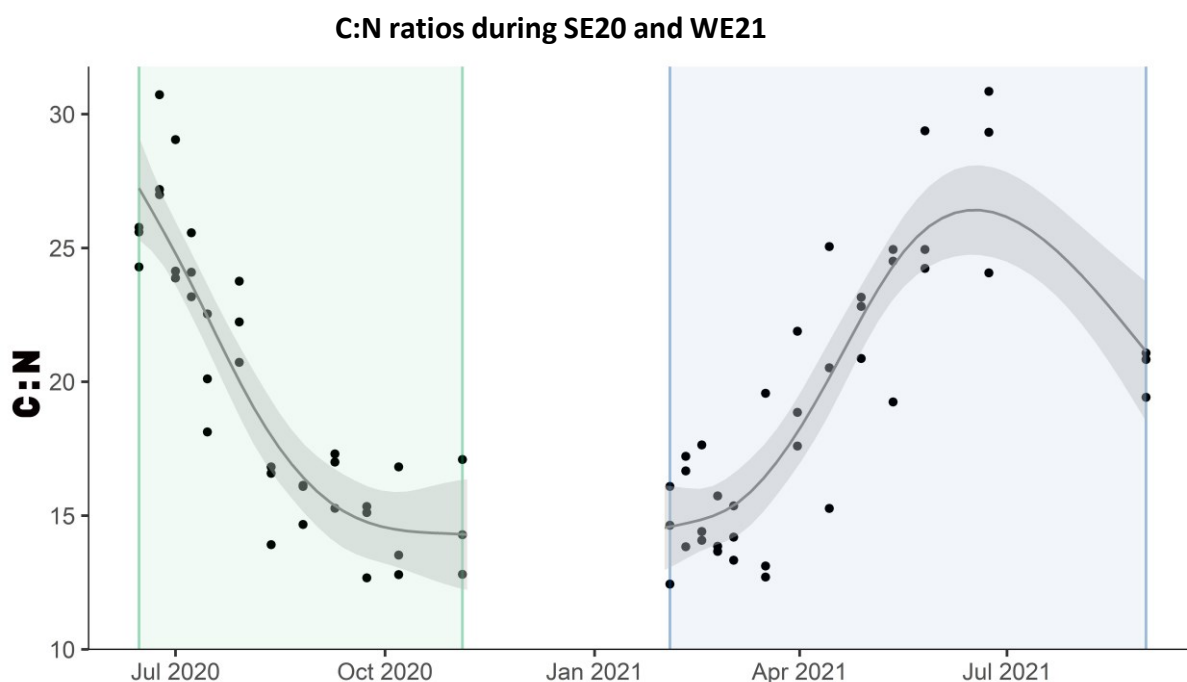


Figure 43: C:N ratios (y-axis) during litterbag decay in a constant aquatic environment; green highlighted time frame represents first experiment starting in summer, and blue frame the experiment starting in winter. Time line (x-axis) is continued between the start of both experiments. Black dots show the respective sample values, with three stacked dots at each sampling point for the three replicates. Black line is the mean value between the three replicates, and the grey highlighted background is the scattering; x-axis represents the retrieval days as a continued timeline, and y-axis the C:N ratio (in M/M).

The C:N ratio in SE20 starts with a high ratio, indicating low biological activity. With the passing of time, the ratio narrows down and biological activity is promoted. In WE21 it is vice versa, with a change after a peak in the second last sampling towards a narrower ratio till the end of the experiment (data given in Table A 8 for SE20 and Table A 9 for WE21).

The same C:N analyses have been done for the seasonal experiments, split into black and white bags. Results are shown in Figure 44.

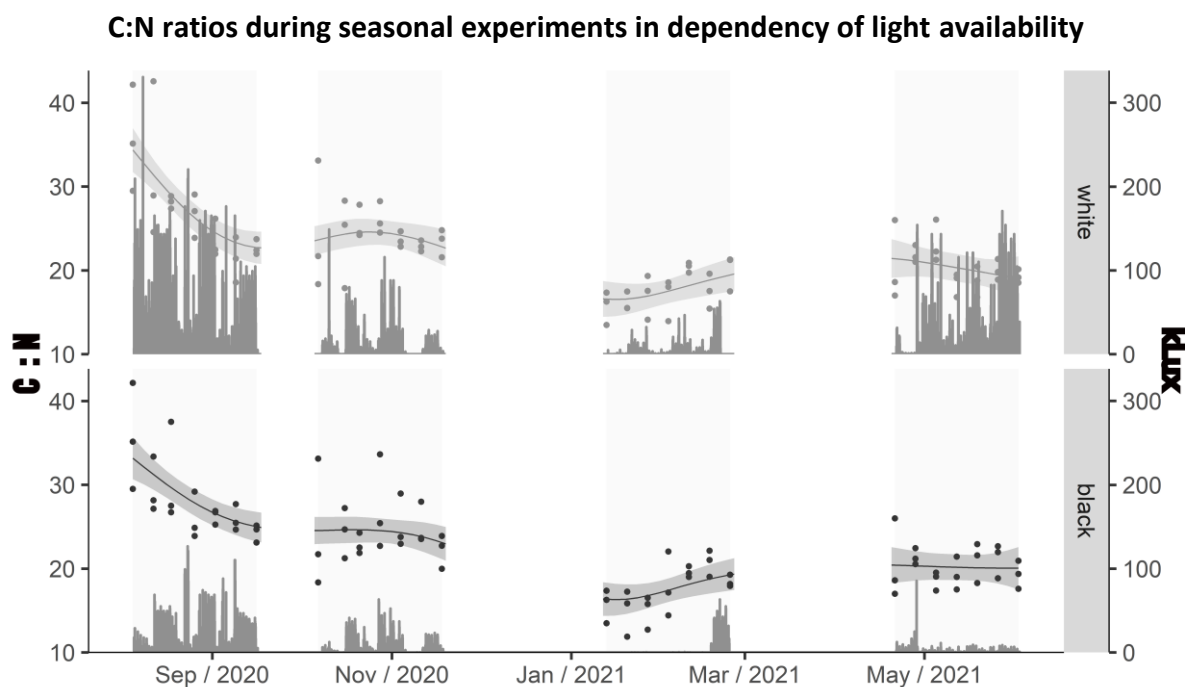


Figure 44: C:N ratios (in M/M, first y-axes, left) split by treatment white (upper y-axis) and black (lower y-axis) mesh bags. Time line (x-axis) is continued between all experiments, with white interruptions when no experiment was executed. Black dots show the respective sample values, with three stacked dots at each sampling point for the three replicates. Black line is the mean value between the three replicates, and the grey highlighted background is the scattering. Additional values for light (in Kilolux) are given in the second y-axis (right).

Comparing the seasonal C:N ratios shows that the ratios are higher in warmer seasons, and lower in cold seasons. The highest ratios are seen in summer, lowest in winter. Autumn and spring look similar, with the autumn having slightly higher ratios. The ratios in summer and autumn scatter more than in during the other seasons. Treating the litterbags with white or black mesh does not affect the ratio, and it remains similar (data given in Table A 10 for SSu20, Table A 11 for SAu20, Table A 12 for SWi21 and Table A 13 for SSp21).

For greater clarity, in Figure 45 the C:N ratios are spread in individual plots. Again, the three replicates per sampling point are featured in stacked dots, with a linear regression put through each season. Here, no separation between black and white litterbag has been done. Additionally, R^2 was calculated. In statistics, the coefficient of determination, also referred to as R^2 , is a key figure for assessing how well a regression fits.

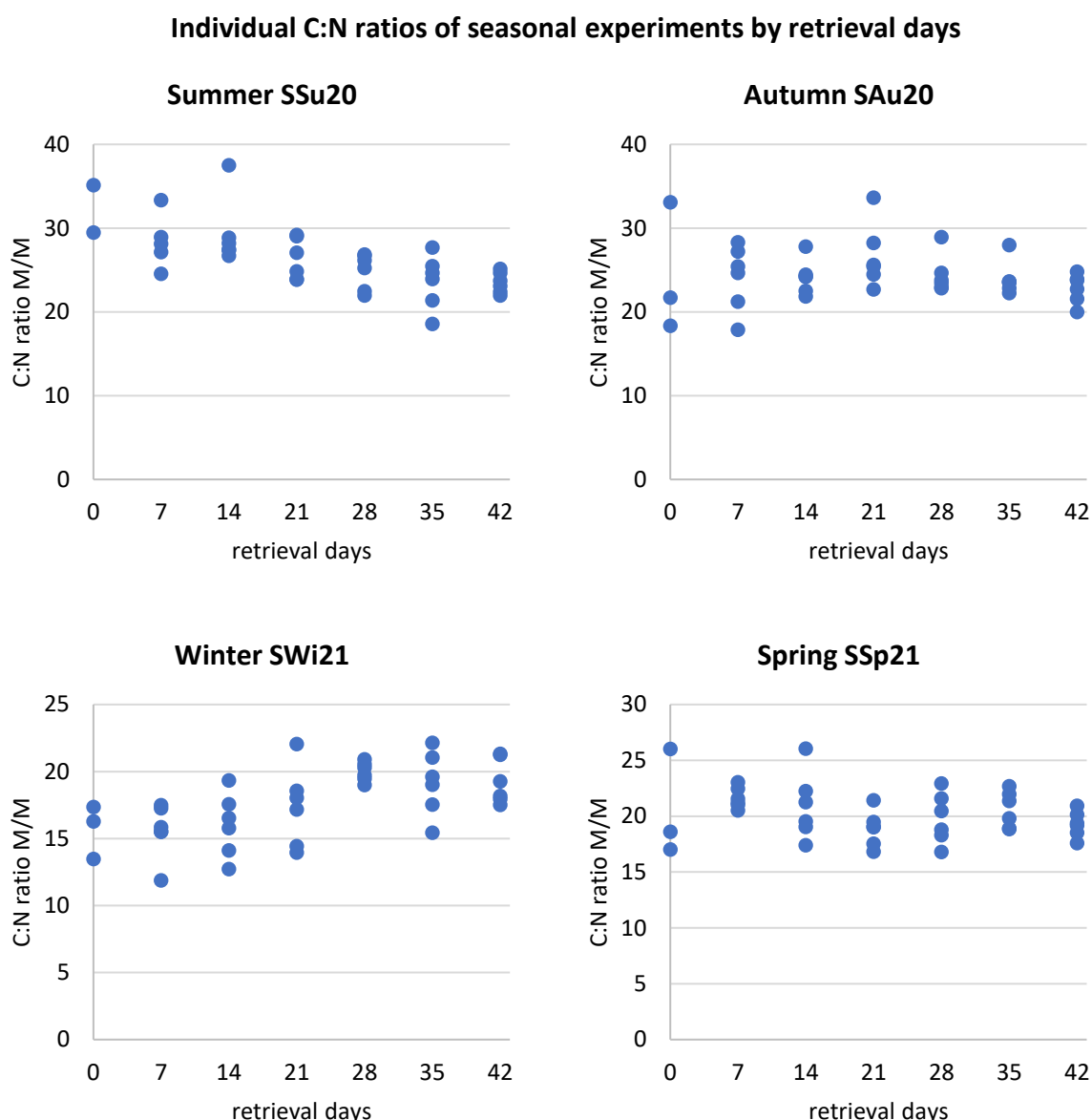


Figure 45: C:N ratios (y-axis) through seasons. Values given (M/M) for a time period of 42 days (x-axis). Blue dots represent respective values for black or white litterbag. A linear regression is put through every season, implying all six values per sampling point. Litterbags changed between aquatic and land exposure every week, starting in the water and finishing after 42 days with a final sampling at land. Please note the adjusted y-axis range for summer and autumn 2020 (up to 40 M/M) opposite to winter (up to 25 M/M) and spring 2021 (up to 30 M/M).

Seasonal plots show a similar trend to the previous figure: in summer the ratio is decreasing, in winter it is increasing. Autumn and spring remain stable through the respective experiment's runtime. The high initial ratios for the first three samplings in summer are noticeable. Looking at R^2 it can be said that summer shows the best fit of the regression with a value of 0.47, followed by winter with 0.35. Spring has a R^2 of 0.06 and autumn the lowest with 0.02.

4 Discussion

Although executing beach management along many coasts worldwide, and leaving significant impacts on beach ecosystems (Kirkman & Kendrick, 1997; Dugan et al., 2003; Davenport & Davenport, 2006; Haydéel & Kathy, 2006), for e.g., the Baltic Sea there is little information regarding beach wrack amounts. A study from 2012 based on an early approach from 1977 at the coast of Schleswig-Holstein (Grave & Möller, 1982) showed an increase of factor 3.15 regarding beach wrack amounts in kg km^{-1} (Weinberger et al., 2020). Nevertheless, data of amounts and species composition in particular for Mecklenburg-Western Pomerania is still rare. The western but also the south-western Baltic Sea area represents the transition between full marine habitat like in the North Sea and the brackish Baltic Proper. Salinity changes have wide variations, and range between 10–18 PSU with random peaks up to 28 PSU (Feldner, 1976; Reusch et al., 1994). Here, limited marine species are mixed with opportunistic benthic fauna (Rumohr et al., 1996) and limnic species, occurring in the northern and inner coastal waters (Bonsdorff, 2006). More pressure is exerted by coastal eutrophication, which has been increasing since the 1970s, with rising nutrient levels (Bonsdorff et al., 1997; Andersen et al., 2017). This is caused by, amongst others, urbanization, land use and agricultural inflow (Rosenberg et al., 1990; Larsson & Granstedt, 2010; Savage et al., 2010) and wrack decomposition processes (Helcom, 2007). This influences the distribution of aquatic plants (Telesh & Khlebovich, 2010; Chubarenko et al., 2021). Wrack deposition is driven by strong hydrodynamically onshore winds (Lenanton et al., 1982; Bird, 1996; Mateo et al., 2003) especially on less exposed coasts (De Falco et al., 2008). When left at the beach, wrack is an additional nutrient source to the local coast (Prasad et al., 2019). The organic content of the sand, after being buried, alters the physical structure of sediments (Rossi & Underwood, 2002) and enhances the build-up of benthic microalgae (Dizon & Yap, 1999; Posey et al., 1999). This work divides beach wrack into new and old wrack. New wrack (NW) is the first wrack line at the splash zone, and old wrack (OW) is further back at the dunes. This differentiation is important because of potential differences in residence time and water availability.

In Kühlungsborn old wrack was most present in autumn, exceeding new wrack amounts. Compared to the dried amounts given for the Kiel area with an average 3.2 kg m^{-1} (Weinberger et al., 2021) the values are relatively moderate with a maximum of 0.73 kg m^{-2} . One needs to be mindful of the differences in the unit of measurement (kg m^{-1} vs. kg m^{-2}). High amounts of seagrass within the old wrack especially during the summer reflect its growth period (Orth et al., 2006) and the intactness of seagrass, having whole or broken leaves, determines the volume of beach wrack, too. Seagrass was often fragmented. No explicit measuring has been executed

on collected seagrass leaves in this study, but random samples in other studies ranged between approximately 30 to 50 cm on average when fresh and unbroken (Feldner, 1976; Reusch et al., 1994). The mean dry weight (DW) of *Zostera marina* was at 0.158 kg m^{-2} and therefore, lower than the previously investigated values from Feldner in 1976, from the Belt Area. This is more saline and approximately 130 km west of Kühlungsborn. Reasons might be the aforementioned eutrophication and thereby water turbidity and the general decline of seagrass meadows. The mean DW of total BW lay at 0.66 kg m^{-2} for NW and 0.73 kg m^{-2} for OW. Species richness showed seven macrophytes plus seagrass at Kühlungsborn. Lots of sand was in the BW, usually exceeding the dry weight (0.93 kg m^{-2} mean sand in NW and 1.61 kg m^{-2} in OW). At Poel an average of 1.22 kg m^{-2} (1.17 kg m^{-2} NW and 1.27 kg m^{-2} OW) of sand was measured. The highest amounts occurred in autumn (3.03 kg m^{-2} sand). The average sand content of freshly piled beach wrack is given with 50–95 % (Chubarenko et al., 2021). Similar data was given in an earlier study stating 50–90 % of the content of beach wrack (Mossbauer, et al., 2012). Generally, NW consisted more of algae. The habitus on algae, depending of the species, being interwoven and sticky favor sand inclusion as seagrass leaves do not adhere as much to sand.

Unlike the exposed coastline of Kühlungsborn towards the Baltic Sea, the coastline of Poel is sheltered through the Wismar Bay. In contrast to Kühlungsborn, at Poel beach wrack tends to get trapped in the Wismar Bay and starts to accumulate. The characteristics of Poel's beach differ. It is wider with more beach vegetation like beach grass, sea hollies and other opportunistic land plants. The examined beach “Schwarzer Busch” is located to the north-western part of Poel, being exposed to the currents of the Wismar Bay. Here, some of the largest local seagrass meadows spread (Helcom, 2007; Hartz et al., 2014; Chubarenko et al., 2021). In these shallow and calm inner bays, especially those known as “Bodden” or “Haff”, seagrass finds optimal growth conditions (von Nordheim & Boedeker, 1998; Lotze et al., 2006; Helcom, 2007). The main part of beach wrack (73 % new and 79 % old wrack) at Poel therefore, consisted of seagrass *Zostera marina*. Both wrack lines were continuously present. Samplings in late April showed wrack mainly consisted of algal biomass, reflecting the terminated growth season of seagrass (Feldner, 1976; Reusch et al., 1994) and thereby its decline in BW. Landings shifted from autumn to summer, and new wrack amounts were highest with 1.05 kg m^{-2} DW, almost the equivalent of the yearly mean 1.35 kg m^{-2} DW. Old wrack reached an average 0.73 kg m^{-2} DW. Mean wrack thickness within NW was 2.4 cm and 4.9 cm for OW. New wrack amounts at Poel were more than double compared to Kühlungsborn, old wrack had similar values (0.75 kg m^{-2} at Poel vs. 0.73 kg m^{-2} in Kühlungsborn). Calculated beach wrack volume piled up to a max. of 25.51 m^3 , exceeding the amount at Kühlungsborn (max. 0.52 m^3). These

findings need to be considered when being compared with values from e.g., the municipality or other literature data where the amounts are usually given in m³.

A clear seasonality was seen. At Kühlungsborn during summer large amounts of red algae dominated, whereas at Poel seagrass dominated throughout the whole year. On both sites in spring BW consisted of red and green algae. In summer red algae reached their peak at Kühlungsborn's beach in the new wrack, accompanied by brown and green algae. Old wrack was dominated by seagrass. Reflecting the lack of seagrass at the local coast, it points towards detached seagrass being washed ashore from nearby meadows. Wrack at Poel consisted to equal parts of red, brown and green algae in spring (own observation). Green algae like *Cladophora* spp., *Fucus vesiculosus* and *Ulva* spp. grow abundantly at the groin pillars. Other personal observations showed charophytes (*Chara aspera*), which flourish plentifully nearby. No specimen was found in the samples. Rhodophytes and chlorophytes had their largest amounts during spring and summer. For the western Baltic Sea there is a total species richness of up to 211 species given (Schories et al., 2009): eight species of charophytes being reduced to six towards the Western Baltic. 52 species of chlorophytes are categorized for the Eastern Baltic Sea and 32 of rhodophytes, respectively (Schories et al., 2009). A limited number of species were found. Besides *Z. marina*, algae of the species *Ceramium diaphanum*, *Ulva* spp., *Fucus vesiculosus*, *Cladophora* spp. and *Pilayella littoralis* were found. Wrack varies during seasons (Suursaar et al., 2014), with *Delesseria sanguinea* being found in autumn.

Decay experiments on land showed interesting results. Up to now, most research had focused on litterbags with pure seagrass material (Jędrzejczak, 2002a) and pre-dried content (Jędrzejczak, 2002b). Here, local BW was collected, containing lots of fragile algae. After the first two months, surface bags gained more weight than buried bags, being almost at the same weight after four months. These weight gains are hard to explain. Methodically, the fragility of used BW did not allow for sand to be washed off after retrieval. Samples were de-sanded as well as possible, however measuring errors cannot be excluded. There were no visible epiphytes. Possible explanations for weight gain, besides adhesive sand, include the colonization with diatoms and other microscopic or phototrophic communities. This is supported by light and higher oxygen availability compared to buried bags. High organic matter contents under the buried bags during the initial month (0.504 %) compared to the bare sand samples (0.329 %) suggests that there was leaching and decay. Bags on top of the sand showed an increase in organic matter content only after four months (from initially 0.304 % to 0.358 % after four months), allowing a secondary pursuit of decay processes. Results are unlike in other

research where over 40 % of the initial weight decayed within the first days (Lastra et al., 2014). However, these experiments were done on the Antarctic Peninsula under different climatic conditions. Temperate beaches like Warnemünde will have different rates of decay. Comparable data for land decay in other regions is rare, and depend on the mixture of beach wrack (Ochieng & Erftemeijer, 1999). It was proven that aquatic freshwater macrophytes decay faster in their natural environment (Bianchi & Findlay, 1991), and conducting the experiments on land might have therefore inhibited decay processes. Degradation is said to be faster underwater and in the dark than under light conditions (Bianchi & Findlay, 1991). This should favor the buried bags, having better water availability and no light. Thereby, no phototrophic communities should have developed. Still, there is no clear pattern of better decay when being buried. In this experiment, throughout the whole year, there is no measurable weight loss to the litterbags. This could be explained by relatively dry conditions (64.8 l m⁻² less water in 2019 than in 2020) with a lot of sunshine (1905.5 hours of sunshine in 2019 and 2054.6 hours in 2020). This is in accordance with Karberg et al. (2008), stating that litter decomposition rates are dependent on moisture. Results reflect, to a certain degree, the influence of temperature, too: microbial activity might double by an increase of 10 °C (Kirschbaum, 1995), and vice versa. With dropping temperatures in autumn, organic matter decreased under buried bags. Underneath surface bags and within the bare sand OM increased in first four months before starting to drop. In March OM dropped in all samples, with higher amounts in surface bags. With increasing growth of fresh annual biomass more nutrients are consumed, causing their loss. Surface sediments gained approx. 33 % OM compared to the initial stage. Litterbags experienced arid conditions, slowing down decay (Urban-Malinga et al., 2008). On the surface they had to face strong UV impacts, solar radiation and temperature, resulting in fewer grazer and microbes fostering shredding and decay. High weight gains (tripling in weight from the start 5.7 g to March/six months 16.2 g) might be due to sand. From the initial to final sampling, the weight of buried bags stayed almost constant. But fragmentation of wrack material was observed. Shifts in the weight of surface bags after six and eight months was explained by plants growing through bags. With this inhibited and, compared to literature (Bianchi & Findlay, 1991), slow decay, methodical errors are apparent.

Experiments under alternating conditions were intended to mimic the natural succession of beach wrack that is flushed to land and backwashed to the water several times during decay. Imitating wrack accumulations with the possibility of getting buried, half of the litterbags were made of black mesh, representing the dark conditions for the buried part of BW. Over time white litterbags gained weight, especially in summer. High temperatures and sufficient light

might have given good conditions for epibiota, like e.g., diatoms, other phototrophic organisms and epiphytic algae. In need of water, growth appeared during aquatic phases (Harlin, 1975). Nutrient leaching might have attracted settlement of microbes, promoting colonization with higher trophic level grazers. In black bags the weights constantly decreased. Without sufficient light for primary production more consumption than production took place. Fungi should be considered with their involvement in decomposition (Das et al., 2008).

There is not much data available regarding the long-term microbial decomposition of seagrass detritus and microbial processes remain poorly understood (Trevathan-Tackett et al., 2020). A large number of prokaryotes and eukaryotes were detected. Hereby the decisive factor between SE20 and WE21 was the differentially abundant pathways, representing the stabilizing transformations. Compared with the genera, the respective seasonal start determined the pathways of microbial development. Both experiments showed a dominance of Alpha- and Gamma Proteobacteria, Bacteroidia and Verrucomicrobiae, and unclassified bacteria. As WE20 started after SE20, it is a continuation of microbial growth through the year. Cyanobacteria and campylobacteria peaked at the beginning of SE20. In the first attempt there were higher amounts of planctomycetes, confirming their important role in decay processes (Das et al., 2008). Acidimicrobiia are a class of species with an abundant appearance in aquatic and marine ecosystems and, so far, they cannot be distinguished from other species in this class (Hu et al., 2019). Clostridia content was higher in WE20, and actinobacteria towards the end. Desulfobulbia represent an anaerobic organism within the 16S rDNA community; litterbags during WE20 silted up during autumn storms, most likely having caused anoxic conditions, favoring desulfobulbia (Kuever et al., 2005; Galushko & Kuever, 2019). Anaerobic conditions are said to slow down nitrogen mobilization during decay (Melillo et al., 1984). Planctomycetes during SE20 point towards faster decay of seagrass during the warm season, representing key factors in carbon and nitrogen cycling (Wiegand et al., 2018). These conditions, combined with the higher fraction of Polyangia, known to play a vital role in the degradation of polymeric lignin (Li et al., 2022), could have broken down seagrass' outer structure. Both classes were present in considerably low amounts in WE20, hence slowing down decay. In both experiments *Shewanella* was present, being able to live as a facultative anaerobic organism (e.g., *S. oneidensis*) (Jiang et al., 2020) In winter its abundance was higher than in summer. Its ability to degrade organic matter (Jiang et al., 2020), might explain the faster decay, especially during the initial 48 days of WE20. Species of *Arcobacter* (*A. nitrofigilis*) have been isolated from roots of salt marsh plants in a brackish lake (Fera et al., 2004). *A. sulfidicus* has been proven to be an autotrophic filamentous sulfur producer by sulfide oxidization in coastal marine waters

(Fera et al., 2004). This supports the results of the differential abundant genera analysis with the high abundance of *A. nitrofigilis_1* in summer. In differential abundant pathways associated sulfur metabolism is shown in SE20. During WE20 there were less Ascomycota compared to SE20, but an abundance of *Methylotenera* (β Proteobacteria) was higher than in summer. *Methylotenera* are known to have exceptional antifungal effects (He et al., 2022), which is why an interspecific suppression might have happened. These results are additionally supported by the FAPROTAX (Functional Annotation of Prokaryotic Taxa) analysis, reflecting ecological and metabolic functions towards the microbial community. In SE20 oxygenic photo(auto)trophy, cyanobacteria and chloroplasts dominated, in WE20 nitrate respiration, reduction and methylotrophy occurred. Dark sulfur and sulfite oxidation, and fermentation happened. Chloroplasts vanished in WE20 after the initial phase of one week. Aerobic chemoheterotrophy and chloroplast, pointing towards photosynthetic activity, dominated SE20 whereas in WE21 fermentation, reductional and oxidational processes together with N respiration were higher (Figure 34). This refers to the important role of light and oxygen availability during decomposition processes, and is confirmed by the results of the correlations between OTUs and physicochemical factors: Here, all OTUs except of Hyphomonadaceae_6 are negatively correlated with temperature, but positively with light (Figure 36).

Comparing microbial analysis of seasonal attempts, the bacterial composition of SE20 and WE20 were reflected. Bacili, planctomycetes and cyanobacteria were most present in SSu20, primarily in white bags, but no desulfobulbia were present. Acidimicrobiia and Actinobacteria were most present in SAu20 and SWi21. Unclassified bacteria occurred less in these experiments which might be interpreted that those classified bacteria are water-bound; as litterbags alternated, they might have lacked constant water availability. Verrucomicrobiae reflected an annual pattern within the seasons. Looking from the alternating experiments perspective it seems that the Bacteroidia class must be water related as they decreased on land: back in the water, they returned. Similar patterns occurred for alpha and gamma proteobacteria. Gamma Proteobacteria started with high levels, which constantly decreased. There were no differences between black and white treatment, or when being transferred from water to land and vice versa. Bacteroida had higher levels during exposure to water and decreased on land, particularly during SSu20. Cyanobacteria were abundant within white bags. This can be explained by being photoautotrophic (Zavřel et al., 2015). Bacilli were highest present in SSu20 in white bags during decay on land. As endospores of *Bacillus* spp. have been proven to be resistant against extreme environments, they might have outlasted the aquatic periods

(Nicholson et al., 2000). Planctomycetes reduced from SSu20 towards SWi21 in abundance. Remaining classes of 16S rDNA did not show a pattern towards specific growth requirements.

Analysis of eukaryotic 18S rDNA within constant aquatic exposure showed a high abundance for Annelida after 28 days in SE20. This can be explained by an approx. 5 cm long estuary ragworm *Nereis diversicolor* in the bag. Although not visually recognizable, there was another peak after 140 days which remains unexplained. During late winter and spring there were high proportions of Bacillariophyta, most probably reflecting their spring bloom in the Baltic Sea during this season (Klais et al., 2011; Wasmund et al., 2013; Spilling et al., 2018). Furthermore, diatoms settle epiphytic on seagrass leaves (Chung & Lee, 2008; Michael et al., 2008). Arthropoda, cnidaria, nematoda and mollusca were omnipresent: Maybe reproductive material was left on the seagrass leaves. As typical grazer (Lewis & Hollingworth, 1982) they might have been responsible for physical breakdown and partial weight loss. During seasonal experiments, Embryophyceae, a class of land plants, reached a peak in winter (SWi21) and spring (SSp21). Reasons might be their blooming during summer and the drift of pollen and seeds. Euglenozoa (SAu20), needing heterotrophic conditions (Tobias-Hünefeldt et al., 2020), might have depended on the primary establishment of a microbial community. Labyrinthulomycetes and unclassified fungi had higher abundances in autumn (SAu20) and spring (SSp21) than in winter (SWi20). They are important species for the decay of leaf litter material in aquatic environments. They make nutrients available to higher trophic levels (Sinsabaugh & Linkins, 1990; Das et al., 2008). Algal species like phaeophytes and Ulvophyceae were present in spring and summer. Starting in summer seems to accelerate decomposition leaving almost no remains. In winter, a minor residue was left.

No direct pattern can be seen when trying to explain weight differences between terrestrial and aquatic phases in seasonal experiments; during the first week in water weight increased in white bags, and decreased in the following week on land. Back in the water, weight dropped in week three. In the fourth week, on land, weight increased again. From week five on weight remained stable in both environments. A detrimental community might need a certain period to develop and be able to act effectively. The short-term changes between aquatic and terrestrial conditions might have prevented the formation of an effective decomposition community. Regarding conductivity the changing conditions might have been an additional challenge to establish a detrimental association (Carstensen & Conley, 2019). The results seem to prove a dependency on water within the microbial community.

Through SSu20 biomass in the white bags increased by 0.005 d^{-1} , in the black bags was decay with -0.006 d^{-1} . Decay in SAu20 was faster in white bags. Black bags kept weights nearly unchanged. Overall degradation seemed to be faster with light, which is underpinned by the PCA (Figure 22). Still, in summer weight was gained. Comparing mesh color treatments for SAu20, the rate of decay rate in black bags was higher with -0.0023 d^{-1} compared to -0.0015 d^{-1} in white bags. Therefore, decay under dark conditions was higher by a factor of ca. 1.5. The same effect was seen in SWi21: the decay coefficient in black bags was almost double (-0.0061 d^{-1}) compared to white bags (-0.0038 d^{-1}). The influence of temperature might be crucial, contradicting the thesis that higher temperatures promote faster decay (Godshalk & Wetzel, 1978c). But the experiments of Lastra et al. (2014) proved under cold, wet and arctic conditions the fast decay of up to 40 % within the initial days. SSp21 showed stable weights in black bags, with decay in first two weeks in white bags. Afterwards the bags reached a plateau, and gained new weight after five weeks. The theory of auto-trophic organisms colonizing seagrass leaves during times of high light availability is supported. Black bags had weight gain, and therefore a negative decay value of 0.0002 d^{-1} , white bags real decay with -0.0001 d^{-1} (both SSp21). In every season white bags gained weight within the first week in water, underpinning the theory that fresh and green seagrass litter might continue to photosynthesize and gain weight during the initial stage of decay (Robertson, 1982). An increase in the respiration rate through death and senescence might contribute here (Bidwell, 1974). After this initial week weight decreased, till week four. Another peak in degradation was after the fifth week in water. With the exception of SSu20, where weight gain continued during the last week on land, in all other treatments weight dropped on land. Generally lower decomposition in white bags might be explained by settlement of autotrophic organisms. No explanation for weight gain during the last week in black bags in spring can be given. Through reduced light, primary production has to be questioned. Decay in black bags was overall negative at first. However, from week four this was reversed in water. It was lower by a factor of 24 when transferred to land. It changed from 0.024 d^{-1} to a value of 0.001 d^{-1} . This development suggests a dependency towards an exposure to water, confirming research stating that, during the initial phase of leaching, rapid microbial growth can be determined (Robertson, 1982; Kenworthy & Thayer, 1984; Blum & Mills, 1991). Despite this, phenolic compounds in seagrasses leachates are said to inhibit microbial growth (Harrison & Chan, 1980; Murray & Hodson, 1986).

Changes of dry weight in SE20 and SW20 showed that the initial weight was virtually stable for the first two weeks. Comparison with previous research is challenging. This has been conducted under laboratory conditions and with pre-dried seagrass material (Pellikaan, 1984).

A slow decomposition was expected as seagrass possesses high concentrations of structural tissue, namely cellulose, hemicellulose and lignin to a total of more than 50 % of its biomass composition (Godschalk & Wetzel, 1978a). After the initial two weeks weight was constantly increasing, reaching an almost quadrupled weight after three weeks. Hence, fresh seagrass leaves did not directly decompose but gained weight by e.g., attracting microbial grazers. The formation of a biofilm, in addition with water flowing through the litterbags, favored binding of sediments. That might have changed structure and resulted in weight gain (Gerbersdorf et al., 2020). Following the (physical) breakdown of leaves, nutrients can translocate among litter of varying degrees of decomposition, resulting in a more rapid and efficient utilization of litter substrate to grazers (Seastedt, 1984). Especially in SE20, a settlement with phototrophic organisms was assumed. But seagrass plants are thought to produce antialgal allelochemicals (Harrison, 1982) and natural biocides (Lamb et al., 2017) during their life. If and to which extent these defense mechanisms and photosynthesis continue to work after leaf senescence is not fully understood yet. After 42 days weight started to drop and decomposition set in. Visual leaf litter breakdown was apparent. This shredding into palatable biomass might have induced delayed microbial digestion, as it is known from vascular plants (Moran & Hodson, 1989). Complete decay within 210 days reflects similar results from Walker & McComb (1985), stating a total time of 200 days for a complete seagrass (*Amphibolis antarctica* and *Posidonia australis*) decomposition (Walker & McComb, 1985).

Decay is predicted to be marginally faster during summer. Previous research by Trevathan-Tackett et al. (2020) proved that microbial breakdown is temperature dependent in seagrass leaves and higher temperatures promote faster decay. Similarities and differences can be seen between starting the experiment in summer (SE20) or winter (WE20). Both experiments were finished after 210 days. Higher decay rates appeared in SE20, with almost empty bags after 140 days. Decay coefficients were calculated, resulting in -0.014 d^{-1} for SE20, -0.004 d^{-1} in WE20. This underpinned the temperature dependency of decay (Pellikaan, 1984; Seastedt, 1984; Moran & Hodson, 1989). Calculated decay coefficients would result in a residue of -0.002 g after 140 days in SE20, sustaining almost empty bags after 140 days. Adapting to WE20, residue should be at 0.006 g after 210 days. With a little sludgy biomass, it can be seen as proven, too. Therefore, the exponential decay model of Petersen & Cummins (1974) seems to be applicable for seagrass decay in the Baltic Sea. The gained results correspond to previous research: *Zostera marina* is decaying much slower than e.g., freshwater angiosperms (Godschalk & Wetzel, 1978a, 1978b). It was proven that, for decomposition processes, a certain temperature and an aerobic environment is vital (Godshalk & Wetzel, 1978c). Harsh

environmental habitat conditions of *Z. marina* are hypothesized to be responsible for its slow decay. The ultrastructure of its tissue is adapted accordingly (Godshalk & Wetzel, 1978c). Limiting decay factors are temperature, followed by dissolved oxygen and nutrient availability etc. (Godshalk & Wetzel, 1978c). During spring and summer increasing temperatures promote decay with higher degrees (Godshalk & Wetzel, 1978c). In the seasonal experiments, temperatures showed similar values in SAu20 (11.07 °C) and SSp21 (12.45 °C), with low temperatures in SWi21 (2.06 °C) and average temperatures in SSu20 that were tenfold higher (21.06 °C). Temperature and light are parallel. With the experiments being conducted in temperate latitudes this reflects the annual cycle. Here gained results indicate a dependency on temperature; but only minor differences of disintegration at low or higher temperatures have been seen (Figure 26). Especially in SE20 the rate of decay is higher in warmer temperatures between 42 and 84 days whereas it is the opposite in WE21, where gains rather than reductions in weight can be seen (Figure 19). Oxygen as a variable has not been measured.

For possible explanations of the development of the microbial community as well as predictions of decomposition other than abiotic parameters (Batistel et al., 2021), C:N ratios were measured. Hereby, the Redfield ratio describes the proportions of the atomic composition of marine phytoplankton if nutrients were available in unlimited quantities (Redfield, 1934). It consists of C, N and P. Here, only C and N were measured. Due to their photosynthetic activities, benthic macroalgae and seagrasses vary greatly from the Redfield ratio in their C and N composition, giving a hint towards the ecological significances of this marine plant biomass (Atkinson & Smith, 1983). Whereas marine algae are said to have a C:N ratio of approx. 0–5, vascular plant debris from coastal marine sediments range from between 30 to 40 (Meyers, 1994). The C:N ratio is said to increase when seagrass leaves are left to decay (Holmer & Bachmann-Olsen, 2002). Previous experiments have shown that seagrass decay is divided into three phases: first with leaching of soluble C_{org}, followed by bacterial decomposition of sugar, storage and structural carbohydrates, and finally bacterially limited decay through lignin and lignocellulose (Kirschbaum, 1995; Landgraf et al., 2006; Satoh & Shigeki, 2022). Hereby the second phase is expected to be terminated within several months (Harrison & Mann, 1975; Buchsbaum et al., 1990; Blum & Mills, 1991). It is known that the initial plant litter quality is of crucial importance for the rate of decay, especially when rich in nitrogen and low in lignin (Melillo et al., 1984). Here the time of harvesting is important. Seagrass flowers between spring and summer, having its biomass peak (Blok et al., 2018). Additionally, the C:N ratio is, in relative terms, higher in reproductive than in vegetative shoots (Wada et al., 2022). High N concentrations in seagrass have been observed when seagrass is picked in the winter months

(Pirc & Wollenweber, 1988). In the experiments carried out here, only seagrass leaves were used. The following discussed C:N ratios have been calculated based on the values from Table A 8 to Table A 13.

The seasonal course of seagrass production is reflected in the experiments with ca. 25 M/M in SE20 and ca. 15 M/M in WE20. The initial quality of the seagrass might be one responsible factor for the development of the long-term experiments. A steady decline through SE20 was shown. In the SE20 experiment, C:N starts with 22:1 and remains stable through the first three weeks, before lowering to 14:1 ($\pm 2:1$) after 56 days, where it remains for the rest of the experiment. The ratio constantly increased in WE20 with 12:1 ($\pm 2:1$) for the first 42 days. Most likely epibiota were binding nutrients, shredding leaf surfaces and making more C:N available through their settlement. The C:N ratio increased from 56 days (17:1) till 140 days (24:1). For last sampling after 210 days C:N is reduced to 18:1. A possible explanation for the rise during WE20 might be a different initial quality of seagrass leaves. Also, seagrass samples have not been washed prior to C:N analysis giving a chance to include all epiphytes and the biofilm. In the last sampling not much biomass was left, and through the burial of the litterbags organic matter from the sediment might have falsified the result. The conducted PCA (Figure 22) further supports the thesis that light, temperature and C:N ratio are the driving factors during decay as PC1 explains more than 53 % of the variability. The final fractioning of the two experiments is explained by the conductivity. The same can be seen in the cluster analysis (Figure 24) where SE20 and WE21 are strictly separated by the respective experiment starting point. In the nMDS plot (Figure 23) it can be seen that the C:N ratio explains the variability within the individual experiments; the axis of C:N runs through SE20 more or less horizontal and separates WE21. The variability of C:N is therefore, larger in SE20, reflecting the higher decay ratios in this experiment. On the other hand, the individual experiments are separated vertically by light, temperature and conductivity. In seasonal experiments the C:N ratio developed differently: in SSu20 there was a steady decline from 27:1 to 18:1 ($\pm 2:1$), SAu20 and SSp21 remained stable ($21:1 \pm 3:1$) and in SWi21 the ratio increased ($15:1 \pm 3:1$), highlighting the relevancy of temperature during the immobilization of nitrogen through decay of plant litter (Melillo et al., 1984). Light availability during the growth of seagrass has an impact towards a higher C:N ratio, too. Nevertheless, this cannot be transferred directly to the decay. There was no difference between litterbags exposed to dark (black mesh) or light (white mesh) conditions. The C:N ratio increased during aquatic periods, with declining values in a terrestrial environment, hinting towards a preferential degradation of N-compounds in an aquatic environment (SSu20). No

clear difference in the development of C:N could be given to a treatment under light or dark conditions.

Previous research on land stated the relevancy of nitrogen especially from *Posidonia oceanica* for vegetated areas (Cardona & García, 2008). However, relating the hypothesis to the aquatic environment, the N-relevancy might be explained by occurrences of epibiota through seasonal changes and the C:N ratio reflects the nutritional value of senescent seagrass leaves (De Los Santos et al., 2012) suggesting its nutritional significance to epibiotic organisms and microbial settlement. Uptake from microalgae is expected (Eyre & Ferguson, 2002) which might have been confirmed by these experiments. Possible varying values of the initial quality might have had the biggest influence on the subsequent decay rate (Melillo et al., 1984). Remineralization of seagrass litter and the thereof gained organic matter to sediments affects the changes in microbial communities towards N-fixation and leads to greater biochemical activity, especially in sediments (Fraser et al., 2016). This enrichment paired with the silting up of the litterbags might have changed the microbial structure towards a more anaerobic community. Increases in the C:N ratio in winter might indicate improved primary production. In contrast, there is reduced light availability. The mixing of the water column and, therefore, redistribution of nutrients might play another role during decay. The results of the PCA with an Eigenvector of -0.559 (PC1), and the nMDS plot underlines the decisive role of the C:N ratio during the settlement with microbial grazer as well as the rate of decay of seagrass. Finally, and with respect to chapter 3.5, the abiotic parameters during the decay of seagrass are of crucial importance. Possible decisive factors for the decay of seagrass seem to be a) the part of the plant, whether leaf, root or flower (Wada et al., 2022) and b) the point when harvested (Pirc & Wollenweber, 1988; Blok et al., 2018) as the nutritional value varies greatly (Wada et al., 2022). Nitrogen rich, and lignin poor material and elevated temperatures foster decay (Melillo et al., 1984). This partly contradicts the results seen here as N contents in SE20 were initially half the amount (1.57 %) compared to WE21 (2.84 %). The lignin content cannot be commented upon as it was not measured. The decay itself seems to be contrary to the temperature in the Baltic Sea. Here, the SE20 experiment, terminating in winter 21, had very few remains whereas the WE21, terminating in summer 21, had more residue in the respective litterbags. Seasonal experiments had too short a runtime to make any conclusive statement. But in the short time available, again winter has the highest rate of decay of all the seasonal experiments that were conducted. In these experiments the influence of light is particularly clearly shown as the higher decomposition rates were obtained in the black litterbags with reduced light availability. Only autumn had higher decay rates in white rather than black litterbags.

5 Conclusion & Outlook

The whole series of experiments worked out and delivered valuable data and information on beach wrack, its life cycle and decay. In terms of current understanding of the topic, it was the first long-term series of experiments in-situ.

Based on the findings the first thesis: **Beach wrack landings on the Baltic Sea coast are mainly influenced by the seasons regarding amounts and species composition** can be accepted. It was shown that beach wrack follows a specific seasonality both, in terms of amounts and species composition.

The second thesis: **There are differences between the decay characteristics of beach wrack on land and in the water** is accepted for the experiment setup as done here. Nevertheless, this could only be proven for pure seagrass litter.

The third and last thesis: **Abiotic factors influence the quantitative and qualitative microbial community composition** can be accepted: species composition and quantitative microbial community showed significant differences between experiments starting in summer or winter. Shifts in the microbial community during seasonal experiments can be seen both between land or water exposure as well as among exposure to dark or light conditions. In these experiments the distinctions are less pronounced than in the constant water treated experiments.

Experiments conducted within this thesis have gained valuable data towards a better understanding of beach wrack landings and decay dynamics. In additional research, further focus should be put on the influence of abiotic parameters like wind, wave heights and approaching directions as well as to water levels. This might result in more precise predictions towards drifted biomass from other areas of the Baltic Sea. A chance to develop a model with predictions of beach wrack landings could be given.

Decomposition processes need more research and a better comparison in future attempts. Not specifically seagrass, but beach wrack of local species composition should be used for further experiments. Hence, in the future decay both in aquatic and terrestrial environments should be examined with the same type of species. The approach to compare the decay of algal biomass on land with seagrass in the water column raises further questions. Especially as seagrass is a vascular plant with other physical properties (lignin, hemi-cellulose and cellulose in its cell walls), it cannot be directly compared to algae. Furthermore, mesh size of the litterbags should be the same to include or exclude same grazer in both environments. As changes in sea levels are thought to have a major influence on decay processes (Nicastro et al., 2012), more research

needs to be conducted towards exposure to aquatic conditions. On the hydrodynamic changing Baltic Sea coast, changes towards higher water levels might make a pivotal difference when assessing decomposition processes in the future. Attempts with a controlled decay under laboratory conditions might be helpful to evaluate and manipulate individual factors. The question about the role of beach wrack in adding nutrients to beaches and coastal waters could not be answered in this context and has left gaps in knowledge to be filled in additional research. The subjacent layer under litterbags should be sampled for its rise or fall in e.g., organic matter content, and to gain insight into nutrient leaching. To prevent the silting up of litterbags under water, re-lifting bags e.g. in a monthly pattern could be done. The basic idea of evaluating the microbial processes during decay showed interesting results, yet in further research replicates should be increased. To secure C:N results, in a future attempt seagrass leaves from different seasons should be analyzed initially. The composition of organic and inorganic compounds might change between seasons, providing different, seasonal raw material. As the C:N ratio increased during aquatic periods, these should be extended. For better comparability experiments should run water to land and at the same time vice versa. This would ensure complete datasets at any stage within any treatment throughout subsequent experiments. Sudden changes especially to conditions on land could be better considered for this.

With regards to beach management strategies this research can conclude that beach wrack will most likely disintegrate faster in water than when left on land. The high amounts of sand within wrack are confirmed. The present technique of pre-washing wrack in shallow water seems to be the best to remove gross sediment weight. As complete decay of seagrass takes about 210 days of time when left in the water, and algal biomass – especially when buried – outlasts the period of a full year, management strategies need to be maintained for recreationally used beaches. Nutrient leaching during initial decay requires quick removal to prevent back-flow into the shallow waters. A potentially high enrichment of the water leading to massive algal blooms and anoxic lagoons around the Baltic Sea beaches might be avoided. This hypothesis requires further research. With consideration of all the examined aspects, beach wrack remains a natural element of a healthy coastline. It is a vital part of the beach ecosystem, giving shelter and food to vertebrates and invertebrates and acts as a natural protection against sand removal by consolidating the beach with incorporated biomass. Pristine and untreated beach sections need to be conserved and, in the interests of both nature and humanity, a nature-compatible handling of beaches has to be established.

6 References

- Aerts, R. (1997). Climate, Leaf Litter Chemistry and Leaf Litter Decomposition in Terrestrial Ecosystems: A Triangular Relationship. *Oikos*, 79(3), 439. <https://doi.org/10.2307/3546886>
- Ainley, L. B., & Bishop, M. J. (2015). Relationships between estuarine modification and leaf litter decomposition vary with latitude. *Estuarine, Coastal and Shelf Science*, 164, 244–252. <https://doi.org/10.1016/j.ecss.2015.07.027>
- Almqvist, J., Bretz, T., & Fondahn, Å. (2021). Beach wrack in a business environment: Guidance and inspiration towards increased resource utilization based on innovative treatment options, Report of the Interreg Project CONTRA, Kristianstad, 40 pp. *Interreg Baltic Sea Region Project CONTRA*.
- Amir, A., McDonald, D., Navas-Molina, J. A., Kopylova, E., Morton, J. T., Zech Xu, Z., Kightley, E. P., Thompson, L. R., Hyde, E. R., Gonzalez, A., & Knight, R. (2017). Deblur Rapidly Resolves Single-Nucleotide Community Sequence Patterns. *mSystems*, 2(2), e00191-16. <https://doi.org/10.1128/mSystems.00191-16>
- Andersen, J. H., Carstensen, J., Conley, D. J., Dromph, K., Fleming-Lehtinen, V., Gustafsson, B. G., Josefson, A. B., Norkko, A., Villnäs, A., & Murray, C. (2017). Long-term temporal and spatial trends in eutrophication status of the Baltic Sea: Eutrophication in the Baltic Sea. *Biological Reviews*, 92(1), 135–149. <https://doi.org/10.1111/brv.12221>
- Atkinson, M. J., & Smith, S. V. (1983). C:N:P ratios of benthic marine plants1. *Limnology and Oceanography*, 28(3), 568–574. <https://doi.org/10.4319/lo.1983.28.3.0568>
- Balestri, E., Vallerini, F., Seggiani, M., Cinelli, P., Menicagli, V., Vannini, C., & Lardicci, C. (2019). Use of bio-containers from seagrass wrack with nursery planting to improve the eco-sustainability of coastal habitat restoration. *Journal of Environmental Management*, 251, 109604. <https://doi.org/10.1016/j.jenvman.2019.109604>
- Bärlocher, F. (2005). Leaf Mass Loss Estimated by Litter Bag Technique. In M. A. S. Graça, F. Bärlocher, & M. O. Gessner (Eds.), *Methods to Study Litter Decomposition* (pp. 37–42). Springer-Verlag. https://doi.org/10.1007/1-4020-3466-0_6
- Barreiro, F., Gómez, M., Lastra, M., López, J., & De La Huz, R. (2011). Annual cycle of wrack supply to sandy beaches: Effect of the physical environment. *Marine Ecology Progress Series*, 433, 65–74. <https://doi.org/10.3354/meps09130>
- Batistel, C. C., Jurasinski, G., & Schubert, H. (2021). Salinity exerted little effect on decomposition of emergent macrophytes in coastal peatlands. *Aquatic Botany*, 175, 103446. <https://doi.org/10.1016/j.aquabot.2021.103446>
- Behbehani, M. I., & Croker, R. A. (1982). Ecology of beach wrack in northern New England with special reference to *Orchestia platensis*. *Estuarine, Coastal and Shelf Science*, 15(6), 611–620. [https://doi.org/10.1016/0272-7714\(82\)90075-0](https://doi.org/10.1016/0272-7714(82)90075-0)

- Bengtsson, M. M., Bühler, A., Brauer, A., Dahlke, S., Schubert, H., & Blindow, I. (2017). Eelgrass Leaf Surface Microbiomes Are Locally Variable and Highly Correlated with Epibiotic Eukaryotes. *Frontiers in Microbiology*, 8, 1312. <https://doi.org/10.3389/fmicb.2017.01312>
- Bianchi, T. S., & Findlay, S. (1991). Decomposition of Hudson Estuary Macrophytes: Photosynthetic Pigment Transformations and Decay Constants. *Estuaries*, 14(1), 65. <https://doi.org/10.2307/1351983>
- Bidwell, R. G. S. (1974). Physiology of plant under stress. *Plant Physiology*, 563–576.
- Bird, E. C. F. (1996). Lateral Grading of Beach Sediments: A Commentary. *Journal of Coastal Research*, 12(3), 774–785.
- Blok, S., Olesen, B., & Krause-Jensen, D. (2018). Life history events of eelgrass *Zostera marina* L. populations across gradients of latitude and temperature. *Marine Ecology Progress Series*, 590, 79–93. <https://doi.org/10.3354/meps12479>
- Blum, L., & Mills, A. (1991). Microbial growth and activity during the initial stages of seagrass decomposition. *Marine Ecology Progress Series*, 70, 73–82. <https://doi.org/10.3354/meps070073>
- Bonsdorff, E. (2006). Zoobenthic diversity-gradients in the Baltic Sea: Continuous post-glacial succession in a stressed ecosystem. *Journal of Experimental Marine Biology and Ecology*, 330(1), 383–391. <https://doi.org/10.1016/j.jembe.2005.12.041>
- Bonsdorff, E., Blomqvist, E. M., Mattila, J., & Norkko, A. (1997). Coastal eutrophication: Causes, consequences and perspectives in the Archipelago areas of the northern Baltic Sea. *Estuarine, Coastal and Shelf Science*, 44, 63–72. [https://doi.org/10.1016/S0272-7714\(97\)80008-X](https://doi.org/10.1016/S0272-7714(97)80008-X)
- Booth, E. (1964). Trace elements and seaweeds. *Proceeding of the 4th International Seaweed Symposium*. Macmillan, London, 385–393.
- Borum, J., Duarte, C. M., Greve, T. M., & Krause-Jensen, D. (2004). *European seagrasses: An introduction to monitoring and management*. M & MS project. https://www.academia.edu/download/40966373/EuropeanSeagrasses_high.pdf
- Braune, W. (2008). Meeresalgen: Ein Farbbildführer zu verbreiteten benthischen Grün-, Braun-und Rotalgen der Weltmeere. (No Title). <https://cir.nii.ac.jp/crid/1130282271944764416>
- Brown, A. C., & McLachlan, A. (2010). *The ecology of sandy shores*. Elsevier. <https://books.google.com/books?hl=de&lr=&id=Y4V5a6Ro3l0C&oi=fnd&pg=PP1&dq=brown+%26+mclachlan+2010&ots=opc9yER2L&sig=RklTS0qllt0e7qi4DuatVO7FeDs>
- Buchsbaum, R. N., Short, F. T., & Cheney, D. P. (1990). Phenolic-nitrogen interactions in eelgrass, *Zostera marina* L.: Possible implications for disease resistance. *Aquatic Botany*, 37(3), 291–297. [https://doi.org/10.1016/0304-3770\(90\)90075-V](https://doi.org/10.1016/0304-3770(90)90075-V)
- Callahan, B. J., McMurdie, P. J., Rosen, M. J., Han, A. W., Johnson, A. J. A., & Holmes, S. P. (2016). DADA2: High-resolution sample inference from Illumina amplicon data. *Nature Methods*, 13(7), 581–583. <https://doi.org/10.1038/nmeth.3869>

- Caporaso, J. G., Ackermann, G., Apprill, A., Bauer, M., Berg-Lyons, D., Betley, J., Fierer, N., Fraser, L., Fuhrman, J. A., & Gilbert, J. A. (2018). *EMP 16S Illumina amplicon protocol*. <https://www.protocols.io/view/emp-16s-illumina-amplicon-protocol-nuudeww.html>
- Cardona, L., & García, M. (2008). Beach-cast seagrass material fertilizes the foredune vegetation of Mediterranean coastal dunes. *Acta Oecologica*, *34*(1), 97–103. <https://doi.org/10.1016/j.actao.2008.04.003>
- Carstensen, J., & Conley, D. J. (2019). Baltic Sea Hypoxia Takes Many Shapes and Sizes. *Limnology and Oceanography Bulletin*, *28*(4), 125–129. <https://doi.org/10.1002/lob.10350>
- Chubarenko, B., Woelfel, J., Hofmann, J., Aldag, S., Beldowski, J., Burlakovs, J., Garrels, T., Gorbunova, J., Guizani, S., Kupczyk, A., Kotwicki, L., Domnin, D., Gajewska, M., Hogland, W., Kotecka, K., Nielsen, J., & Schubert, H. (2021). Converting beach wrack into a resource as a challenge for the Baltic Sea (an overview). *Ocean & Coastal Management*, *200*, 105413. <https://doi.org/10.1016/j.ocecoaman.2020.105413>
- Chung, M.-H., & Lee, K.-S. (2008). Species composition of the epiphytic diatoms on the leaf tissues of three *Zostera* species distributed on the southern coast of Korea. *Algae*, *23*(1), 75–81.
- Clarke, K. R., & Gorley, R. N. (2015). Getting started with PRIMER v7. *PRIMER-E: Plymouth, Plymouth Marine Laboratory*, *20*(1).
- Clarke: *User manual/tutorial—Google Scholar*. (2001). https://scholar.google.com/scholar_lookup?&title=PRIMER%20v5%3A%20User%20Manual%2FTutorial&publication_year=2001&author=Clarke%2CK.%20R.&author=Gorley%2CR.%20N.
- Cole, A. J., Paul, N. A., De Nys, R., & Roberts, D. A. (2017). Good for sewage treatment and good for agriculture: Algal based compost and biochar. *Journal of Environmental Management*, *200*, 105–113. <https://doi.org/10.1016/j.jenvman.2017.05.082>
- Colombini, I., Chelazzi, L., Gibson, R. N., & Atkinson, R. J. A. (2003). Influence of marine allochthonous input on sandy beach communities. *Oceanography and Marine Biology: An Annual Review*, *41*, 115–159.
- Colombini, I., Mateo, M. Á., Serrano, O., Fallaci, M., Gagnarli, E., Serrano, L., & Chelazzi, L. (2009). On the role of *Posidonia oceanica* beach wrack for macroinvertebrates of a Tyrrhenian sandy shore. *Acta Oecologica*, *35*(1), 32–44. <https://doi.org/10.1016/j.actao.2008.07.005>
- Costanza, R., d'Arge, R., De Groot, R., Farber, S., Grasso, M., Hannon, B., Limburg, K., Naeem, S., O'Neill, R. V., & Paruelo, J. (1997). The value of the world's ecosystem services and natural capital. *Nature*, *387*(6630), 253–260.
- Cummins, K. W., Spengler, G. L., Ward, G. M., Speaker, R. M., Ovink, R. W., Mahan, D. C., & Mattingly, R. L. (1980). Processing of confined and naturally entrained leaf litter in a woodland stream ecosystem. *Limnology and Oceanography*, *25*(5), 952–957. <https://doi.org/10.4319/lo.1980.25.5.0952>

- Das, M., Royer, T. V., & Leff, L. G. (2008). Fungal communities on decaying leaves in streams: A comparison of two leaf species. *Mycological Progress*, 7(4), 267–275. <https://doi.org/10.1007/s11557-008-0569-x>
- Davenport, J., & Davenport, J. L. (2006). The impact of tourism and personal leisure transport on coastal environments: A review. *Estuarine, Coastal and Shelf Science*, 67(1–2), 280–292. <https://doi.org/10.1016/j.ecss.2005.11.026>
- Davis, T. J., & Keppel, G. (2021). Fine-scale environmental heterogeneity and conservation management: Beach-cast wrack creates microhabitats for thermoregulation in shorebirds. *Journal of Applied Ecology*, 58(6), 1291–1301. <https://doi.org/10.1111/1365-2664.13865>
- De Falco, G., Simeone, S., & Baroli, M. (2008). Management of Beach-Cast *Posidonia oceanica* Seagrass on the Island of Sardinia (Italy, Western Mediterranean). *Journal of Coastal Research*, 4, 69–75. <https://doi.org/10.2112/06-0800.1>
- De Los Santos, C., Brun, F., Onoda, Y., Cambridge, M., Bouma, T., Vergara, J., & Pérez-Lloréns, J. (2012). Leaf-fracture properties correlated with nutritional traits in nine Australian seagrass species: Implications for susceptibility to herbivory. *Marine Ecology Progress Series*, 458, 89–102. <https://doi.org/10.3354/meps09757>
- Deidun, A., Saliba, S., & Schembri, P. J. (2009). Considerations on the Ecological Role of Wrack Accumulations on Sandy Beaches in the Maltese Islands and Recommendations for Their Conservation Management. *Journal of Coastal Research*, , Special Issue No. 56. *Proceedings of the 10th International Coastal Symposium ICS 2009*, 410–414.
- Del Vecchio, S., Jucker, T., Carboni, M., & Acosta, A. T. R. (2017). Linking plant communities on land and at sea: The effects of *Posidonia oceanica* wrack on the structure of dune vegetation. *Estuarine, Coastal and Shelf Science*, 184, 30–36. <https://doi.org/10.1016/j.ecss.2016.10.041>
- Dizon, R. M., & Yap, H. T. (1999). Short-term responses of coral reef microphytobenthic communities to inorganic nutrient loading. *Limnology and Oceanography*, 44(5), 1259–1267. <https://doi.org/10.4319/lo.1999.44.5.1259>
- Duarte, C. (1990). Seagrass nutrient content. *Marine Ecology Progress Series*, 67, 201–207. <https://doi.org/10.3354/meps067201>
- Duarte, C. M., Losada, I. J., Hendriks, I. E., Mazarrasa, I., & Marbà, N. (2013). The role of coastal plant communities for climate change mitigation and adaptation. *Nature Climate Change*, 3(11), 961–968. <https://doi.org/10.1038/nclimate1970>
- Dugan, J. E., & Hubbard, D. M. (2010). Loss of Coastal Strand Habitat in Southern California: The Role of Beach Grooming. *Estuaries and Coasts*, 33(1), 67–77. <https://doi.org/10.1007/s12237-009-9239-8>
- Dugan, J. E., Hubbard, D. M., McCrary, M. D., & Pierson, M. O. (2003). The response of macrofauna communities and shorebirds to macrophyte wrack subsidies on exposed sandy beaches of southern California. *Estuarine, Coastal and Shelf Science*, 58, 25–40. [https://doi.org/10.1016/S0272-7714\(03\)00045-3](https://doi.org/10.1016/S0272-7714(03)00045-3)

- Dugan, J. E., Hubbard, D. M., Rodil, I. F., Revell, D. L., & Schroeter, S. (2008). Ecological effects of coastal armoring on sandy beaches. *Marine Ecology*, 29(s1), 160–170. <https://doi.org/10.1111/j.1439-0485.2008.00231.x>
- Estaki, M., Jiang, L., Bokulich, N. A., McDonald, D., González, A., Kosciolk, T., Martino, C., Zhu, Q., Birmingham, A., Vázquez-Baeza, Y., Dillon, M. R., Bolyen, E., Caporaso, J. G., & Knight, R. (2020). QIIME 2 Enables Comprehensive End-to-End Analysis of Diverse Microbiome Data and Comparative Studies with Publicly Available Data. *Current Protocols in Bioinformatics*, 70(1), e100. <https://doi.org/10.1002/cpbi.100>
- Eyras, M. C., Rostagno, C. M., & Defossé, G. E. (1998). Biological Evaluation of Seaweed Composting. *Compost Science & Utilization*, 6(4), 74–81. <https://doi.org/10.1080/1065657X.1998.10701943>
- Eyre, B., & Ferguson, A. (2002). Comparison of carbon production and decomposition, benthic nutrient fluxes and denitrification in seagrass, phytoplankton, benthic microalgae- and macroalgae-dominated warm-temperate Australian lagoons. *Marine Ecology Progress Series*, 229, 43–59. <https://doi.org/10.3354/meps229043>
- Feldner, J. (1976). *Ökologische und produktionsbiologische Untersuchungen am Seegrass Zostera marina L. in der Kieler Bucht (westliche Ostsee)* [PhD Thesis, Christian-Albrechts-Universität Kiel]. <https://oceanrep.geomar.de/id/eprint/40098>
- Fera, M. T., Maueri, T. L., Gugliandolo, C., Beninati, C., Giannone, M., La Camera, E., & Carbone, M. (2004). Detection of *Arcobacter* spp. In the Coastal Environment of the Mediterranean Sea. *Applied and Environmental Microbiology*, 70(3), 1271–1276. <https://doi.org/10.1128/AEM.70.3.1271-1276.2004>
- Ford, R., Thrush, S., & Probert, P. (1999). Macrobenthic colonisation of disturbances on an intertidal sandflat: the influence of season and buried algae. *Marine Ecology Progress Series*, 191, 163–174. <https://doi.org/10.3354/meps191163>
- Fraser, M. W., Statton, J., Hovey, R. K., Laverock, B., & Kendrick, G. A. (2016). Seagrass derived organic matter influences biogeochemistry, microbial communities, and seedling biomass partitioning in seagrass sediments. *Plant and Soil*, 400(1–2), 133–146. <https://doi.org/10.1007/s11104-015-2721-0>
- Galushko, A., & Kuever, J. (2019). Lawsonia. In W. B. Whitman (Ed.), *Bergey's Manual of Systematics of Archaea and Bacteria* (1st ed., pp. 1–8). Wiley. <https://doi.org/10.1002/9781118960608.gbm01036.pub2>
- Garbary, D. J., Fraser, S., Ferguson, C., & Lauff, R. F. (2004). Use of Eelgrass, *Zostera marina*, Wrack by Three Species of Ladybird Beetles (Coleoptera: Coccinellidae) in Prince Edward Island. *The Canadian Field-Naturalist*, 118(2), 225. <https://doi.org/10.22621/cfn.v118i2.917>
- Garden, C. J., & Smith, A. M. (2015). Voyages of seaweeds: The role of macroalgae in sediment transport. *Sedimentary Geology*, 318, 1–9. <https://doi.org/10.1016/j.sedgeo.2014.11.007>

- Gerbersdorf, S. U., Koca, K., de Beer, D., Chennu, A., Noss, C., Risse-Buhl, U., Weitere, M., Eiff, O., Wagner, M., & Aberle, J. (2020). Exploring flow-biofilm-sediment interactions: Assessment of current status and future challenges. *Water Research*, *185*, 116182.
- Gessner, M. O., & Chauvet, E. (2002). A CASE FOR USING LITTER BREAKDOWN TO ASSESS FUNCTIONAL STREAM INTEGRITY. *Ecological Applications*, *12*(2), 498–510. [https://doi.org/10.1890/1051-0761\(2002\)012\[0498:ACFULB\]2.0.CO;2](https://doi.org/10.1890/1051-0761(2002)012[0498:ACFULB]2.0.CO;2)
- Gibilisco, P. E., Lancelotti, J. L., Negrin, V. L., & Idaszkin, Y. L. (2020). Composting of seaweed waste: Evaluation on the growth of *Sarcocornia perennis*. *Journal of Environmental Management*, *274*, 111193. <https://doi.org/10.1016/j.jenvman.2020.111193>
- Giovannoni, S. J., Mullins, T. D., & Field, K. G. (1995). Microbial Diversity in Oceanic Systems: rRNA Approaches to the Study of Unculturable Microbes. In I. Joint (Ed.), *Molecular Ecology of Aquatic Microbes* (pp. 217–248). Springer Berlin Heidelberg. https://doi.org/10.1007/978-3-642-79923-5_13
- Godschalk, G. L., & Wetzel, R. G. (1978a). Decomposition of aquatic angiosperms c. *Zostera Marina*, 329–354.
- Godschalk, G. L., & Wetzel, R. G. (1978b). Decomposition of aquatic angiosperms. II. *Particulate Components. Aquatic Botany*, *5*, 301–927.
- Godshalk, G. L., & Wetzel, R. G. (1978). Decomposition of aquatic angiosperms. III. *Zostera marina* L. and a conceptual model of decomposition. *Aquatic Botany*, *5*, 329–354. [https://doi.org/10.1016/0304-3770\(78\)90075-X](https://doi.org/10.1016/0304-3770(78)90075-X)
- Gómez, M., Barreiro, F., DE LA HUZ, R., Lastra, M., & López, J. (2009). Degradative processes in macroalgal wrack on sheltered beaches: Ecological effects. *Sandy Beaches and Coastal Zone Management—Proceedings of the Fifth International Symposium on Sandy Beaches, Rabat, Morocco*, 117–118. <http://www.israbat.ac.ma/wp-content/uploads/2015/02/22%20Gomez.pdf>
- Gómez, M., Barreiro, F., López, J., & Lastra, M. (2018). Effect of upper beach macrofauna on nutrient cycling of sandy beaches: Metabolic rates during wrack decay. *Marine Biology*, *165*(8), 133. <https://doi.org/10.1007/s00227-018-3392-1>
- Gómez, M., Barreiro, F., López, J., Lastra, M., & De La Huz, R. (2013). Deposition patterns of algal wrack species on estuarine beaches. *Aquatic Botany*, *105*, 25–33. <https://doi.org/10.1016/j.aquabot.2012.12.001>
- Goulter, P. F. E., & Allaway, W. G. (1979). Litter Fall and Decomposition in a Mangrove Stand, *Avicennia marina* (Forsk.) Vierh., in Middle Harbour, Sydney. *Marine and Freshwater Research*, *30*(4), 541–546.
- Graca, B., Jędruch, A., Bełdowska, M., Bełdowski, J., Kotwicki, L., Siedlewicz, G., Korejwo, E., Popińska, W., & Łukawska-Matuszewska, K. (2022). Effects of beach wrack on the fate of mercury at the land-sea interface – A preliminary study. *Environmental Pollution*, *315*, 120394. <https://doi.org/10.1016/j.envpol.2022.120394>
- Grafals-Soto, R., & Nordstrom, K. (2009). Sand Fences in the Coastal Zone: Intended and Unintended Effects. *Environmental Management*, *44*(3), 420–429. <https://doi.org/10.1007/s00267-009-9331-7>

- Grave, H., & Möller, H. (1982). *Quantifizierung des pflanzlichen Strandanwurfs an der westdeutschen Ostseeküste*.
- Griffiths, C. L., Stenton-Dozey, J. M. E., & Koop, K. (1983). *Kelp Wrack and the Flow of Energy through a Sandy Beach Ecosystem*. In: McLachlan, A., Erasmus, T. (eds) *Sandy Beaches as Ecosystems. Developments in Hydrobiology, vol 19*. Springer, Dordrecht. https://doi.org/10.1007/978-94-017-2938-3_42
- Gwózdź, B., & Schikan, J. S. (2022). *The seaweed archives: A material study of seaweed as a building material and its implementation on two buildings on North Koster, Sweden*. <https://odr.chalmers.se/items/ef445737-e270-42f1-b4da-52273684f6d3>
- Haller, I., Stybel, N., Schumacher, S., & Mossbauer, M. (2011). Will Beaches be enough? Future Changes for Coastal Tourism at the German Baltic Sea. *Journal of Coastal Research*, 61, 70–80. <https://doi.org/10.2112/SI61-001.68>
- Harb, T. B., & Chow, F. (2022). An overview of beach-cast seaweeds: Potential and opportunities for the valorization of underused waste biomass. *Algal Research*, 62, 102643. <https://doi.org/10.1016/j.algal.2022.102643>
- Harlin, M. M. (1975). Epiphyte—Host relations in seagrass communities. *Aquatic Botany*, 1, 125–131. [https://doi.org/10.1016/0304-3770\(75\)90017-0](https://doi.org/10.1016/0304-3770(75)90017-0)
- Harrison, P. G. (1982). Control of microbial growth and of amphipod grazing by water-soluble compounds from leaves of *Zostera marina*. *Marine Biology*, 67(2), 225–230. <https://doi.org/10.1007/BF00401288>
- Harrison, P. G. (1989). Detrital processing in seagrass systems: A review of factors affecting decay rates, remineralization and detritivory. *Aquatic Botany*, 35(3–4), 263–288. [https://doi.org/10.1016/0304-3770\(89\)90002-8](https://doi.org/10.1016/0304-3770(89)90002-8)
- Harrison, P. G., & Chan, A. T. (1980). Inhibition of the growth of micro-algae and bacteria by extracts of eelgrass (*Zostera marina*) leaves. *Marine Biology*, 61(1), 21–26. <https://doi.org/10.1007/BF00410338>
- Harrison, P. G., & Mann, K. H. (1975). Detritus formation from eelgrass (*Zostera marina* L.): The relative effects of fragmentation, leaching, and decay: Detritus formation from eelgrass. *Limnology and Oceanography*, 20(6), 924–934. <https://doi.org/10.4319/lo.1975.20.6.0924>
- Hartz, S., Jöns, H., Lübke, H., & Schmölcke, U. (2014). *Prehistoric Settlements in the southwestern Baltic Sea area and Development of the Regional Stone Age Economy*.
- Harwell, M. C., & Orth, R. J. (2002). *Long-Distance Dispersal Potential in a Marine Macrophyte*. 83(12).
- Haydéel, D., & Kathy, B. (2006). *Manual beach cleaning in Belgium: An ecological alternative*.
- He, R., Cui, Y., Li, Y., & Ge, X. (2022). Tetrahydroisoquinoline N-methyltransferase from *Methylotenera* Is an Essential Enzyme for the Biodegradation of Berberine in Soil Water. *Molecules*, 27(17), 5442.

- Heerhartz, S. M., Dethier, M. N., Toft, J. D., Cordell, J. R., & Ogston, A. S. (2014). Effects of Shoreline Armoring on Beach Wrack Subsidies to the Nearshore Ecotone in an Estuarine Fjord. *Estuaries and Coasts*, 37(5), 1256–1268. <https://doi.org/10.1007/s12237-013-9754-5>
- Helcom, B. (2007). HELCOM Baltic Sea action plan. *Krakow, Poland*, 15, 2007.
- Hemminga, M. A., & Duarte, C. M. (2000). *Seagrass ecology*. Cambridge University Press. https://books.google.com/books?hl=de&lr=&id=uet0dSgzhrsC&oi=fnd&pg=PP1&dq=hemminga+%26+duarte+2000&ots=vGdeyNA5Oo&sig=ltATMSlw7_3pGgpdhom6643fdnw
- Herlemann, D. P., Labrenz, M., Jürgens, K., Bertilsson, S., Waniek, J. J., & Andersson, A. F. (2011). Transitions in bacterial communities along the 2000 km salinity gradient of the Baltic Sea. *The ISME Journal*, 5(10), 1571–1579. <https://doi.org/10.1038/ismej.2011.41>
- Hodson, R. E., Christian, R. R., & Maccubbin, A. E. (1984). Lignocellulose and lignin in the salt marsh grass *Spartina alterniflora*: Initial concentrations and short-term, post-depositional changes in detrital matter. *Marine Biology*, 81(1), 1–7. <https://doi.org/10.1007/BF00397619>
- Hofmann, J., & Banovec, M. (2021). Socioeconomic impacts of beach wrack management: Report of the Interreg Project CONTRA. *Rostock. Tillgänglig via: https://Eucc-d-Inline.Databases.EUCC-D.de/Files/Documents/00001272_CONTRA-Output02-W_EB.Pdf [Hämtad 2022-03-03]*.
- Holden, J. J., MacNeill, S. K., Juanes, F., & Dudas, S. E. (2018). Beach-cast deposition and commercial harvesting of a non-indigenous alga, *Mazzaella japonica*: Implications for macrofauna communities in Baynes Sound, British Columbia. *Estuarine, Coastal and Shelf Science*, 210, 162–171. <https://doi.org/10.1016/j.ecss.2018.06.008>
- Holmer, M., & Bachmann Olsen, A. (2002). Role of decomposition of mangrove and seagrass detritus in sediment carbon and nitrogen cycling in a tropical mangrove forest. *Marine Ecology Progress Series*, 230, 87–101. <https://doi.org/10.3354/meps230087>
- Holmquist, J. (1997). Disturbance and gap formation in a marine benthic mosaic: influence of shifting macroalgal patches on seagrass structure and mobile invertebrates. *Marine Ecology Progress Series*, 158, 121–130. <https://doi.org/10.3354/meps158121>
- Hooton, N., Miller, D. L., Thetford, M., & Sean Claypool, B. (2014). Survival and Growth of Planted *Uniola paniculata* and Dune Building Using Surrogate Wrack on Perdido Key Florida, U.S.A.: Use of Surrogate Wrack. *Restoration Ecology*, 22(5), 701–707. <https://doi.org/10.1111/rec.12129>
- Hu, Xu, Gao, Li, Jiang, Liu, Su, & Yang. (2019). Long-Chain Bases from Sea Cucumber Alleviate Obesity by Modulating Gut Microbiota. *Marine Drugs*, 17(8), 455. <https://doi.org/10.3390/md17080455>

- Huang, S., Chen, C., Wu, Y., Wu, Q., & Zhang, R. (2011). Characterization of depth-related bacterial communities and their relationships with the environmental factors in the river sediments. *World Journal of Microbiology and Biotechnology*, 27(11), 2655–2664. <https://doi.org/10.1007/s11274-011-0739-x>
- Hubbard, D. M., Dugan, J. E., Schooler, N. K., & Viola, S. M. (2014). Local extirpations and regional declines of endemic upper beach invertebrates in southern California. *Estuarine, Coastal and Shelf Science*, 150, 67–75. <https://doi.org/10.1016/j.ecss.2013.06.017>
- Hull, S. C. (1987). Macroalgal mats and species abundance: A field experiment. *Estuarine, Coastal and Shelf Science*, 25(5), 519–532.
- Hyndes, G. A., Berdan, E. L., Duarte, C., Dugan, J. E., Emery, K. A., Hambäck, P. A., Henderson, C. J., Hubbard, D. M., Lastra, M., Mateo, M. A., Olds, A., & Schlacher, T. A. (2022). The role of inputs of marine wrack and carrion in sandy-beach ecosystems: A global review. *Biological Reviews*, 97(6), 2127–2161. <https://doi.org/10.1111/brv.12886>
- Ince, R., Hyndes, G. A., Lavery, P. S., & Vanderklift, M. A. (2007). Marine macrophytes directly enhance abundances of sandy beach fauna through provision of food and habitat. *Estuarine, Coastal and Shelf Science*, 74(1–2), 77–86. <https://doi.org/10.1016/j.ecss.2007.03.029>
- Inglis, G. (1989). The colonisation and degradation of stranded *Macrocystis pyrifera* (L.) C. Ag. By the macrofauna of a New Zealand sandy beach. *Journal of Experimental Marine Biology and Ecology*, 125(3), 203–217.
- Innocenti, R. A., Feagin, R. A., & Huff, T. P. (2018). The role of Sargassum macroalgal wrack in reducing coastal erosion. *Estuarine, Coastal and Shelf Science*, 214, 82–88. <https://doi.org/10.1016/j.ecss.2018.09.021>
- Jankowska, E., De Troch, M., Michel, L. N., Lepoint, G., & Włodarska-Kowalczyk, M. (2018). Modification of benthic food web structure by recovering seagrass meadows, as revealed by trophic markers and mixing models. *Ecological Indicators*, 90, 28–37. <https://doi.org/10.1016/j.ecolind.2018.02.054>
- Jędrzejczak, M. F. (2002a). Spatio-temporal decay 'hot spots' of stranded wrack in a Baltic sandy coastal system. Part I. Comparative study of the pattern: 1 type of wrack vs 3 beach sites. *Oceanologia*, 44(4). <https://bibliotekanauki.pl/articles/48627.pdf>
- Jędrzejczak, M. F. (2002b). Stranded *Zostera marina* L. vs wrack fauna community interactions on a Baltic sandy beach (Hel, Poland): A short-term pilot study. Part II. Driftline effects of succession changes and colonisation of beach fauna. *Oceanologia*, 44(3). <https://agro.icm.edu.pl/agro/element/bwmeta1.element.agro-article-bbcd5bb4-74b3-4b48-bcb9-ce5d3445901f>
- Jensen, A. (1993). *Present and future needs for algae and algal products*.
- Jiang, Z., Shi, M., & Shi, L. (2020). Degradation of organic contaminants and steel corrosion by the dissimilatory metal-reducing microorganisms *Shewanella* and *Geobacter* spp. *International Biodeterioration & Biodegradation*, 147, 104842.

- Kanehisa, M., Araki, M., Goto, S., Hattori, M., Hirakawa, M., Itoh, M., Katayama, T., Kawashima, S., Okuda, S., Tokimatsu, T., & Yamanishi, Y. (2007). KEGG for linking genomes to life and the environment. *Nucleic Acids Research*, *36* (Database), D480–D484. <https://doi.org/10.1093/nar/gkm882>
- Karberg, N. J., Scott, N. A., & Giardina, C. P. (2008). Methods for Estimating Litter Decomposition. In C. M. Hoover (Ed.), *Field Measurements for Forest Carbon Monitoring* (pp. 103–111). Springer Netherlands. https://doi.org/10.1007/978-1-4020-8506-2_8
- Kassambara, A. (2018). Ggpubr: 'ggplot2' based publication ready plots. *R Package Version*, 2.
- Kenworthy, W. J., & Thayer, G. W. (1984). Production and Decomposition of the Roots and Rhizomes of Seagrasses, *Zostera marina* and *Thalassia testudinum*, in temperate and subtropical marine Ecosystems. *BULLETIN OF MARINE SCIENCE*, *35*.
- Kirkman, H., & Kendrick, G. A. (1997). Ecological significance and commercial harvesting of drifting and beach-cast macro-algae and seagrasses in Australia: A review. *Journal of Applied Phycology*, *9*(4), 311–326. <https://doi.org/10.1023/A:1007965506873>
- Kirschbaum, M. U. F. (1995). The temperature dependence of soil organic matter decomposition, and the effect of global warming on soil organic C storage. *Soil Biology and Biochemistry*, *27*(6), 753–760. [https://doi.org/10.1016/0038-0717\(94\)00242-S](https://doi.org/10.1016/0038-0717(94)00242-S)
- Klais, R., Tamminen, T., Kremp, A., Spilling, K., & Olli, K. (2011). Decadal-scale changes of dinoflagellates and diatoms in the anomalous Baltic Sea spring bloom. *PLoS One*, *6*(6), e21567.
- Kobiyama, A., Rashid, J., Reza, Md. S., Ikeda, Y., Yamada, Y., Kudo, T., Mizusawa, N., Yanagisawa, S., Ikeda, D., Sato, S., Ogata, T., Ikeo, K., Kaga, S., Watanabe, S., Naiki, K., Kaga, Y., Segawa, S., Tada, Y., Musashi, T., ... Watabe, S. (2021). Seasonal and annual changes in the microbial communities of Ofunato Bay, Japan, based on metagenomics. *Scientific Reports*, *11*(1), 17277. <https://doi.org/10.1038/s41598-021-96641-9>
- Kornmann, P., & Sahling, P. H. (1977). Meeresalgen von Helgoland. *Helgoländer Wissenschaftliche Meeresuntersuchungen*, *29*(1–2), 1–289. <https://doi.org/10.1007/BF01611137>
- Kornmann, P., & Sahling, P.-H. (1983). Meeresalgen von Helgoland: Ergänzung. *Helgoländer Meeresuntersuchungen*, *36*(1), 1–65. <https://doi.org/10.1007/BF01995795>
- Kornmann, P., & Sahling, P.-H. (1994). Meeresalgen von Helgoland: Zweite Ergänzung. *Helgoländer Meeresuntersuchungen*, *48*(4), 365–406. <https://doi.org/10.1007/BF02366253>
- Krause-Jensen, D., Duarte, C. M., Sand-Jensen, K., & Carstensen, J. (2021). Century-long records reveal shifting challenges to seagrass recovery. *Global Change Biology*, *27*(3), 563–575. <https://doi.org/10.1111/gcb.15440>
- Krause-Jensen, D., Sagert, S., Schubert, H., & Boström, C. (2008). Empirical relationships linking distribution and abundance of marine vegetation to eutrophication. *Ecological Indicators*, *8*(5), 515–529. <https://doi.org/10.1016/j.ecolind.2007.06.004>

- Kuever, J., Rainey, F. A., & Widdel, F. (2005). *Desulfobulbus* Widdel 1981, 382 VP (Effective publication: Widdel 1980, 374). In D. J. Brenner, N. R. Krieg, G. M. Garrity, J. T. Staley, D. R. Boone, P. Vos, M. Goodfellow, F. A. Rainey, & K.-H. Schleifer (Eds.), *Bergey's Manual® of Systematic Bacteriology* (pp. 988–992). Springer-Verlag. https://doi.org/10.1007/0-387-29298-5_240
- Kuliński, K., Kędra, M., Legeżyńska, J., Gluchowska, M., & Zaborska, A. (2014). Particulate organic matter sinks and sources in high Arctic fjord. *Journal of Marine Systems*, *139*, 27–37. <https://doi.org/10.1016/j.jmarsys.2014.04.018>
- Kupczyk, A., KołECKA, K., & Gajewska, M. (2019). Solving the Beach Wrack Problems by On Site Treatment with Reed Beds Towards Fertilizer Amendments. *Journal of Ecological Engineering*, *20*(8), 252–261. <https://doi.org/10.12911/22998993/111717>
- Lafferty, K. D., Rodriguez, D. A., & Chapman, A. (2013). Temporal and spatial variation in bird and human use of beaches in southern California. *SpringerPlus*, *2*(1), 38. <https://doi.org/10.1186/2193-1801-2-38>
- Lamb, J. B., Van De Water, J. A. J. M., Bourne, D. G., Altier, C., Hein, M. Y., Fiorenza, E. A., Abu, N., Jompa, J., & Harvell, C. D. (2017). Seagrass ecosystems reduce exposure to bacterial pathogens of humans, fishes, and invertebrates. *Science*, *355*(6326), 731–733. <https://doi.org/10.1126/science.aal1956>
- Lammel, D. R., Arlt, T., Manke, I., & Rillig, M. C. (2019). Testing Contrast Agents to Improve Micro Computerized Tomography (μ CT) for Spatial Location of Organic Matter and Biological Material in Soil. *Frontiers in Environmental Science*, *7*, 153. <https://doi.org/10.3389/fenvs.2019.00153>
- Landgraf, D., Leinweber, P., & Makeschin, F. (2006). Cold and hot water–extractable organic matter as indicators of litter decomposition in forest soils. *Journal of Plant Nutrition and Soil Science*, *169*(1), 76–82. <https://doi.org/10.1002/jpln.200521711>
- Langille, M. G. I., Zaneveld, J., Caporaso, J. G., McDonald, D., Knights, D., Reyes, J. A., Clemente, J. C., Burkepile, D. E., Vega Thurber, R. L., Knight, R., Beiko, R. G., & Huttenhower, C. (2013). Predictive functional profiling of microbial communities using 16S rRNA marker gene sequences. *Nature Biotechnology*, *31*(9), 814–821. <https://doi.org/10.1038/nbt.2676>
- Larkum, A., Orth, R. J., & Duarte, C. M. (2006). *Seagrasses: Biology, Ecology and Conservation*. Springer Netherlands. <https://doi.org/10.1007/978-1-4020-2983-7>
- Larsson, M., & Granstedt, A. (2010). Sustainable governance of the agriculture and the Baltic Sea—Agricultural reforms, food production and curbed eutrophication. *Ecological Economics*, *69*(10), 1943–1951. <https://doi.org/10.1016/j.ecolecon.2010.05.003>
- Lastra, M., Rodil, I. F., Sánchez-Mata, A., García-Gallego, M., & Mora, J. (2014). Fate and processing of macroalgal wrack subsidies in beaches of Deception Island, Antarctic Peninsula. *Journal of Sea Research*, *88*, 1–10. <https://doi.org/10.1016/j.seares.2013.12.011>

- Lavery, P., McMahon, K., Weyers, J., Boyce, M., & Oldham, C. (2013). Release of dissolved organic carbon from seagrass wrack and its implications for trophic connectivity. *Marine Ecology Progress Series*, *494*, 121–133. <https://doi.org/10.3354/meps10554>
- Lenanton, R., Robertson, A., & Hansen, J. (1982). Nearshore Accumulations of Detached Macrophytes as Nursery Areas for Fish. *Marine Ecology Progress Series*, *9*, 51–57. <https://doi.org/10.3354/meps009051>
- Lepoint, G., & Hyndes, G. A. (2022). Tropicalization of seagrass macrophytodebris accumulations and associated food webs. *Frontiers in Marine Science*, *9*, 943841. <https://doi.org/10.3389/fmars.2022.943841>
- Lewis, J. B., & Hollingworth, C. E. (1982). Leaf epifauna of the seagrass *Thalassia testudinum*. *Marine Biology*, *71*(1), 41–49. <https://doi.org/10.1007/BF00396991>
- Lewis, W. H., Tahon, G., Geesink, P., Sousa, D. Z., & Ettema, T. J. (2021). Innovations to culturing the uncultured microbial majority. *Nature Reviews Microbiology*, *19*(4), 225–240.
- Li, J.-L., Duan, L., Wu, Y., Ahmad, M., Yin, L.-Z., Luo, X.-Q., Wang, X., Fang, B.-Z., Li, S.-H., Huang, L.-N., Wu, J.-X., Mou, X.-Z., Wang, P., & Li, W.-J. (2022). Unraveling microbe-mediated degradation of lignin and lignin-derived aromatic fragments in the Pearl River Estuary sediments. *Chemosphere*, *296*, 133995. <https://doi.org/10.1016/j.chemosphere.2022.133995>
- Lian, J., Wijffels, R. H., Smidt, H., & Sipkema, D. (2018). The effect of the algal microbiome on industrial production of microalgae. *Microbial Biotechnology*, *11*(5), 806–818. <https://doi.org/10.1111/1751-7915.13296>
- Liebowitz, D. M., Nielsen, K. J., Dugan, J. E., Morgan, S. G., Malone, D. P., Largier, J. L., Hubbard, D. M., & Carr, M. H. (2016). Ecosystem connectivity and trophic subsidies of sandy beaches. *Ecosphere*, *7*(10), e01503. <https://doi.org/10.1002/ecs2.1503>
- Liu, S., Trevathan-Tackett, S. M., Ewers Lewis, C. J., Ollivier, Q. R., Jiang, Z., Huang, X., & Macreadie, P. I. (2019). Beach-cast seagrass wrack contributes substantially to global greenhouse gas emissions. *Journal of Environmental Management*, *231*, 329–335. <https://doi.org/10.1016/j.jenvman.2018.10.047>
- López, B. A., Macaya, E. C., Jeldres, R., Valdivia, N., Bonta, C. C., Tala, F., & Thiel, M. (2019). Spatio-temporal variability of strandings of the southern bull kelp *Durvillaea antarctica* (Fucales, Phaeophyceae) on beaches along the coast of Chile—Linked to local storms. *Journal of Applied Phycology*, *31*(3), 2159–2173. <https://doi.org/10.1007/s10811-018-1705-x>
- Lotze, H. K., Lenihan, H. S., Bourque, B. J., Bradbury, R. H., Cooke, R. G., Kay, M. C., Kidwell, S. M., Kirby, M. X., Peterson, C. H., & Jackson, J. B. C. (2006). Depletion, Degradation, and Recovery Potential of Estuaries and Coastal Seas. *Science*, *312*(5781), 1806–1809. <https://doi.org/10.1126/science.1128035>
- Love, M. I., Huber, W., & Anders, S. (2014). Moderated estimation of fold change and dispersion for RNA-seq data with DESeq2. *Genome Biology*, *15*(12), 550. <https://doi.org/10.1186/s13059-014-0550-8>

- Lozupone, C. A., & Knight, R. (2007). Global patterns in bacterial diversity. *Proceedings of the National Academy of Sciences*, *104*(27), 11436–11440. <https://doi.org/10.1073/pnas.0611525104>
- Mateo, M.-Á., Sánchez-Lizaso, J.-L., & Romero, J. (2003). Posidonia oceanica ‘banquettes’: A preliminary assessment of the relevance for meadow carbon and nutrients budget. *Estuarine, Coastal and Shelf Science*, *56*(1), 85–90. [https://doi.org/10.1016/S0272-7714\(02\)00123-3](https://doi.org/10.1016/S0272-7714(02)00123-3)
- Mathuriau, C., & Chauvet, E. (2002). Breakdown of leaf litter in a neotropical stream. *Journal of the North American Benthological Society*, *21*(3), 384–396. <https://doi.org/10.2307/1468477>
- McDonald, D., Price, M. N., Goodrich, J., Nawrocki, E. P., DeSantis, T. Z., Probst, A., Andersen, G. L., Knight, R., & Hugenholtz, P. (2012). An improved Greengenes taxonomy with explicit ranks for ecological and evolutionary analyses of bacteria and archaea. *The ISME Journal*, *6*(3), 610–618. <https://doi.org/10.1038/ismej.2011.139>
- McLachlan, A., Wooldridge, T., & Dye, A. H. (1981). The ecology of sandy beaches in southern Africa. *South African Journal of Zoology*, *16*(4), 219–231. <https://doi.org/10.1080/02541858.1981.11447760>
- McMurdie, P. J., & Holmes, S. (2013). phyloseq: An R Package for Reproducible Interactive Analysis and Graphics of Microbiome Census Data. *PLoS ONE*, *8*(4), e61217. <https://doi.org/10.1371/journal.pone.0061217>
- Melillo, J. M., Naiman, R. J., Aber, J. D., & Linkins, A. E. (1984). *Factors Controlling Mass Loss and Nitrogen Dynamics of Plant Litter Decaying in Northern Streams*.
- Menéndez, M., Abril, M., Colls, M., & Quintana, X. D. (2019). Decomposition processes in coastal lagoons and their implications for the assessment of ecological health. *Aquatic Conservation: Marine and Freshwater Ecosystems*, *29*(3), 450–460. <https://doi.org/10.1002/aqc.3018>
- Meyers, P. A. (1994). Preservation of elemental and isotopic source identification of sedimentary organic matter. *Chemical Geology*, *114*(3–4), 289–302. [https://doi.org/10.1016/0009-2541\(94\)90059-0](https://doi.org/10.1016/0009-2541(94)90059-0)
- Michael, T. S., Shin, H. W., Hanna, R., & Spafford, D. C. (2008). A review of epiphyte community development: Surface interactions and settlement on seagrass. *Journal of Environmental Biology*, *29*(4), 629–638.
- Michaud, K. M., Emery, K. A., Dugan, J. E., Hubbard, D. M., & Miller, R. J. (2019). Wrack resource use by intertidal consumers on sandy beaches. *Estuarine, Coastal and Shelf Science*, *221*, 66–71. <https://doi.org/10.1016/j.ecss.2019.03.014>
- Mir, K., Neuhaus, K., Bossert, M., & Schober, S. (2013). Short Barcodes for Next Generation Sequencing. *PLoS ONE*, *8*(12), e82933. <https://doi.org/10.1371/journal.pone.0082933>
- Möller, T., Woelfel, J., Beldowski, J., Busk, T., Gorbunova, J., Hogland, W., Kotwicki, L., Martin, G., Quintana, C. O., & Sachpazidou, V. (2021). Ecological aspects of sustainable beach wrack management. *Rostocker Meeresbiologische Beiträge*, *31*, 56–107.

- Moran, M. A., & Hodson, R. E. (1989). Bacterial secondary production on vascular plant detritus: Relationships to detritus composition and degradation rate. *Applied and Environmental Microbiology*, 55(9), 2178–2189. <https://doi.org/10.1128/aem.55.9.2178-2189.1989>
- Mossbauer, M., Haller, I., Dahlke, S., & Schernewski, G. (2012). Management of stranded eelgrass and macroalgae along the German Baltic coastline. *Ocean & Coastal Management*, 57, 1–9. <https://doi.org/10.1016/j.ocecoaman.2011.10.012>
- Mossbauer, M., Schernewski, G., & Bock, S. (2012). The effectiveness of coastal management web portals – a critical analysis. *Journal of Coastal Conservation*, 16(4), 439–448. <https://doi.org/10.1007/s11852-012-0186-3>
- Murray, R. E., & Hodson, R. E. (1986). Influence of Macrophyte Decomposition on Growth Rate and Community Structure of Okefenokee Swamp Bacterioplankton. *Applied and Environmental Microbiology*, 51(2), 293–301. <https://doi.org/10.1128/aem.51.2.293-301.1986>
- Nagpal, S., Singh, R., Yadav, D., & Mande, S. S. (2020). MetagenoNets: Comprehensive inference and meta-insights for microbial correlation networks. *Nucleic Acids Research*, 48(W1), W572–W579. <https://doi.org/10.1093/nar/gkaa254>
- Nicastro, A., Onoda, Y., & Bishop, M. (2012). Direct and indirect effects of tidal elevation on eelgrass decomposition. *Marine Ecology Progress Series*, 456, 53–62. <https://doi.org/10.3354/meps09635>
- Nichols, S. (1997). On the interpretation of principal components analysis in ecological contexts. *Vegetatio*, 34(3), 191–197. <https://doi.org/10.1007/BF00055215>
- Nicholson, W. L., Munakata, N., Horneck, G., Melosh, H. J., & Setlow, P. (2000). Resistance of *Bacillus* Endospores to Extreme Terrestrial and Extraterrestrial Environments. *Microbiology and Molecular Biology Reviews*, 64(3), 548–572. <https://doi.org/10.1128/MMBR.64.3.548-572.2000>
- Nielsen, S. L., Sand-Jensen, K., Borum, J., & Geertz-Hansen, O. (2002). Depth Colonization of Eelgrass (*Zostera marina*) and Macroalgae as Determined by Water Transparency in Danish Coastal Waters. *Estuaries*, 25(5), 1025–1032.
- Nordstrom, K. F., Jackson, N. L., Freestone, A. L., Korotky, K. H., & Puleo, J. A. (2012). Effects of beach raking and sand fences on dune dimensions and morphology. *Geomorphology*, 179, 106–115. <https://doi.org/10.1016/j.geomorph.2012.07.032>
- Nordstrom, K. F., Jackson, N. L., & Korotky, K. H. (2011). Aeolian Sediment Transport Across Beach Wrack. *Journal of Coastal Research*, 59, 211–217. <https://doi.org/10.2112/SI59-022.1>
- Norkko, J., Bonsdorff, E., & Norkko, A. (2000). Drifting algal mats as an alternative habitat for benthic invertebrates: Species specific responses to a transient resource. *J. Exp. Mar. Biol. Ecol.*
- Ochieng, C. A., & Erftemeijer, P. L. A. (1999). Accumulation of seagrass beach cast along the Kenyan coast: A quantitative assessment. *Aquatic Botany*, 65(1–4), 221–238. [https://doi.org/10.1016/S0304-3770\(99\)00042-X](https://doi.org/10.1016/S0304-3770(99)00042-X)

- Olabarria, C., Lastra, M., & Garrido, J. (2007). Succession of macrofauna on macroalgal wrack of an exposed sandy beach: Effects of patch size and site. *Marine Environmental Research*, 63(1), 19–40. <https://doi.org/10.1016/j.marenvres.2006.06.001>
- Oldham, C., McMahon, K., Brown, E., Bosserelle, C., & Lavery, P. (2014). A preliminary exploration of the physical properties of seagrass wrack that affect its offshore transport, deposition, and retention on a beach. *Limnology and Oceanography: Fluids and Environments*, 4(1), 120–135. <https://doi.org/10.1215/21573689-2844703>
- Ondiviela, B., Losada, I. J., Lara, J. L., Maza, M., Galván, C., Bouma, T. J., & Van Belzen, J. (2014). The role of seagrasses in coastal protection in a changing climate. *Coastal Engineering*, 87, 158–168. <https://doi.org/10.1016/j.coastaleng.2013.11.005>
- Orr, M., Zimmer, M., Jelinski, D. E., & Mews, M. (2005). Wrack Deposition on Different Beach Types: Spatial and Temporal Variation in the Pattern of Subsidy. *Ecology*, 86(6), 1496–1507.
- Orth, R. J., Carruthers, T. J. B., Dennison, W. C., Duarte, C. M., Fourqurean, J. W., Heck, K. L., Hughes, A. R., Kendrick, G. A., Kenworthy, W. J., Olyarnik, S., Short, F. T., Waycott, M., & Williams, S. L. (2006). A Global Crisis for Seagrass Ecosystems. *BioScience*, 56(12), 987. [https://doi.org/10.1641/0006-3568\(2006\)56\[987:AGCFSE\]2.0.CO;2](https://doi.org/10.1641/0006-3568(2006)56[987:AGCFSE]2.0.CO;2)
- Pedregosa, F., Varoquaux, G., Gramfort, A., Michel, V., Thirion, B., Grisel, O., Blondel, M., Prettenhofer, P., Weiss, R., Dubourg, V., Vanderplas, J., Passos, A., & Cournapeau, D. (2011). Scikit-learn: Machine Learning in Python. *MACHINE LEARNING IN PYTHON*.
- Pellikaan, G. C. (1984). Laboratory experiments on eelgrass (*Zostera marina* L.) decomposition. *Netherlands Journal of Sea Research*, 18(3–4), 360–383.
- Petersen, R. C., & Cummins, K. W. (1974). Leaf processing in a woodland stream*. *Freshwater Biology*, 4(4), 343–368. <https://doi.org/10.1111/j.1365-2427.1974.tb00103.x>
- Pirc, H., & Wollenweber, B. (1988). Seasonal Changes in Nitrogen, Free Amino Acids, and C/N Ratio in Mediterranean Seagrasses. *Marine Ecology*, 9(2), 167–179. <https://doi.org/10.1111/j.1439-0485.1988.tb00206.x>
- Piriz, M. L., Eyra, M. C., & Rostagno, C. M. (2003). *Changes in biomass and botanical composition of beach-cast seaweeds in a disturbed coastal area from Argentine Patagonia*.
- Plag, H.-P., & Tsimplis, M. N. (1999). Temporal variability of the seasonal sea-level cycle in the North Sea and Baltic Sea in relation to climate variability. *Global and Planetary Change*, 20(2–3), 173–203. [https://doi.org/10.1016/S0921-8181\(98\)00069-1](https://doi.org/10.1016/S0921-8181(98)00069-1)
- Porri, F., Hill, J., & McQuaid, C. (2011). Associations in ephemeral systems: The lack of trophic relationships between sandhoppers and beach wrack. *Marine Ecology Progress Series*, 426, 253–262. <https://doi.org/10.3354/meps08951>
- Posey, M. H., Alphin, T. D., Cahoon, L., Lindquist, D., & Becker, M. E. (1999). Interactive Effects of Nutrient Additions and Predation on Infaunal Communities. *Estuaries*, 22(3), 785. <https://doi.org/10.2307/1353111>
- Prairie, Y. T. (1996). Evaluating the predictive power of regression models. *Canadian Journal of Fisheries and Aquatic Sciences*, 53(3), 490–492. <https://doi.org/10.1139/f95-204>

- Prasad, M. H. K., Ganguly, D., Paneerselvam, A., Ramesh, R., & Purvaja, R. (2019). Seagrass litter decomposition: An additional nutrient source to shallow coastal waters. *Environmental Monitoring and Assessment*, *191*(1), 5. <https://doi.org/10.1007/s10661-018-7127-z>
- Pruesse, E., Quast, C., Knittel, K., Fuchs, B. M., Ludwig, W., Peplies, J., & Glockner, F. O. (2007). SILVA: A comprehensive online resource for quality checked and aligned ribosomal RNA sequence data compatible with ARB. *Nucleic Acids Research*, *35*(21), 7188–7196. <https://doi.org/10.1093/nar/gkm864>
- Quast, C., Pruesse, E., Yilmaz, P., Gerken, J., Schweer, T., Yarza, P., Peplies, J., & Glöckner, F. O. (2012). The SILVA ribosomal RNA gene database project: Improved data processing and web-based tools. *Nucleic Acids Research*, *41*(D1), D590–D596. <https://doi.org/10.1093/nar/gks1219>
- Raffaelli, D., & Hawkins, S. J. (1996). *Intertidal ecology*. Springer Science & Business Media. <https://books.google.com/books?hl=de&lr=&id=ecUNr6m2R4gC&oi=fnd&pg=PR7&dq=chemical+physical+beech+characteristics+raffaelli&ots=MIHqsjx4Wt&sig=zgeTjZtA oobl4JNi-Ty9s-qubjU>
- Ray, G. C., & Hayden, B. P. (1992). Coastal Zone Ecotones. In A. J. Hansen & F. Di Castri (Eds.), *Landscape Boundaries* (Vol. 92, pp. 403–420). Springer New York. https://doi.org/10.1007/978-1-4612-2804-2_21
- Ray, J., Althammer, J., Skaar, K. S., Simonelli, P., Larsen, A., Stoecker, D., Sazhin, A., Ijaz, U. Z., Quince, C., Nejstgaard, J. C., Frischer, M., Pohnert, G., & Troedsson, C. (2016). Metabarcoding and metabolome analyses of copepod grazing reveal feeding preference and linkage to metabolite classes in dynamic microbial plankton communities. *Molecular Ecology*, *25*(21), 5585–5602. <https://doi.org/10.1111/mec.13844>
- Reboul, G., Moreira, D., Annenkova, N. V., Bertolino, P., Vershinin, K. E., & López-García, P. (2021). Marine signature taxa and core microbial community stability along latitudinal and vertical gradients in sediments of the deepest freshwater lake. *The ISME Journal*, *15*(11), 3412–3417. <https://doi.org/10.1038/s41396-021-01011-y>
- Redfield, A. C. (1934). *On the proportions of organic derivatives in sea water and their relation to the composition of plankton* (Vol. 1). university press of liverpool Liverpool. https://www.researchgate.net/profile/Yair-Suari/publication/344709447_ON_THE_PROPORTIONS_OF_ORGANIC_DERIVATIVES_IN_SEA_WATER_AND_THEIR_RELATION_TO_THE_COMPOSITION_OF_PLANKTON_This_is_the_text_from_Alfred_Charles_Redfield_paper/links/5f8d5b04a6fdccfd7b6c0caf/ON-THE-PROPORTIONS-OF-ORGANIC-DERIVATIVES-IN-SEA-WATER-AND-THEIR-RELATION-TO-THE-COMPOSITION-OF-PLANKTON-This-is-the-text-from-Alfred-Charles-Redfield-paper.pdf
- Remane, A. (1934). Die Brackwasserfauna: Mit besonderer Berücksichtigung der Ostsee. *Zoologischer Anzeiger*. <https://oceanrep.geomar.de/id/eprint/43967>

- Renaud, O., & Victoria-Feser, M.-P. (2010). A robust coefficient of determination for regression. *Journal of Statistical Planning and Inference*, *140*(7), 1852–1862.
- Reusch, T., Chapman, A., & Groger, J. (1994). Blue mussels *Mytilus edulis* do not interfere with eelgrass *Zostera marina* but fertilize shoot growth through biodeposition. *Marine Ecology Progress Series*, *108*, 265–282. <https://doi.org/10.3354/meps108265>
- Robbe, E., Woelfel, J., Balčiūnas, A., & Schernewski, G. (2021). An Impact Assessment of Beach Wrack and Litter on Beach Ecosystem Services to Support Coastal Management at the Baltic Sea. *Environmental Management*, *68*(6), 835–859. <https://doi.org/10.1007/s00267-021-01533-3>
- Robertson, M. L. (1982). *The effects of species origin and environmental setting on the decomposition of two tropical seagrasses, Thalassia testudinum and Syringodium filiforme* [PhD Thesis]. University of Virginia.
- Rodil, I. F., Lastra, M., López, J., Mucha, A. P., Fernandes, J. P., Fernandes, S. V., & Olabarria, C. (2019). Sandy Beaches as Biogeochemical Hotspots: The Metabolic Role of Macroalgal Wrack on Low-productive Shores. *Ecosystems*, *22*(1), 49–63. <https://doi.org/10.1007/s10021-018-0253-1>
- Rognes, T., Flouri, T., Nichols, B., Quince, C., & Mahé, F. (2016). VSEARCH: A versatile open source tool for metagenomics. *PeerJ*, *4*, e2584. <https://doi.org/10.7717/peerj.2584>
- Rosenberg, R., Elmgren, R., Fleischer, S., Jonsson, P., Persson, G., & Dahlin, H. (1990). Marine Eutrophication Case Studies in Sweden. *Ambio*, *19*(3), 102–108.
- Rossi, F., & Underwood, A. (2002). Small-scale disturbance and increased nutrients as influences on intertidal macrobenthic assemblages: Experimental burial of wrack in different intertidal environments. *Marine Ecology Progress Series*, *241*, 29–39. <https://doi.org/10.3354/meps241029>
- Ruiz-Delgado, M. C., Reyes-Martínez, M. J., Sánchez-Moyano, J. E., López-Pérez, J., & García-García, F. J. (2015). Distribution patterns of supralittoral arthropods: Wrack deposits as a source of food and refuge on exposed sandy beaches (SW Spain). *Hydrobiologia*, *742*(1), 205–219. <https://doi.org/10.1007/s10750-014-1986-2>
- Rumohr, H., Bonsdorff, E., & Pearson, T. H. (1996). *Zoobenthic succession in Baltic sedimentary habitats*.
- Salonen, A., Salojärvi, J., Lahti, L., & De Vos, W. M. (2012). The adult intestinal core microbiota is determined by analysis depth and health status. *Clinical Microbiology and Infection*, *18*, 16–20. <https://doi.org/10.1111/j.1469-0691.2012.03855.x>
- Satoh, Y., & Shigeki, W. (2022). Organic matter composition regulates residual potential of organic carbon of the seagrass *Zostera marina* L. during its decomposition process in seawater. *Marine Environmental Research*, *182*, 105790.
- Savage, C., Leavitt, P. R., & Elmgren, R. (2010). Effects of land use, urbanization, and climate variability on coastal eutrophication in the Baltic Sea. *Limnology and Oceanography*, *55*(3), 1033–1046. <https://doi.org/10.4319/lo.2010.55.3.1033>

- Schlacher, T. A., & Hartwig, J. (2013). Bottom-up control in the benthos of ocean-exposed sandy beaches?: DONOR CONTROL ON SANDY BEACHES. *Austral Ecology*, *38*(2), 177–189. <https://doi.org/10.1111/j.1442-9993.2012.02390.x>
- Schories, D., Selig, U., & Schubert, H. (2009). Species and synonym list of the German marine macroalgae based on historical and recent records. *Rostocker Meeresbiologische Beiträge*, *21*, 7–135.
- Schückel, U., & Kröncke, I. (2013). Temporal changes in intertidal macrofauna communities over eight decades: A result of eutrophication and climate change. *Estuarine, Coastal and Shelf Science*, *117*, 210–218. <https://doi.org/10.1016/j.ecss.2012.11.008>
- Seastedt, T. R. (1984). The Role of Microarthropods in Decomposition and Mineralization Processes. *Annual Review of Entomology*, *29*(1), 25–46. <https://doi.org/10.1146/annurev.en.29.010184.000325>
- Shetty, S. A., Hugenholtz, F., Lahti, L., Smidt, H., & De Vos, W. M. (2017). Intestinal microbiome landscaping: Insight in community assemblage and implications for microbial modulation strategies. *FEMS Microbiology Reviews*, *41*(2), 182–199. <https://doi.org/10.1093/femsre/fuw045>
- Sinsabaugh, R. L., & Linkins, A. E. (1990). Enzymic and chemical analysis of particulate organic matter from a boreal river. *Freshwater Biology*, *23*(2), 301–309. <https://doi.org/10.1111/j.1365-2427.1990.tb00273.x>
- Smith, A. M., Guastella, L. A., Botes, Z. A., Bundy, S. C., & Mather, A. A. (2014). Forecasting cyclic coastal erosion on a multi-annual to multi-decadal scale: Southeast African coast. *Estuarine, Coastal and Shelf Science*, *150*, 86–91. <https://doi.org/10.1016/j.ecss.2013.12.010>
- Snoeijs-Leijonmalm, P., Schubert, H., & Radziejewska, T. (2017). *Biological oceanography of the Baltic Sea*. Springer Science & Business Media. <https://books.google.com/books?hl=de&lr=&id=ycGaDgAAQBAJ&oi=fnd&pg=PR9&dq=biological+oceanography+of+the+baltic+sea&ots=8ytpZNUv-v&sig=35xC2E3wflFnH10VBdzgQziPr2M>
- Spilling, K., Olli, K., Lehtoranta, J., Kremp, A., Tedesco, L., Tamelander, T., Klais, R., Peltonen, H., & Tamminen, T. (2018). Shifting Diatom—Dinoflagellate Dominance During Spring Bloom in the Baltic Sea and its Potential Effects on Biogeochemical Cycling. *Frontiers in Marine Science*, *5*, 327. <https://doi.org/10.3389/fmars.2018.00327>
- Suursaar, Ü., Torn, K., Martin, G., Herkül, K., & Kullas, T. (2014). Formation and species composition of stormcast beach wrack in the Gulf of Riga, Baltic Sea **The study was supported by the EU Life+project MARMONI ‘Innovative approaches for marine biodiversity monitoring and assessment of conservation status of nature values in the Baltic Sea’, ESF grant No. 8980, Estonian target financed project SF0180104s08 and Institutional research funding IUT2-20 of the Estonian Research Council. *Oceanologia*, *56*(4), 673–695. <https://doi.org/10.5697/oc.56-4.673>

- Taylor, R. (1999). The green tide threat in the UK — a brief overview with particular reference to Langstone Harbour, south coast of England and the Ythan Estuary, east coast of Scotland. *Botanical Journal of Scotland*, 51(2), 195–203. <https://doi.org/10.1080/03746609908684935>
- Telesh, I. V., & Khlebovich, V. V. (2010). Principal processes within the estuarine salinity gradient: A review. *Marine Pollution Bulletin*, 61(4–6), 149–155. <https://doi.org/10.1016/j.marpolbul.2010.02.008>
- Tobias-Hünefeldt, S. P., Wenley, J., Baltar, F., & Morales, S. E. (2020). Predation impacts late but not early community assembly in model marine biofilms. *bioRxiv*, 2020–08.
- Trevathan-Tackett, S., Allnut, T., Sherman, C., Richardson, M., Crowley, T., & Macreadie, P. (2020). Spatial variation of bacterial and fungal communities of estuarine seagrass leaf microbiomes. *Aquatic Microbial Ecology*, 84, 59–74. <https://doi.org/10.3354/ame01926>
- Unsworth, R. K. F., McKenzie, L. J., Nordlund, L. M., & Cullen-Unsworth, L. C. (2018). A changing climate for seagrass conservation? *Current Biology*, 28(21), R1229–R1232. <https://doi.org/10.1016/j.cub.2018.09.027>
- Urban-Malinga, B., Gheskiere, T., Degraer, S., Derycke, S., Opalinski, K. W., & Moens, T. (2008). Gradients in biodiversity and macroalgal wrack decomposition rate across a macrotidal, ultradissipative sandy beach. *Marine Biology*, 155(1), 79–90. <https://doi.org/10.1007/s00227-008-1009-9>
- Valiela, I., & Rietsma, C. S. (1995). Disturbance of salt marsh vegetation by wrack mats in Great Sippewissett Marsh. *Oecologia*, 102(1), 106–112. <https://doi.org/10.1007/BF00333317>
- Van Egmond, E. M., Van Bodegom, P. M., Van Hal, J. R., Van Logtestijn, R. S. P., Broekman, R. A., Berg, M. P., & Aerts, R. (2019). Growth of pioneer beach plants is strongly driven by buried macroalgal wrack, whereas macroinvertebrates affect plant nutrient dynamics. *Journal of Experimental Marine Biology and Ecology*, 514–515, 87–94. <https://doi.org/10.1016/j.jembe.2019.03.015>
- Van Loo, D., Bouckaert, L., Leroux, O., Pauwels, E., Dierick, M., Van Hoorebeke, L., Cnudde, V., De Neve, S., & Sleutel, S. (2014). Contrast agents for soil investigation with X-ray computed tomography. *Geoderma*, 213, 485–491. <https://doi.org/10.1016/j.geoderma.2013.08.036>
- Van Wychen, S., & Laurens, L. M. L. (2013). Determination of total lipids as fatty acid methyl esters (FAME) by in situ transesterification. *Contract*, 303(December), 275–3000.
- von Nordheim, & Boedeker. (1998). *Umweltvorsorge bei der marinen Sand- und Kiesgewinnung*.
- Wada, S., Satoh, Y., & Hama, T. (2022). Massive loss and microbial decomposition in reproductive biomass of *Zostera marina*. *Estuarine, Coastal and Shelf Science*, 275, 107986.

- Walker, D. I., & McComb, A. J. (1985). Decomposition of Leaves from *Amphibolis antarctica* (Labill.) Sonder et Aschers, and *Posidonia australis* Hook. F. The Major Seagrass Species of Shark Bay, Western Australia. *Botm*, 28(9), 407–414. <https://doi.org/10.1515/botm.1985.28.9.407>
- Walker, D. I., Pergent, G., & Fazi, S. (2001). Seagrass decomposition. *Global Seagrass Research Methods*, 313–324.
- Walters, W., Hyde, E. R., Berg-Lyons, D., Ackermann, G., Humphrey, G., Parada, A., Gilbert, J. A., Jansson, J. K., Caporaso, J. G., Fuhrman, J. A., Apprill, A., & Knight, R. (2016). Improved Bacterial 16S rRNA Gene (V4 and V4-5) and Fungal Internal Transcribed Spacer Marker Gene Primers for Microbial Community Surveys. *mSystems*, 1(1), e00009-15. <https://doi.org/10.1128/mSystems.00009-15>
- Ward, T., Larson, J., Meulemans, J., Hillmann, B., Lynch, J., Sidiropoulos, D., Spear, J. R., Caporaso, G., Blekhman, R., Knight, R., Fink, R., & Knights, D. (2017). *BugBase predicts organism-level microbiome phenotypes* [Preprint]. Bioinformatics. <https://doi.org/10.1101/133462>
- Wasmund, N. (2002). Harmful Algal Blooms in Coastal Waters of the South-Eastern Baltic Sea. In G. Schernewski & U. Schiewer (Eds.), *Baltic Coastal Ecosystems* (pp. 93–116). Springer Berlin Heidelberg. https://doi.org/10.1007/978-3-662-04769-9_8
- Wasmund, N., Nausch, G., & Feistel, R. (2013). Silicate consumption: An indicator for long-term trends in spring diatom development in the Baltic Sea. *Journal of Plankton Research*, 35(2), 393–406. <https://doi.org/10.1093/plankt/fbs101>
- Waycott, M., Duarte, C. M., Carruthers, T. J. B., Orth, R. J., Dennison, W. C., Olyarnik, S., Calladine, A., Fourqurean, J. W., Heck, K. L., Hughes, A. R., Kendrick, G. A., Kenworthy, W. J., Short, F. T., & Williams, S. L. (2009). Accelerating loss of seagrasses across the globe threatens coastal ecosystems. *Proceedings of the National Academy of Sciences*, 106(30), 12377–12381. <https://doi.org/10.1073/pnas.0905620106>
- Weinberger, F., Paalme, T., & Wikström, S. A. (2020). Seaweed resources of the Baltic Sea, Kattegat and German and Danish North Sea coasts. *Botanica Marina*, 63(1), 61–72. <https://doi.org/10.1515/bot-2019-0019>
- Weinberger, F., Sundt, S., Staerck, N., Merk, C., Karez, R., & Rehdanz, K. (2021). Shifting beach wrack composition in the SW Baltic Sea and its effect on beach use. *Ecology and Society*, 26(4), art43. <https://doi.org/10.5751/ES-12759-260443>
- Wetzel, R. G. (2001). *Limnology: Lake and River Ecosystems*. Gulf Professional Publishing.
- Whitney, L. L. (1987). *Macroalgal commercialization in the United States*.
- Wiegand, S., Jogler, M., & Jogler, C. (2018). On the maverick Planctomycetes. *FEMS Microbiology Reviews*, 42(6), 739–760. <https://doi.org/10.1093/femsre/fuy029>
- Williams, A., & Feagin, R. (2010). Sargassum as a Natural Solution to Enhance Dune Plant Growth. *Environmental Management*, 46(5), 738–747. <https://doi.org/10.1007/s00267-010-9558-3>
- Wright, E., S. (2016). Using DECIPHER v2.0 to Analyze Big Biological Sequence Data in R. *The R Journal*, 8(1), 352. <https://doi.org/10.32614/RJ-2016-025>

- Wright, J. P., & Jones, C. G. (2006). The Concept of Organisms as Ecosystem Engineers Ten Years On: Progress, Limitations, and Challenges. *BioScience*, *56*(3), 203. [https://doi.org/10.1641/0006-3568\(2006\)056\[0203:TCCOOAE\]2.0.CO;2](https://doi.org/10.1641/0006-3568(2006)056[0203:TCCOOAE]2.0.CO;2)
- Wu, Q. L., Zwart, G., Schauer, M., Kamst-van Agterveld, M. P., & Hahn, M. W. (2006). Bacterioplankton Community Composition along a Salinity Gradient of Sixteen High-Mountain Lakes Located on the Tibetan Plateau, China. *Applied and Environmental Microbiology*, *72*(8), 5478–5485. <https://doi.org/10.1128/AEM.00767-06>
- Wyllie-Echeverria, S., & Cox, P. A. (1999). The Seagrass (*Zostera marina* [Zosteraceae]) Industry of Nova Scotia (1907-1960). *Economic Botany*, *53*(4), 419–426.
- Zavřel, T., Sinetova, M. A., Búzová, D., Literáková, P., & Červený, J. (2015). Characterization of a model cyanobacterium *Synechocystis* sp. PCC 6803 autotrophic growth in a flat-panel photobioreactor. *Engineering in Life Sciences*, *15*(1), 122–132. <https://doi.org/10.1002/elsc.201300165>
- Zhang, W., Schneider, R., Kolb, J., Teichmann, T., Dudzinska-Nowak, J., Harff, J., & Hanebuth, T. J. J. (2015). Land–sea interaction and morphogenesis of coastal foredunes—A modeling case study from the southern Baltic Sea coast. *Coastal Engineering*, *99*, 148–166. <https://doi.org/10.1016/j.coastaleng.2015.03.005>
- Zielinski, S., Botero, C. M., & Yanes, A. (2019). To clean or not to clean? A critical review of beach cleaning methods and impacts. *Marine Pollution Bulletin*, *139*, 390–401. <https://doi.org/10.1016/j.marpolbul.2018.12.027>

List of figures

- Figure 1:** Stranded beach wrack, consisting mainly of seagrass, after a storm event at the beach “Schwarzer Busch” (16.10.2020). Shown is the unmanaged part of the beach without beach management activities. 5
- Figure 2:** Seagrass accumulations around a groin in the shallow water at the island of Poel, “Schwarzer Busch” (15.07.2020). Such accumulated amounts are especially during autumn and after storms observed. 8
- Figure 3:** Experiment location sites along the Western Baltic Sea coast in Germany, Mecklenburg Western-Pomerania. Beach wrack amounts and species composition were evaluated at the beach “Schwarzer Busch” (Island of Poel) and in Kühlungsborn, decay under constant water exposure Poel, solely, and alternating experiment regarding the decay of seagrass was conducted at the Island of Poel and in Warnemünde. Map created with QGIS version 3.14.16-Pi (QGIS Development Team. (2023). QGIS geographic information system. QGIS Association: <https://www.qgis.org/>). 10
- Figure 4:** Beach transects and their sampling frames for the different areas of old and new wrack. Length in total: 100 m, beach width depending on water level. One square for sampling equals an area of 20 cm x 20 cm = 400 cm² of beach wrack. Three replicates per area. Red arrows indicate beach length and width limitations. 12
- Figure 5:** Litterbag installation at Warnemünde. On the left, the litterbags on the sediment can be seen. Covered by sand, on the right, are the buried litterbags. Installation: 10.10.2019. 15
- Figure 6:** Litterbag cage as installed on the groin in Poel. Poles in the bag represent groin poles. Black rectangle shows the two cages filled with the litterbags. Symbolical numbers are shown to represent plastic checks. Red rectangle is a close-up of some bags to show their securing against rip-off. Blue line symbolizes water level. Green bush on the right side is representative for the adjacent seagrass meadow. 16
- Figure 7:** Transmission of light in percent of used meshes for the litterbags. blue line representing bare light, green light representing white mesh, and black representing black mesh. X-axis is giving the spectrum in nm, y-axis is giving the percentage of transmission of individual meshes. All values measured with a Macam SR-9910-PC (Macam Photometrics Ltd., Livingston, Scotland, UK). 19

Figure 8: Gel electrophoresis picture of tested kits for DNA extraction. Marker: 100 bp DNA Ladder (New England Biolabs, Ipswich, MA; US). First row shows marker and its ladder at 100 bp, 300 bp and 500 bp. From left to right: Qiagen PowerSoil pro, Qiagen PowerBiofilm, Macherey-Nagel NucleoSpin Soil. Upper lane represents prokaryotic 16S rDNA, lower lane eukaryotic 18S rDNA. Neg is the negative control of the PCR. Used was a random seagrass test sample that was extracted for evaluating the DNA kits. These samples were not used in any following analyze 23

Figure 9: Gel electrophoresis of DNA extraction as run by 23.11.21. First band shows marker (λ / EcoRI+ Hind III; Fermentas), followed by the five respective samples. It can be seen that sub-samples needed to be pooled to yield enough DNA-concentration and to get a proper signal. Negative control at the end. As negative control is empty, a clean extraction is received. 24

Figure 10: Beach wrack landings in 2019 at the beach "Schwarzer Busch" (Poel) with shares of new (green) and old (brown) wrack and sand (yellow). All values are given in mean dry weight kg m^{-2} on y-axis, x-axis including retrieval dates and wrack status (\pm SE, $n=3$). 31

Figure 11: Beach wrack amounts between April 2019 and November 2019 in Kühlungsborn and at Poel. Amounts given cumulated for each season (x-axis), with dry weight (DW) given in kg m^{-2} (y-axis). NW = new wrack, OW = old wrack (\pm SD). For definition of seasonal time frames please refer to Table 2. 32

Figure 12: Beach wrack species composition at Kühlungsborn. In spring, there has been no old wrack line. Bars display relative abundance per species in percentage, calculated to a total of 100 % (y-axis). NW = new wrack, OW = old wrack (x-axis). Blue = angiosperms (consisting of seagrass *Zostera marina* only in this data collection), green = chlorophytes, brown = phaeophytes, red = rhodophytes. 33

Figure 13: Beach wrack species composition at "Schwarzer Busch" at the Island of Poel. Bars display relative abundance per species in percentage, calculated to a total of 100 % (y-axis). NW = new wrack, OW = old wrack (x-axis). Blue = angiosperms (consisting of seagrass *Zostera marina* only in this data collection), green = chlorophytes, brown = phaeophytes, red = rhodophytes. 34

Figure 14: Unmanaged beach of Kühlungsborn at 19.06.2019. Beach transect = 100 m length, varying beach width. On the left the so called “Riedenbach” and its estuary can be seen. Few beach wracks lie at the beach, more macrophytes can be seen in the shallow water (bottom of picture). The shore is sandy at the beach and rockier in the shallow adjacent water. 35

Figure 15: Unmanaged beach of Poel, beach “Schwarzer Busch” at 19.06.2019. Beach transect = 100 m length, varying beach width. On the left the last groin separates the managed (left of groin) to the unmanaged (right of groin) beach section. Shore and shallow water are both sandy. 35

Figure 16: Decay of beach wrack in litterbags over the course of one year. Installation was done in September 2019, sampling was executed after 1, 2 and 4 months (year 2019), and after 6, 8 and 12 months (year 2020). Half of litterbags were buried in approx. 10 cm depth (brown), another half laid at the surface (green). Experiment site was in Warnemünde at the back of the beach without exposure to water and waves in the measuring field from the DWD ((Deutscher Wetterdienst, German Weather Service; fenced area, Figure 5); x-axis sampling dates, y-axis mean dry weight in g; \pm SE, n = 3). 36

Figure 17: Organic matter content of sediment samples taken underneath and besides the litterbags in Warnemünde. Values are given in chronological order, ranging from after 1, 2 and 4 months (year 2019), and after 6, 8 and 12 months (year 2020). Brown = organic matter content in sediment = underneath buried bags, green = underneath surface bags and yellow = within bare sand, all in % (x-axis sampling month, y-axis organic matter of sediments in %, \pm SE, n = 3). 37

Figure 18: Decay of seagrass litterbags being constantly exposed to water. Given are remaining dry weights in grams after indicated days on x-axis. The two different approaches are labeled in yellow (starting in summer) and blue (starting in winter) dots. Light grey dots mark initial bag dry weight for summer, dark grey for winter experiment (x-axis retrieval days, y-axis dry weight in g, n = 3). 39

Figure 19: Weight loss given as decay: $k d^{-1}$ in the x-axes: decay; yellow = experiment starting in summer (SE20), blue = experiment starting in winter (WE21; x-axis decay $k d^{-1}$, y-axis retrieval days, \pm SE, n = 3). 40

Figure 20: Experiments with constant exposure to water. Left two columns represent decay starting in summer (17.06.2020, SE20), right two columns starting in winter (02.02.2021, WE21). Initial t_0 and final t_{13} are not shown; initial sample has not been packed in litterbags and final sample has been empty without any content being left due to complete decomposition. 41

Figure 21: Conductivity profile given in mS cm^{-1} during the complete run-time of experiments. Left graphic representing values for experiment that started in summer 2020 (SE20), and right graphic showing conductivity values for experiment starting in winter 2021 (WE21). As seasonal experiments were taken out of the water every second week, this conductivity profile represents values for all experiments (x-axes respective date, y-axes conductivity in mS cm^{-1}). 42

Figure 22: Principal component analyzes (PCA) to determine abiotic influences on the two consecutive experiments with 210 days runtime each. Pretreatment: normalizing data as environmental data set. Parameters: light, temperature, conductivity and C:N ratio. Red dots = experiment that started in summer (SE20), blue rhombs = in winter (WE21). Small numbers indicate sampling after respective days. Associated Eigenvalues and Eigenvectors are given in Table 6. 43

Figure 23: Non-metric multidimensional scaling of abiotic factors during the two consecutive 210 days experiments. Pretreatments: transformation to fourth root, standardizing samples by total and calculating resemblance to Bray-Curtis similarity. Red dots = start in summer (SE20), blue rhombs = start in winter (WE21). Small numbers next to the symbols indicate sampling after respective days. Parameters: light, temperature, conductivity and C:N ratio. Points closer together are more similar than those further apart. 44

Figure 24: Cluster analysis, comparing samples with their respective similarities. Pretreatment: transformation of fourth root, standardizing samples by total and creating resemblance matrix by S17 Bray-Curtis similarity. Red dots = samples from SE20, blue rhombs = WE21; x-axis showing samples and y-axis showing similarity in %. 45

Figure 25: Seasonal values for light and temperature. Light availability is given on the first y-axis on the left. Brown columns show logged values for logger without any coverage, grey columns show values in white bags and black columns in black bags. Light blue background displays temperature, with the scale on the second (right) y-axis, x-axis giving respective dates, a) and b) in 2020, c) and d) in 2021. Please note: due to a broad range between the seasons, it was not possible to set the same scales for the light- or temperature-axis in all graphs. 47

Figure 26: Seasonal decay experiments. Blue dots = initial weights, orange dots = white litterbags, black dots = black litterbags; x-axis indicating sampling points in days, and y-axis giving dry weights of litterbag contents in grams. R^2 = coefficient of determination for the respective experiment and season (n = 3 per treatment). 49

Figure 27: 16S rDNA genus composition by a) samples and b) season for SE20 and WE21. Stack bars show genus composition in relative abundance, extrapolated to a total of 1.00 equaling 100%. On the x-axis in Figure a), time points of collection of samples is shown, in Figure b) respective experiment starting point. In both graphics the two blocks are divided by season, with its starting date interpreted as season: left representing experiment starting in summer and right experiment starting in winter. A prevalence cutoff of 0.01 in 50% of the samples was used, and a detection limit of 0.6% as a classifier for the lowest possible abundant species within the samples (Graphics created by I. Barrantes, adapted). 52

Figure 28: 16S rDNA class composition for SE20 and WE21. Bubbles represent abundance of classes, with increasing abundance along with increasing bubble size; x-axis is time line, with retrieval days given for both experiments, y-axis representing individual classes (Graphic created by K. Keszy). 53

Figure 29: 16S rDNA class composition for the seasonal experiments under changing conditions (SSu20, SAu20, SWi21, SSp21). Exposure to water and land changed weekly, starting in water (0 days) and finishing at land (42 days). Bubbles represent abundance of classes, with increasing bubble size; x-axis shows retrieval days for each seasonal experiment, y-axis representing individual classes. Additionally, results are split into black or white litterbags, respectively; please refer to headlines in each plot to distinguish. Note: initial samples have only been taken once, and are therefore, listed together with the graphs for the white litterbags – although being fresh from nature and hence not having any pre-treatment regarding light availability (Graphic created by K. Keszy). 54

Figure 30: 16S rDNA phylum composition by a) samples and b) season for SE20 and WE21. Stack bars show genus composition in relative abundance, extrapolated to a total of 1.00 equaling 100%. On the x-axis in Figure a), time points of collection of samples is shown, in Figure b) respective experiment starting point. In both graphics the two blocks are divided by experiment, with its starting date interpreted as season: left representing experiment starting in summer and right experiment starting in winter. A prevalence cutoff of 0.01 in 50% of the samples was used, and a detection limit of 0.1% as a classifier for the lowest possible abundant species within the samples (Graphics created by I. Barrantes, adapted). 55

Figure 31: 16S rDNA core microbiome in the first experiment, starting in a) summer (SE20) and the second experiment starting in b) winter (WE21). On the x-axis the relative abundance of genera is given in percent, on the y-axis respective genera are listed. Least abundant genus white/light blue, and getting darker and changing color from white/light blue towards blue, abundance of genus is increasing. Most abundant genera are marked dark blue. A prevalence cutoff of 0.3 in 80 % of the samples was used, and a detection limit of 0.1 % as a classifier for the lowest possible abundant species within the samples. Please note the difference on the x-axis' extent, with the summer core microbiome ranging from 1 % to 9.5 % and the winter microbiome ranging from 1 % to 13.8 % relative abundance (Graphics created by I. Barrantes). 56

Figure 32: 16S rDNA a) α and b) β diversity. Both diversities are represented by experiment, with boxplots for SE20 on the left in blue and WE21 in yellow on the right. Horizontal lines indicate the median, with upper and lower quartile, vertical lines show upper and lower Whisker. In these box-plots there has been only one outlier within the α diversity in summer, below the boxplot. The α diversity is the mean species diversity in a site at a local scale, whereas β diversity is the Bray divergence, the ratio between regional and local species diversity. The Wilcoxon test checks whether two dependent samples differ significantly from each other. The p-value is a probability measure for the indications against the acceptance of the null hypothesis with a p-value <0.05 providing stronger evidence to decline the null hypothesis. This applies, in this test, to both α and β diversity (\pm SD, graphics created by I. Barrantes). 58

Figure 33: Correlation analysis of differential abundant a) genera and b) pathways in 16S rDNA for SE20 (turquoise) and WE21 (red). Used method: DESeq2, which is automatically performing data normalization and adjusts the p-value. With the Wald test the null hypothesis is kept while the distribution of a suitable test statistic is performed. Please note that the fit-type for genera in a) is local (numerical integration for dispersion), whereas in b) for pathways parametric (closed-form expression for the variance stabilizing transformation of dispersion), and x-axis have different measuring units. FDR (False Discovery Rate) has been set to <0.01 for both analyses. X-axis is the log2 transformed fold change and y-axis for a) genera and b) KEGG (Kyoto Encyclopedia of Genes and Genomes) pathways (Graphics created by I. Barrantes). 59

Figure 34: Results of a FAPROTAX (Functional Annotation of Prokaryotic Taxa) plotted as bubble chart, comparing SE20 (left, green) and WE21 (right, red) cycles. It predicts bacterial or archaeal taxa and their respective ecological and metabolic relevant functions. X-axis shows retrieval days for the two experiments, and y-axis the annotation, according to the ecological or metabolic function. The size of bubbles shows its percentage weight; the larger the bubble the more relevant is its respective function (Graphic created by I. Barrantes, adapted). 60

Figure 35: Time trajectory for omnipresent prokaryotic 16S rDNA genera, a) *Shewanella*, b) *Flavobacteriaceae*, c) *Rhodobacteraceae*; x-axis representing timeline, with the two experiments divided by the black bar: SE20 on the left, WE21 on the right. Both ranging from 0 to 210 days runtime. Y-axis showing relative abundance per genus in percent; out_id=operational taxonomic unit-identifier, that is used to classify groups of closely related individuals, given as additional number behind the id (Graphic created by I. Barrantes, adapted). 61

Figure 36: Analysis of correlations between OTU (Operational Taxonomic Unit) and physicochemical factors. Here, abiotic factors of both experiments (SE20 and WE21) are combined for analysis. Correlation is color coded: red shows positive correlation, and blue negative correlation. X-axis is representing the factors light in lux and temperature in degree Celsius, y-axis shows the respective out_id (operational taxonomic unit-identifier) (Graphic created by I. Barrantes). 62

Figure 37: 18S rDNA genus composition by a) samples and b) season for SE20 and WE21. Stack bars show genus composition in relative abundance, extrapolated to a total of 1.00 equaling 100%. On the x-axis in Figure a), time points of collection of samples is shown, in Figure b) respective experiment starting point. In both graphics the two blocks are divided by season, with its starting date interpreted as season: left representing experiment starting in summer and right experiment starting in winter. A prevalence cutoff of 0.01 in 50% of the samples was used, and a detection limit of 0.1% as a classifier for the lowest possible abundant species within the samples (Graphics created by I. Barrantes, adapted). 65

Figure 38: 18S rDNA class composition for SE20 (left) and WE21 (right). Bubbles represent abundance of classes, with increasing abundance along with increasing bubble size; x-axis is time line, with retrieval days given for both experiments, y-axis representing individual classes (Graphic created by K. Kesy). 66

Figure 39: 18S rDNA class composition for the seasonal experiments under changing conditions (SSu20, SAu20, SWi21, SSp21). Exposure to water and land changed weekly, starting in water (0 days) and finishing at land (42 days). Bubbles represent abundance of classes, with increasing abundance along with increasing bubble size; x-axis shows retrieval days for each seasonal experiment, y-axis representing individual classes. Additionally, results are split into black or white litterbags, respectively; please refer to headlines in each plot to distinguish. Note: initial samples have only been taken once, and are therefore, listed together with the graphs for the white litterbags – although being fresh from nature and hence not having any pre-treatment regarding light availability (Graphic created by K. Keszy). 67

Figure 40: 18S rDNA phylum composition by a) samples and b) season for SE20 and WE21. Stack bars show genus composition in relative abundance, extrapolated to a total of 1.00 equaling 100 %. On the x-axis in Figure a, time points of collection of samples is shown, in Figure b) respective experiment starting point. In both graphics the two blocks are divided by experiment, with its starting date interpreted as season: left representing experiment starting in summer and right experiment starting in winter. A prevalence cutoff of 0.01 in 50 % of the samples was used, and a detection limit of 0.1 % as a classifier for the lowest possible abundant species within the samples (Graphics created by I. Barrantes, adapted). 68

Figure 41: 18S rDNA core microbiome in the first experiment, starting in a) summer (SE20) and the second experiment starting in b) winter (WE21). On the x-axis the relative abundance of genera is given in percent, on the y-axis respective genera are listed. Least abundant genus dark blue, and getting lighter and changing color from blue towards yellow, abundance of genus is increasing. Most abundant genera are marked bright yellow. A prevalence cutoff of 0.4 in 50 % of the samples was used in summer, and a prevalence cutoff of 0.5 in 50 % in winter. Detection limit was set to 0.1 % as a classifier for the lowest possible abundant species within the samples. Please note the difference on the y-axis' prevalence extent, with the core microbiome ranging from 0.2 to 0.6 in summer and the microbiome ranging from 0.2 to 0.8 in winter (Graphics created by I. Barrantes). 69

Figure 42: 18S rDNA α diversity. Diversity is represented by experiment, with boxplots for summer (SE20) on the left in blue and winter (WE21) in yellow on the right. Horizontal lines indicate the median, with upper and lower quartile, vertical lines show upper and lower Whisker. In these box-plots there has been only one outlier within the α diversity in winter, below the boxplot. The α diversity is the mean species diversity in a site at a local scale. The Wilcoxon test checks whether two dependent samples differ significantly from each other. The p-value is a probability measure for the indications against the acceptance of the null hypothesis with a p-value < 0.05 providing stronger evidence to decline the null hypothesis. In this test, α diversity is > 0.05 with a value of 0.29 meaning that there is evidence to reject the null hypothesis, and therefore, having no different diversities between the two experiments (\pm SD, graphic created by I. Barrantes). 70

Figure 43: C:N ratios (y-axis) during litterbag decay in a constant aquatic environment; green highlighted time frame represents first experiment starting in summer, and blue frame the experiment starting in winter. Time line (x-axis) is continued between the start of both experiments. Black dots show the respective sample values, with three stacked dots at each sampling point for the three replicates. Black line is the mean value between the three replicates, and the grey highlighted background is the scattering; x-axis represents the retrieval days as a continued timeline, and y-axis the C:N ratio (in M/M). 71

Figure 44: C:N ratios (in M/M, first y-axis, left) split by treatment white (upper y-axis) and black (lower y-axis) mesh bags. Time line (x-axis) is continued between all experiments, with white interruptions when no experiment was executed. Black dots show the respective sample values, with three stacked dots at each sampling point for the three replicates. Black line is the mean value between the three replicates, and the grey highlighted background is the scattering. Additional values for light (in Kilolux) are given in the second y-axis (right). 72

Figure 45: C:N ratios (y-axis) through seasons. Values given (M/M) for a time period of 42 days (x-axis). Blue dots represent respective values, and are not separated by black or white litterbag. A linear regression is put through every season, implying all six values per sampling point. Litterbags changed between aquatic and land exposure every week, starting in the water and finishing after 42 days with a final sampling at land. Please note the adjusted y-axis range for summer and autumn 2020 (up to 40 M/M) opposite to winter (up to 25 M/M) and spring 2021 (up to 30 M/M). 73

List of tables

- Table 1:** GPS coordinates of respective 100 m transects at the experiment conduction sites. 11
- Table 2:** Seasonal classification of sampling dates in 2019. 12
- Table 3:** Sampling dates for the two litterbag experiments with constant exposure to water for 210 days. Acronyms are given in parentheses, as SE20 = summer experiment 2020 and WE21 = winter experiment 2021. Please note last sampling from SE20 was done in January 2021. 17
- Table 4:** Seasonal experiments with sampling dates. Column “exposure” shows from which exposure to which alternating exposure the litterbags were transferred from and to. Acronyms are given in parentheses, as SSu20 = seasonal summer experiment 2020, SAu20 = seasonal autumn experiment 2020, SWi21 = seasonal winter experiment 2021 and SSp21 = seasonal spring experiment 2021. Please note that the spring experiment run over the meteorological spring and until June (last sampling at land in Warnemünde) in the early summer of 2021. 20
- Table 5:** Beach characteristics and beach wrack found at Poel and Kühlungsborn. Values are given as average. Beach length was given as 100 m for each sampling. Abbreviations: BW = beach wrack, NW = new wrack, OW = old wrack. Beach wrack coverage is given as percentage of total beach’s surface. Please note difference in unity regarding beach wrack thickness. 30
- Table 6:** Table of associated Eigenvalues and Eigenvectors of previous PCA (Figure 22). 44
- Table 7:** Mean litterbag dry weights in grams through seasonal experiments, separated in white and black mesh bags respectively. Initial weight given as “start” with collected material from respective season. Start serves as reference weight for the decay during the experiment. 48
- Table 8:** Decay coefficients $k \text{ d}^{-1}$ for the seasonal experiments in white and black litterbags, respectively. 50

Appendix

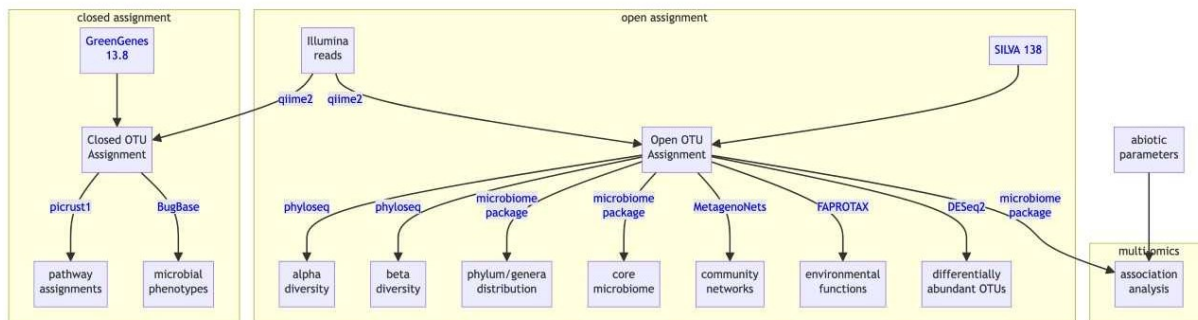


Figure A 1: Flowchart of procedures for microbial data evaluation (figure created by I. Barrantes).

Table A 1: Retrieval weights of litterbag experiment at Warnemünde. Continuous exposure to land conditions, buried bags and surface bags. Runtime between march 2020 and september 2020.

Date	Sampling point	Months	Buried bags in g	Surface bags in g
13.09.19	t_0	0	6.73	6.45
			7.48	5.44
			5.91	5.31
10.10.19	t_1	1	19.6	6.18
			7.43	5.83
			9.52	5.51
13.11.19	t_2	2	9.86	13.90
			8.86	10.11
			9.59	10.24
13.01.20	t_4	4	14.10	13.09
			12.95	11.52
			10.81	13.20
13.03.20	t_6	6	17.84	15.78
			16.47	13.57
			10.97	19.25
13.05.20	t_8	8	6.95	9.38
			6.31	12.43
			6.11	15.73
14.09.20	t_{12}	12	5.59	8.03
			4.72	5.11
			11.21	7.79

Table A 2: DNA contents in ng/ μ l of individual samples for the two experiments with 210 days runtime. Additional information given by full sample ID: SE20 = Summer Experiment 2020, WE21 = Winter Experiment 2021. To evaluate extractions and handling, blank controls were included.

sample nr.	full sample ID	sampling date	mean DNA content ng/ μ l
1.	SE20 t0	17.06.20	14,7
2.	SE20 t1	24.06.20	33,5
3.	SE20 t2	01.07.20	2,7
4.	SE20 t3	08.07.20	15,1
5.	SE20t4	15.07.20	24,2
6.	SE20 t5	29.07.20	15,4
7.	SE20 t6	12.08.20	9,52
8.	SE20 t7	26.08.20	20,55
9.	SE20 t8	09.09.20	23,05
10.	SE20 t9	23.09.20	23,4
11.	SE20 t10	07.10.20	34,5
12.	SE20 t11	04.11.20	28,1
13.	SE20 t12	13.01.21	10,75
14.	<i>Blank Control</i>	<i>06.12.21</i>	<i>DNA-free Water</i>
15.	WE21 t0	03.02.21	2,67
16.	WE21 t1	10.02.21	3,945
17.	WE21 t2	17.02.21	16,0
18.	WE21 t3	24.02.21	5,755
19.	WE21 t4	03.03.21	36,5
20.	WE21 t5	17.03.21	40,5
21.	WE21 t6	31.03.21	34,4
22.	WE21 t7	14.04.21	43,7
23.	WE21 t8	28.04.21	19,85
24.	WE21 t9	12.05.21	9,375
25.	WE21 t10	26.05.21	22,85
26.	WE21 t11	23.06.21	15,15
27.	WE21 t12	01.09.21	10,95
28.	<i>Blank Control</i>	<i>06.12.21</i>	<i>DNA-free Water</i>

Table A 3: DNA contents in ng/ μ l of individual samples for the seasonal experiments with 42 days runtime each. Additional information given by full sample ID: SSu20 = Seasonal Summer Experiment 2020, SAu20 = Seasonal Autumn Experiment 2020. L = light conditions in white mesh bags, D = dark conditions in black mesh bags. To evaluate extractions and handling, random blank controls and different dilutions have been added.

sample nr.	full sample ID	sampling date	mean DNA content ng/ μ l
29.	SSu20 t0	05.08.20	32.5
30.	SSu20 t1 L	12.08.20	18.05
31.	SSu20 t1 D	12.08.20	39.7
32.	SSu20 t2 L	19.08.20	3.36
33.	SSu20 t2 D	19.08.20	3.17
34.	SSu20 t3 L	26.08.20	21.75
35.	SSu20 t3 D	26.08.20	6.78
36.	SSu20 t4 L	02.09.20	19.2
37.	SSu20 t4 D	02.09.20	16.85
38.	SSu20 t5 L	09.09.20	11.2
39.	SSu20 t5 D	09.09.20	5.77
40.	SSu20 t6 L	16.09.20	2.45
41.	SSu20 t6 D	16.09.20	4.14
42.	SAu20 t0	07.10.20	1.49
43.	SAu20 t1 L	16.10.20	54.5
44.	SAu20 t1 L	06.12.21	Dilution 1:100
45.	SAu20 t1 D	16.10.20	31.1
46.	SAu20 t2 L	21.10.20	20.65
47.	SAu20 t2 D	21.10.20	31.1
48.	SAu20 t3 L	28.10.20	11.1
49.	SAu20 t3 D	28.10.20	46.8
50.	SAu20 t3 D	06.12.21	Dilution 1:10
51.	SAu20 t4 L	04.11.20	21.35
52.	SAu20 t4 D	04.11.20	32.8
53.	SAu20 t5 L	11.11.20	40.5
54.	SAu20 t5 D	11.11.20	51.0
55.	SAu20 t5 D	06.12.21	Dilution 1:100
56.	SAu20 t6 L	18.11.20	30.05
57.	SAu20 t6 D	18.11.20	51.0
58.	SAu20 t6 D	06.12.21	Dilution 1:10

Table A 4: DNA contents in ng/ μ l of individual samples for the seasonal experiments with 42 days runtime each. Additional information given by full sample ID: SWi21 = Seasonal Winter Experiment 2021, SSp21 = Seasonal Spring Experiment 2021. L = light conditions in white mesh bags, D = dark conditions in black mesh bags. To evaluate extractions and handling, random blank controls and different dilutions have been added.

sample nr.	full sample ID	sampling date	mean DNA content ng/ μ l
59.	SWi21 t0	12.01.21	2.41
60.	SWi21 t1 L	20.01.21	8.98
61.	SWi21 t1 D	20.01.21	10.8
62.	<i>Blank Control</i>	<i>06.12.21</i>	<i>DNA-free Water</i>
63.	SWi21 t2 L	27.01.21	14.2
64.	SWi21 t2 D	27.01.21	13.1
65.	SWi21 t3 L	03.02.21	4.44
66.	<i>Blank Control</i>	<i>06.12.21</i>	<i>DNA-free Water</i>
67.	SWi21 t3 D	03.02.21	27.7
68.	SWi21 t4 L	10.02.21	2.28
69.	SWi21 t4 D	10.02.21	4.95
70.	SWi21 t5 L	17.02.21	6.23
71.	SWi21 t5 D	17.02.21	9.48
72.	SWi21 t6 L	24.02.21	4.44
73.	SWi21 t6 D	24.02.21	6.52
74.	SSp21 t0	20.04.21	10.65
75.	SSp21 t0	<i>06.12.21</i>	Dilution 1:10
76.	SSp21 t1 L	28.04.21	7.36
77.	SSp21 t1 D	28.04.21	16.2
78.	SSp21 t2 L	05.05.21	12.3
79.	SSp21 t2 D	05.05.21	12.25
80.	SSp21 t3 L	12.05.21	11.3
81.	SSp21 t3 D	12.05.21	16.75
82.	SSp21 t3 D	<i>06.12.21</i>	Dilution 1:10
83.	<i>Blank Control</i>	<i>06.12.21</i>	<i>DNA-free Water</i>
84.	SSp21 t4 L	19.05.21	3.38
85.	SSp21 t4 D	19.05.21	14.8
86.	SSp21 t5 L	26.05.21	21.8
87.	SSp21 t5 D	26.05.21	16.15
88.	SSp21 t6 L	02.06.21	11.05
89.	SSp21 t6 D	02.06.21	7.51
90.	<i>Blank Control</i>	<i>06.12.21</i>	<i>DNA-free Water</i>
91.	SE20 t1	<i>06.12.21</i>	Dilution 1:10
92.	WE21 t10	<i>06.12.21</i>	Dilution 1:10
93.	SAu20 t1 D	<i>06.12.21</i>	Dilution 1:50
94.	SAu20 t3 D	<i>06.12.21</i>	Dilution 1:50
95.	SAu20 t6 L	<i>06.12.21</i>	Dilution 1:10
96.	SSp21 t5 L	<i>06.12.21</i>	Dilution 1:10

Table A 5: Content weights of respective litterbags in grams during long-time decay in water. Left part of chart SE20 = Summer Experiment 2020, right part of chart WE21 = Winter Experiment 2021. Runtime: 210 days each.

Date SE20	Days	DW in g	Date WE21	Days	DW in g
17.06.20	0	1.44	02.02.21	0	1.46
17.06.20	0	1.5	02.02.21	0	1.3
17.06.20	0	1.42	02.02.21	0	1.17
24.06.20	7	1.63	10.02.21	7	1.54
24.06.20	7	1.73	10.02.21	7	1.32
24.06.20	7	1.66	10.02.21	7	1.73
01.07.20	14	1.59	17.02.21	14	1.39
01.07.20	14	1.7	17.02.21	14	1.54
01.07.20	14	1.9	17.02.21	14	1.58
08.07.20	21	2	24.02.21	21	1.52
08.07.20	21	1.78	24.02.21	21	1.61
08.07.20	21	3.31	24.02.21	21	1.64
15.08.20	28	6.83	03.03.21	28	1.75
15.08.20	28	3.51	03.03.21	28	1.56
15.08.20	28	3.69	03.03.21	28	1.56
29.08.20	42	1.46	17.03.21	42	1.46
29.08.20	42	2	17.03.21	42	1.67
29.08.20	42	3.37	17.03.21	42	1.48
12.08.20	56	1.1	31.03.21	56	2.19
12.08.20	56	0.97	31.03.21	56	1.69
12.08.20	56	0.72	31.03.21	56	1.74
26.08.20	70	0.31	14.04.21	70	1.22
26.08.20	70	0.51	14.04.21	70	1.24
26.08.20	70	0.6	14.04.21	70	1.26
09.09.20	84	0.16	28.04.21	84	1.41
09.09.20	84	0.07	28.04.21	84	1.71
09.09.20	84	0.18	28.04.21	84	1.33
23.09.20	98	0.15	12.05.21	98	1.26
23.09.20	98	0.53	12.05.21	98	1.26
23.09.20	98	0.13	12.05.21	98	2.64
07.10.20	112	1.08	26.05.21	112	0.96
07.10.20	112	1.41	26.05.21	112	1.65
07.10.20	112	1.99	26.05.21	112	0.87
04.11.20	140	0.0571	23.06.21	140	1.43
04.11.20	140	0.3025	23.06.21	140	2.4
04.11.20	140	0.3149	23.06.21	140	1.98
13.01.21	210	0.19	01.09.21	210	0.92
13.01.21	210	0.44	01.09.21	210	0.03
13.01.21	210	0.004	01.09.21	210	0.81

Table A 6: Content weights of respective litterbags in grams during seasonal experiments. Weights are given for initial, white and black bags. SSu20 = Seasonal Summer Experiment 2020, SAu20 = Seasonal Autumn Experiment 2020. Runtime 42 days each.

Date	Season – sampling day	Initial g	White g	Black g
05.08.20	SSu20 - 0	1.51		
05.08.20	SSu20 - 0	1.44		
05.08.20	SSu20 - 0	1.39		
12.08.20	SSu20 - 7		1.99	1.47
12.08.20	SSu20 - 7		2.01	1.55
12.08.20	SSu20 - 7		1.80	1.43
19.08.20	SSu20 - 14		1.79	1.27
19.08.20	SSu20 - 14		1.78	1.13
19.08.20	SSu20 - 14		1.69	1.14
26.08.20	SSu20 - 21		1.33	1.07
26.08.20	SSu20 - 21		1.23	1.22
26.08.20	SSu20 - 21		1.49	1.29
02.09.20	SSu20 - 28		1.51	1.09
02.09.20	SSu20 - 28		1.71	1.13
02.09.20	SSu20 - 28		1.74	1.24
09.09.20	SSu20 - 35		1.73	1.06
09.09.20	SSu20 - 35		1.77	1.28
09.09.20	SSu20 - 35		1.89	1.21
16.09.20	SSu20 - 42		1.71	1.08
16.09.20	SSu20 - 42		1.77	1.15
16.09.20	SSu20 - 42		1.84	1.14
07.10.20	SAu20 - 0	1.71		
07.10.20	SAu20 - 0	1.75		
07.10.20	SAu20 - 0	1.69		
16.10.20	SAu20 - 7		2.25	1.89
16.10.20	SAu20 - 7		1.78	2.51
16.10.20	SAu20 - 7		2.76	1.8
21.10.20	SAu20 - 14		1.77	1.76
21.10.20	SAu20 - 14		1.69	1.78
21.10.20	SAu20 - 14		1.7	1.82
28.10.20	SAu20 - 21		1.64	1.69
28.10.20	SAu20 - 21		1.52	2.17
28.10.20	SAu20 - 21		1.41	1.73
04.11.20	SAu20 - 28		1.51	2.12
04.11.20	SAu20 - 28		1.5	1.74
04.11.20	SAu20 - 28		1.47	2.2
11.11.20	SAu20 - 35		1.77	2.24
11.11.20	SAu20 - 35		1.67	2.14
11.11.20	SAu20 - 35		1.78	1.76
18.11.20	SAu20 - 42		1.52	1.47
18.11.20	SAu20 - 42		1.64	1.55
18.11.20	SAu20 - 42		1.67	1.64

Table A 7: Content weights of respective litterbags in grams during seasonal experiments. Weights are given for initial, white and black bags in grams. SWi21 = Seasonal Winter Experiment 2021, SSp21 = Seasonal Spring Experiment 2021. Runtime: 42 days each.

Date	Season – sampling day	Initial g	White g	Black g
12.01.21	SWi21 - 0	1.57		
12.01.21	SWi21 - 0	1.46		
12.01.21	SWi21 - 0	1.49		
20.01.21	SWi21 - 7		2.18	1.8
20.01.21	SWi21 - 7		2.25	2.03
20.01.21	SWi21 - 7		2.05	2.12
27.01.21	SWi21 - 14		1.57	1.56
27.01.21	SWi21 - 14		1.67	1.61
27.01.21	SWi21 - 14		1.53	1.78
03.02.21	SWi21 - 21		1.68	1.86
03.02.21	SWi21 - 21		1.59	1.62
03.02.21	SWi21 - 21		2.04	1.83
10.02.21	SWi21 - 28		1.57	1.56
10.02.21	SWi21 - 28		1.42	1.56
10.02.21	SWi21 - 28		1.48	1.42
17.02.21	SWi21 - 35		1.52	1.4
17.02.21	SWi21 - 35		1.82	1.47
17.02.21	SWi21 - 35		1.55	1.41
24.02.21	SWi21 - 42		1.23	1.22
24.02.21	SWi21 - 42		1.32	1.16
24.02.21	SWi21 - 42		1.3	1.12
21.04.21	SSp21 - 0	1.46		
21.04.21	SSp21 - 0	1.41		
21.04.21	SSp21 - 0	1.3		
28.04.21	SSp21 - 7		3.06	1.75
28.04.21	SSp21 - 7		2.42	1.85
28.04.21	SSp21 - 7		2.19	1.75
05.05.21	SSp21 - 14		1.59	1.73
05.05.21	SSp21 - 14		1.63	1.72
05.05.21	SSp21 - 14		1.75	1.68
12.05.21	SSp21 - 21		1.38	1.56
12.05.21	SSp21 - 21		1.39	1.52
12.05.21	SSp21 - 21		1.63	1.43
19.05.21	SSp21 - 28		1.37	1.24
19.05.21	SSp21 - 28		1.43	1.17
19.05.21	SSp21 - 28		1.33	1.12
26.05.21	SSp21 - 35		1.39	1.8
26.05.21	SSp21 - 35		1.51	1.3
26.05.21	SSp21 - 35		1.9	1.08
02.06.21	SSp21 - 42		1.34	1.25
02.06.21	SSp21 - 42		1.26	1.44
02.06.21	SSp21 - 42		1.55	1.52

Table A 8: Results of C and N analyses for the Summer Experiment 2020. Full sample ID given, weight of sample in mg, percentage of N, $\delta^{15}\text{N}$, C, $\delta^{13}\text{C}$ and C:N in M/M ($n = 3$).

sample	sample ID	weight [mg]	N [%]	$\delta^{15}\text{N}$ [‰]	C [%]	$\delta^{13}\text{C}$ [‰]	C/N [M/M]
1	SE20_t0_0days_bag501	1.575	1.57	4.75	34.49	-10.75	25.6
2	SE20_t0_0days_bag502	1.556	1.65	4.35	36.42	-10.85	25.8
3	SE20_t0_0days_bag503	1.52	1.65	4.18	34.36	-10.46	24.3
4	SE20_t1_7days_bag504	3.064	1.35	4.23	31.37	-11.17	27.2
5	SE20_t1_7days_bag505	3.04	1.17	3.08	30.70	-11.71	30.7
6	SE20_t1_7days_bag506	3.078	1.47	3.74	34.12	-12.44	27.0
7	SE20_t2_14days_bag507	3.02	1.40	3.70	34.90	-12.19	29.0
8	SE20_t2_14days_bag508	3.058	1.31	3.64	26.75	-10.76	23.9
9	SE20_t2_14days_bag509	3.084	1.01	3.90	20.89	-13.00	24.1
10	SE20_t3_21days_bag510	3.03	1.31	3.80	27.10	-11.49	24.1
11	SE20_t3_21days_bag511	3.048	1.51	4.06	29.97	-11.85	23.2
12	SE20_t3_21days_bag512	3.034	1.06	4.03	23.27	-11.69	25.6
13	SE20_t4_28days_bag513	3.079	1.54	3.98	23.98	-12.53	18.1
14	SE20_t4_28days_bag514	3.039	1.22	3.44	21.05	-9.49	20.1
15	SE20_t4_28days_bag515	3.036	1.21	4.17	23.40	-12.35	22.5
16	SE20_t5_42days_bag516	3.042	1.42	3.95	28.98	-12.39	23.8
17	SE20_t5_42days_bag517	3.07	1.40	4.06	24.84	-11.77	20.7
18	SE20_t5_42days_bag518	3.086	1.06	3.78	20.23	-11.84	22.2
19	SE20_t6_56days_bag519	3.064	1.75	4.05	20.89	-13.18	13.9
20	SE20_t6_56days_bag520	3.002	1.97	3.78	28.39	-11.68	16.8
21	SE20_t6_56days_bag521	3.008	2.11	3.65	29.97	-12.71	16.6
22	SE20_t7_70days_bag522	3.002	2.39	3.96	32.97	-12.74	16.1
23	SE20_t7_70days_bag523	3.044	2.28	3.96	31.51	-12.47	16.1
24	SE20_t7_70days_bag524	3.066	2.26	3.97	28.44	-13.00	14.7
25	SE20_t8_84days_bag525	3.044	2.41	3.78	31.59	-12.25	15.3
26	SE20_t8_84days_bag526	3.095	1.71	4.20	24.97	-10.90	17.0
27	SE20_t8_84days_bag527	3.05	1.76	4.00	26.09	-12.97	17.3
28	SE20_t9_98days_bag528	3.004	1.88	4.10	24.66	-13.08	15.3
29	SE20_t9_98days_bag529	3.031	1.47	4.72	15.98	-13.76	12.7
30	SE20_t9_98days_bag530	3.029	1.47	3.73	19.08	-11.53	15.1
31	SE20_t10_112days_bag531	3.07	0.43	4.26	6.17	-11.28	16.8
32	SE20_t10_112days_bag532	3.051	0.61	4.74	6.74	-13.68	12.8
33	SE20_t10_112days_bag533	3.078	0.83	5.48	9.65	-12.49	13.5
34	SE20_t11_140days_bag534	3.003	1.16	4.89	16.97	-12.09	17.1
35	SE20_t11_140days_bag535	3.076	0.54	4.25	6.61	-12.88	14.3
36	SE20_t11_140days_bag536	2.973	0.46	4.35	5.04	-13.08	12.8
37	SE20_t12_210days_bag537	empty	empty	empty	empty	empty	empty
38	SE20_t12_210days_bag538	empty	empty	empty	empty	empty	empty
39	SE20_t12_210days_bag539	empty	empty	empty	empty	empty	empty

Table A 9: Results of C and N analyses for the Winter Experiment 2021. Full sample ID given, weight of sample in mg, percentage of N, $\delta^{15}\text{N}$, C, $\delta^{13}\text{C}$ and C:N in M/M ($n = 3$).

sample	sample ID	weight [mg]	N [%]	$\delta^{15}\text{N}$ [‰]	C [%]	$\delta^{13}\text{C}$ [‰]	C/N [M/M]
40	WE21_t0_0days_bag501	1.516	2.84	5.95	35.66	-15.69	14.6
41	WE21_t0_0days_bag502	1.515	2.54	6.26	35.05	-15.53	16.1
42	WE21_t0_0days_bag503	1.558	3.38	7.26	36.06	-16.27	12.4
43	WE21_t1_7days_bag504	3.067	2.93	6.69	34.76	-15.70	13.8
44	WE21_t1_7days_bag505	3.008	2.23	5.66	32.96	-14.72	17.2
45	WE21_t1_7days_bag506	3.6	1.92	6.29	27.38	-15.15	16.7
46	WE21_t2_14days_bag507	3.049	2.38	5.55	35.97	-15.56	17.6
47	WE21_t2_14days_bag508	3.065	2.91	6.70	35.13	-15.66	14.1
48	WE21_t2_14days_bag509	3.089	2.81	6.52	34.69	-15.76	14.4
49	WE21_t3_21days_bag510	3.033	3.10	6.93	36.82	-15.86	13.9
50	WE21_t3_21days_bag511	3.092	2.44	6.94	32.98	-15.69	15.7
51	WE21_t3_21days_bag512	3.037	2.99	6.85	35.04	-16.26	13.7
52	WE21_t4_28days_bag513	3.094	2.93	7.85	33.48	-15.89	13.3
53	WE21_t4_28days_bag514	3.033	2.50	7.02	32.96	-15.04	15.4
54	WE21_t4_28days_bag515	3.035	2.86	6.93	34.75	-15.48	14.2
55	WE21_t5_42days_bag516	3.082	3.28	6.89	35.71	-16.42	12.7
56	WE21_t5_42days_bag517	3.073	2.98	6.83	33.48	-15.89	13.1
57	WE21_t5_42days_bag518	3.089	2.02	6.77	33.96	-14.67	19.6
58	WE21_t6_56days_bag519	3.025	1.90	6.37	28.59	-14.93	17.6
59	WE21_t6_56days_bag520	3.018	2.10	4.93	33.86	-15.67	18.9
60	WE21_t6_56days_bag521	3.001	1.79	5.11	33.50	-15.82	21.9
61	WE21_t7_70days_bag522	3.02	1.52	5.30	32.57	-14.61	25.1
62	WE21_t7_70days_bag523	3.068	1.73	5.47	30.35	-16.04	20.5
63	WE21_t7_70days_bag524	3.037	2.54	7.11	33.18	-15.99	15.3
64	WE21_t8_84days_bag525	3.086	1.71	4.93	30.64	-16.28	20.9
65	WE21_t8_84days_bag526	3.076	1.16	4.98	23.12	-15.12	23.2
66	WE21_t8_84days_bag527	3.032	1.45	4.93	28.29	-14.78	22.8
67	WE21_t9_98days_bag528	3.013	1.86	5.08	30.76	-16.18	19.2
68	WE21_t9_98days_bag529	3.005	1.39	5.47	29.71	-14.20	24.9
69	WE21_t9_98days_bag530	3.031	1.31	5.18	27.62	-14.38	24.5
70	WE21_t10_112days_bag531	3.027	1.66	4.99	34.46	-14.81	24.2
71	WE21_t10_112days_bag532	3.089	1.41	4.77	30.08	-15.25	24.9
72	WE21_t10_112days_bag533	3.085	1.15	4.81	29.06	-14.46	29.4
73	WE21_t11_140days_bag534	3.03	1.09	4.73	27.50	-13.88	29.3
74	WE21_t11_140days_bag535	3.094	0.94	4.56	24.93	-14.62	30.9
75	WE21_t11_140days_bag536	3.005	1.34	4.54	27.74	-15.56	24.1
76	WE21_t12_210days_bag537	3.091	0.89	3.93	16.09	-15.20	21.1
77	WE21_t12_210days_bag538	3.068	0.82	3.48	13.62	-15.40	19.4
78	WE21_t12_210days_bag539	3.015	0.89	3.34	15.94	-15.59	20.8

Table A 10: Results of C and N analyses for the Seasonal Summer Experiment 2020. Full sample ID given, weight of sample in mg, percentage of N, $\delta^{15}\text{N}$, C, $\delta^{13}\text{C}$ and C:N in M/M. L = light conditions in white mesh bags, D = dark conditions in black mesh bags (n = 3).

sample	sample ID	weight [mg]	N [%]	$\delta^{15}\text{N}$ [‰]	C [%]	$\delta^{13}\text{C}$ [‰]	C/N [M/M]
79	SSu20_t0_0days_bag551	1.568	1.18	5.02	35.54	-10.13	35.1
80	SSu20_t0_0days_bag552	1.554	1.43	4.88	36.16	-9.38	29.5
81	SSu20_t0_0days_bag553	1.583	0.96	4.46	34.85	-9.69	42.1
82	SSu20_t1_7days_bag554_L	3.059	1.16	5.57	28.84	-11.01	28.9
83	SSu20_t1_7days_bag555_L	3.08	0.92	5.04	33.44	-10.04	42.6
84	SSu20_t1_7days_bag556_L	3.032	1.57	6.40	33.08	-10.17	24.6
85	SSu20_t1_7days_bag557_D	3.01	1.54	5.62	35.72	-8.29	27.1
86	SSu20_t1_7days_bag558_D	3	1.41	5.91	33.92	-9.40	28.1
87	SSu20_t1_7days_bag559_D	3.013	1.19	5.62	33.97	-10.33	33.4
88	SSu20_t2_14days_bag560_L	3.032	1.48	5.22	36.62	-10.06	28.9
89	SSu20_t2_14days_bag561_L	3.063	1.51	5.59	35.43	-9.53	27.4
90	SSu20_t2_14days_bag562_L	3.075	1.36	5.09	32.96	-9.56	28.2
91	SSu20_t2_14days_bag563_D	3.091	1.54	5.58	36.32	-10.85	27.5
92	SSu20_t2_14days_bag564_D	3.041	1.62	5.01	37.09	-10.19	26.7
93	SSu20_t2_14days_bag565_D	3.049	1.07	4.64	34.45	-9.76	37.5
94	SSu20_t3_21days_bag566_L	3.018	1.76	5.17	35.94	-8.84	23.9
95	SSu20_t3_21days_bag567_L	3.026	1.38	5.13	34.46	-9.48	29.1
96	SSu20_t3_21days_bag568_L	3.015	1.48	6.03	34.31	-10.93	27.1
97	SSu20_t3_21days_bag569_D	3.071	1.38	5.56	34.47	-9.46	29.2
98	SSu20_t3_21days_bag570_D	3.004	1.64	5.00	34.94	-10.24	24.9
99	SSu20_t3_21days_bag571_D	3.04	1.70	5.91	34.91	-8.49	23.9
100	SSu20_t4_28days_bag572_L	3.036	1.53	5.24	34.33	-10.66	26.2
101	SSu20_t4_28days_bag573_L	3.017	1.60	5.49	30.09	-10.39	22.0
102	SSu20_t4_28days_bag574_L	3.007	1.53	5.08	29.47	-9.90	22.5
103	SSu20_t4_28days_bag575_D	3.027	1.64	5.45	35.56	-10.00	25.3
104	SSu20_t4_28days_bag576_D	3.043	1.56	5.77	35.71	-8.45	26.7
105	SSu20_t4_28days_bag577_D	3.058	1.49	5.81	34.21	-9.31	26.9
106	SSu20_t5_35days_bag578_L	3.063	1.62	4.69	25.79	-10.58	18.6
107	SSu20_t5_35days_bag579_L	3.084	1.18	4.92	24.27	-9.65	24.0
108	SSu20_t5_35days_bag580_L	3.028	1.74	5.81	31.82	-9.66	21.4
109	SSu20_t5_35days_bag581_D	3.068	1.59	6.39	34.65	-9.29	25.5
110	SSu20_t5_35days_bag582_D	3.087	1.55	5.71	32.85	-9.96	24.7
111	SSu20_t5_35days_bag583_D	3.01	1.39	5.24	33.03	-9.91	27.7
112	SSu20_t6_42days_bag584_L	3.02	1.68	5.50	31.66	-9.38	22.0
113	SSu20_t6_42days_bag585_L	3.017	1.33	5.78	27.08	-10.53	23.7
114	SSu20_t6_42days_bag586_L	3.047	1.43	5.26	27.50	-10.44	22.4
115	SSu20_t6_42days_bag587_D	3.016	1.39	5.67	27.57	-10.38	23.1
116	SSu20_t6_42days_bag588_D	3.086	1.40	5.54	30.10	-10.61	25.1
117	SSu20_t6_42days_bag589_D	3.027	1.56	5.61	32.95	-11.21	24.7

Table A 11: Results of C and N analyses for the Seasonal Autumn Experiment 2020. Full sample ID given, weight of sample in mg, percentage of N, $\delta^{15}\text{N}$, C, $\delta^{13}\text{C}$ and C:N in M/M. L = light conditions in white mesh bags, D = dark conditions in black mesh bags (n = 3).

sample	sample ID	weight [mg]	N [%]	$\delta^{15}\text{N}$ [‰]	C [%]	$\delta^{13}\text{C}$ [‰]	C/N [M/M]
118	SAu20_t0_0days_bag601	1.509	1.98	4.99	36.75	-14.46	21.7
119	SAu20_t0_0days_bag602	1.511	2.27	5.53	35.67	-13.10	18.4
120	SAu20_t0_0days_bag603	1.531	1.24	4.01	35.09	-13.05	33.1
121	SAu20_t1_7days_bag604_L	3.092	1.41	4.27	34.28	-12.76	28.3
122	SAu20_t1_7days_bag605_L	3.015	1.48	5.14	32.19	-12.54	25.4
123	SAu20_t1_7days_bag606_L	3.051	2.34	4.86	35.91	-13.86	17.9
124	SAu20_t1_7days_bag607_D	3.056	1.90	4.12	34.51	-14.21	21.2
125	SAu20_t1_7days_bag608_D	3.035	1.34	4.16	31.35	-13.59	27.2
126	SAu20_t1_7days_bag609_D	3.076	1.60	4.13	33.75	-13.53	24.7
127	SAu20_t2_14days_bag610_L	3.029	1.74	4.02	36.39	-13.83	24.5
128	SAu20_t2_14days_bag611_L	3.079	1.49	3.97	35.47	-12.80	27.8
129	SAu20_t2_14days_bag612_L	3.086	1.80	3.87	37.27	-13.49	24.2
130	SAu20_t2_14days_bag613_D	3.094	1.86	5.06	35.95	-13.13	22.5
131	SAu20_t2_14days_bag614_D	3.068	1.87	4.51	35.07	-13.52	21.9
132	SAu20_t2_14days_bag615_D	3.091	1.51	3.90	31.39	-13.06	24.3
133	SAu20_t3_21days_bag616_L	3.083	1.65	2.65	36.21	-14.85	25.6
134	SAu20_t3_21days_bag617_L	3.029	1.51	3.11	36.67	-14.73	28.3
135	SAu20_t3_21days_bag618_L	3.029	1.75	3.28	36.76	-12.56	24.5
136	SAu20_t3_21days_bag619_D	3.066	0.86	3.78	24.87	-12.33	33.6
137	SAu20_t3_21days_bag620_D	3.082	1.72	3.52	33.55	-14.32	22.7
138	SAu20_t3_21days_bag621_D	3.027	1.54	4.24	33.54	-14.36	25.4
139	SAu20_t4_28days_bag622_L	3.009	1.88	4.29	37.72	-14.88	23.4
140	SAu20_t4_28days_bag623_L	3.064	1.68	4.37	35.59	-13.36	24.7
141	SAu20_t4_28days_bag624_L	3.013	1.88	4.30	36.76	-13.32	22.8
142	SAu20_t4_28days_bag625_D	3.023	1.42	4.08	35.21	-13.31	28.9
143	SAu20_t4_28days_bag626_D	3.055	1.62	3.44	32.97	-13.77	23.8
144	SAu20_t4_28days_bag627_D	3.067	1.70	3.64	33.50	-13.93	23.0
145	SAu20_t5_35days_bag628_L	3.045	1.79	3.31	36.07	-14.45	23.6
146	SAu20_t5_35days_bag629_L	3.085	1.71	3.50	32.72	-13.34	22.3
147	SAu20_t5_35days_bag630_L	3.089	1.47	3.69	28.68	-12.77	22.8
148	SAu20_t5_35days_bag631_D	3.081	1.47	3.22	29.67	-14.05	23.5
149	SAu20_t5_35days_bag632_D	3.006	1.43	3.42	34.36	-12.90	28.0
150	SAu20_t5_35days_bag633_D	3.004	1.73	3.36	34.98	-13.01	23.7
151	SAu20_t6_42days_bag634_L	3.044	1.54	4.42	32.79	-13.57	24.8
152	SAu20_t6_42days_bag635_L	3.025	1.90	4.00	35.17	-12.59	21.6
153	SAu20_t6_42days_bag636_L	3.03	1.41	4.01	28.67	-13.96	23.8
154	SAu20_t6_42days_bag637_D	3.056	1.84	3.60	35.84	-13.64	22.7
155	SAu20_t6_42days_bag638_D	3.047	1.85	4.76	31.64	-13.58	20.0
156	SAu20_t6_42days_bag639_D	3.076	1.67	3.89	34.10	-13.33	23.9

Table A 12: Results of C and N analyses for the Seasonal Winter Experiment 2021. Full sample ID given, weight of sample in mg, percentage of N, $\delta^{15}\text{N}$, C, $\delta^{13}\text{C}$ and C:N in M/M. L = light conditions in white mesh bags, D = dark conditions in black mesh bags (n = 3).

sample	sample ID	weight [mg]	N [%]	$\delta^{15}\text{N}$ [‰]	C [%]	$\delta^{13}\text{C}$ [‰]	C/N [M/M]
157	SWi21_t0_0days_bag651	1.567	3.07	7.20	35.50	-15.17	13.5
158	SWi21_t0_0days_bag652	1.542	2.51	5.70	34.97	-14.72	16.3
159	SWi21_t0_0days_bag653	1.507	2.35	6.16	34.96	-15.75	17.4
160	SWi21_t1_7days_bag654_L	3.033	2.29	6.39	34.26	-15.31	17.5
161	SWi21_t1_7days_bag655_L	3.054	2.30	8.06	30.56	-16.12	15.5
162	SWi21_t1_7days_bag656_L	3.081	2.61	7.47	34.67	-14.95	15.5
163	SWi21_t1_7days_bag657_D	3.033	2.34	6.85	34.58	-14.00	17.2
164	SWi21_t1_7days_bag658_D	3.023	3.36	8.55	34.23	-14.18	11.9
165	SWi21_t1_7days_bag659_D	3.063	2.47	6.75	33.56	-14.27	15.8
166	SWi21_t2_14days_bag660_L	3.075	2.40	6.90	36.13	-13.85	17.5
167	SWi21_t2_14days_bag661_L	3.029	3.04	6.21	36.80	-14.50	14.1
168	SWi21_t2_14days_bag662_L	3.058	2.24	7.13	37.05	-13.25	19.3
169	SWi21_t2_14days_bag663_D	3.053	2.77	6.82	37.48	-14.61	15.8
170	SWi21_t2_14days_bag664_D	3.092	2.31	7.20	32.70	-15.10	16.5
171	SWi21_t2_14days_bag665_D	3.078	3.28	7.54	35.78	-14.20	12.7
172	SWi21_t3_21days_bag666_L	3.038	3.10	6.52	37.07	-16.31	14.0
173	SWi21_t3_21days_bag667_L	3.059	2.30	5.87	36.63	-14.78	18.6
174	SWi21_t3_21days_bag668_L	3.007	2.13	6.48	32.87	-15.29	18.0
175	SWi21_t3_21days_bag669_D	3.077	2.39	6.11	35.16	-15.90	17.2
176	SWi21_t3_21days_bag670_D	3.05	1.74	6.88	32.86	-13.91	22.0
177	SWi21_t3_21days_bag671_D	3.039	2.74	8.23	33.83	-14.65	14.4
178	SWi21_t4_28days_bag672_L	3.016	2.09	5.23	37.48	-14.77	20.9
179	SWi21_t4_28days_bag673_L	3.055	2.25	5.35	38.10	-14.85	19.7
180	SWi21_t4_28days_bag674_L	3.084	2.18	5.69	38.40	-15.57	20.5
181	SWi21_t4_28days_bag675_D	3.043	2.20	5.78	38.24	-13.71	20.3
182	SWi21_t4_28days_bag676_D	3.098	2.34	5.18	38.08	-15.22	19.0
183	SWi21_t4_28days_bag677_D	3.054	2.19	9.22	36.54	-13.35	19.5
184	SWi21_t5_35days_bag678_L	3.034	2.81	5.47	37.22	-14.69	15.4
185	SWi21_t5_35days_bag679_L	3.052	2.49	5.14	37.40	-15.34	17.5
186	SWi21_t5_35days_bag680_L	3.027	2.19	5.39	36.81	-14.84	19.6
187	SWi21_t5_35days_bag681_D	3.058	1.91	8.30	36.15	-14.05	22.1
188	SWi21_t5_35days_bag682_D	3.05	1.78	6.61	32.05	-15.09	21.0
189	SWi21_t5_35days_bag683_D	3.011	2.24	5.67	36.55	-15.21	19.0
190	SWi21_t6_42days_bag684_L	3.091	2.07	5.50	37.81	-14.76	21.3
191	SWi21_t6_42days_bag685_L	3.066	2.09	5.94	38.02	-13.88	21.2
192	SWi21_t6_42days_bag686_L	3.03	2.59	7.58	38.83	-15.58	17.5
193	SWi21_t6_42days_bag687_D	3.058	2.55	4.33	39.70	-16.56	18.2
194	SWi21_t6_42days_bag688_D	3.014	2.37	5.75	39.20	-14.15	19.3
195	SWi21_t6_42days_bag689_D	3.038	2.57	5.86	39.48	-14.83	17.9

Table A 13: Results of C and N analyses for the Seasonal Spring Experiment 2021. Full sample ID given, weight of sample in mg, percentage of N, $\delta^{15}\text{N}$, C, $\delta^{13}\text{C}$ and C:N in M/M. L = light conditions in white mesh bags, D = dark conditions in black mesh bags (n = 3).

sample	sample ID	weight [mg]	N [%]	$\delta^{15}\text{N}$ [‰]	C [%]	$\delta^{13}\text{C}$ [‰]	C/N [M/M]
196	SSp21_t0_0days_bag701	1.533	1.74	3.82	38.74	-11.47	26.0
197	SSp21_t0_0days_bag702	1.561	2.39	4.95	38.08	-11.62	18.6
198	SSp21_t0_0days_bag703	1.51	2.59	4.72	37.68	-11.55	17.0
199	SSp21_t1_7days_bag704_L	3.025	1.97	4.08	35.57	-11.35	21.0
200	SSp21_t1_7days_bag705_L	3.035	1.92	2.61	35.49	-12.90	21.6
201	SSp21_t1_7days_bag706_L	3.016	1.80	4.05	35.59	-11.82	23.0
202	SSp21_t1_7days_bag707_D	3.02	1.94	3.98	35.21	-11.72	21.2
203	SSp21_t1_7days_bag708_D	3.086	2.02	4.03	35.51	-12.15	20.5
204	SSp21_t1_7days_bag709_D	3.023	1.84	4.94	35.34	-13.05	22.4
205	SSp21_t2_14days_bag710_L	3.034	1.91	4.76	36.50	-13.47	22.2
206	SSp21_t2_14days_bag711_L	3.066	2.14	3.64	38.94	-13.68	21.3
207	SSp21_t2_14days_bag712_L	3.002	1.73	4.28	38.65	-12.83	26.0
208	SSp21_t2_14days_bag713_D	3.053	2.57	4.71	38.23	-12.10	17.4
209	SSp21_t2_14days_bag714_D	3.065	2.28	3.52	38.20	-13.03	19.5
210	SSp21_t2_14days_bag715_D	3.054	2.36	3.95	38.50	-12.53	19.0
211	SSp21_t3_21days_bag716_L	3.09	2.60	2.51	37.42	-12.96	16.8
212	SSp21_t3_21days_bag717_L	3.057	2.39	3.18	39.05	-12.97	19.1
213	SSp21_t3_21days_bag718_L	3.018	2.39	3.74	39.84	-12.88	19.5
214	SSp21_t3_21days_bag719_D	3.019	2.31	3.66	34.69	-12.32	17.5
215	SSp21_t3_21days_bag720_D	3.05	2.11	3.20	34.46	-12.61	19.0
216	SSp21_t3_21days_bag721_D	3.035	1.91	3.84	34.99	-12.21	21.4
217	SSp21_t4_28days_bag722_L	3.019	2.69	4.17	38.72	-12.64	16.8
218	SSp21_t4_28days_bag723_L	3.084	2.29	4.00	40.13	-13.54	20.5
219	SSp21_t4_28days_bag724_L	3.015	2.47	4.57	39.84	-11.73	18.8
220	SSp21_t4_28days_bag725_D	3.031	2.02	4.86	39.66	-12.18	22.9
221	SSp21_t4_28days_bag726_D	3.05	2.55	3.37	39.97	-12.55	18.3
222	SSp21_t4_28days_bag727_D	3.014	2.15	3.70	39.84	-11.72	21.6
223	SSp21_t5_35days_bag728_L	3.004	1.97	2.58	36.12	-13.06	21.4
224	SSp21_t5_35days_bag729_L	3.064	2.21	2.17	35.71	-13.60	18.9
225	SSp21_t5_35days_bag730_L	3.029	1.95	2.50	33.07	-11.55	19.8
226	SSp21_t5_35days_bag731_D	3.072	2.39	2.26	38.61	-11.52	18.8
227	SSp21_t5_35days_bag732_D	3.021	2.02	4.79	37.95	-10.57	22.0
228	SSp21_t5_35days_bag733_D	3.061	1.93	3.08	37.58	-12.46	22.7
229	SSp21_t6_42days_bag734_L	3.055	2.13	2.77	36.81	-11.49	20.1
230	SSp21_t6_42days_bag735_L	3.076	2.35	4.87	37.28	-11.99	18.5
231	SSp21_t6_42days_bag736_L	3.064	2.35	3.91	38.56	-12.70	19.2
232	SSp21_t6_42days_bag737_D	3.035	2.39	4.36	39.69	-13.29	19.4
233	SSp21_t6_42days_bag738_D	3.06	2.61	4.66	39.37	-12.50	17.6
234	SSp21_t6_42days_bag739_D	3.011	2.19	4.27	39.36	-12.61	20.9

Acknowledgements

First and foremost, I would like to thank Prof. Dr. Hendrik Schubert for the supervision of this thesis. You gave me your trust, know-how and the confidence to complete a doctorate under your supervision. Our long and helpful discussions and resulting ideas always pushed me forward. Thank you for your unremitting support.

Dr. Petra Nowak: I thank you very much for your unconditional support at any stage of this thesis. Our discussions, collaboration and coffee breaks gave me important input for making considerable progress. And thank you for proofreading this work.

Dr. Israel Barrantes I cannot thank you enough for giving me basic conception for my dataset and supporting me with the statistical analyses as well as their graphical representation. Many ideas, even seemingly impossible ones, were realized. I am grateful for your ongoing support.

Dr. Mia Bengtsson and Dr. Katharina Keszy from the University of Greifswald: Thank you for introducing me to functional genomics of microbes and letting me participate in the Amplicon Analyses Workshops at your University. It gave me understanding of microbial analyses and communities for my thesis.

Dr. Karol Kuliński and Dr. Katarzyna Koziorowska-Makuch: I am grateful for your willingness to analyze my samples at the IOPAN for their C and N contents. Our discussions in Vienna and Rostock gave great input to my work.

Dr. Katharina Romoth, Dr. Christian Porsche and Dr. Marjan Janßen: You all taught me knowledge of data processing by the use of R and Primer. This has made my analyses more feasible. I am grateful to you for your patience and dedication.

Claudia Lott: You did not miss a single sampling day during my field work. I could always rely on you to accompany me when I was working in the Baltic Sea. With this in mind, I was able to retrieve my samples from the waters of the Baltic Sea, even during the worst conditions

To Aquatic Ecology Team and all the divers from the University of Rostock and IOW: Thank you all for supporting me and giving me the best possible work place.

I thank Baltic TRANSCOAST, for welcoming me as an associated PhD student. Unfortunately, and due to my sampling regime, it was not always possible for me to participate in your many activities. Therefore, I am deeply sorry.

Special thanks go to my native friend Rosie Pearson for English proofreading. Thank you to all my friends for your continued support through any stage of this thesis.

Wissenschaftlicher Lebenslauf

Geburtsdaten: Geboren am 13.01.1983 in Wiesbaden, Hessen, Deutschland

Akademische Mai 2023 – heute

Berufserfahrung: wissenschaftlicher Mitarbeiter

Universität Rostock, Fachbereich aquatische Ökologie

Anstellung im EU-geförderten Projekt NOVAFOODIES

„Demonstration of innovative functional food production systems based on a more sustainable value chain of marine and freshwater raw materials for conscientious European consumers“

Mai 2020 – April 2023

Wissenschaftlicher Mitarbeiter und Promotionsstudent

Universität Rostock, Fachbereich aquatische Ökologie

Forschungsschwerpunkt: „Abbau mariner Makrophyten-Biomasse in der Ostsee“

März 2019 – Juni 2021

wissenschaftlicher Mitarbeiter

Universität Rostock, Fachbereich aquatische Ökologie

Anstellung im EU-geförderten Projekt CONTRA

„Beach Wrack - Conversion Of a Nuisance To a Resource and Asset“

Akademische März 2019 – Juli 2024

Ausbildung: Promotionsstudium in der aquatischen Ökologie der Universität Rostock zur Erlangung des akademischen Grades doctor rerum naturalium (Dr. rer. nat.)

Thema der Dissertation:

„Ecology of Beach Wrack“

Universität Rostock, Mecklenburg-Vorpommern, Deutschland

Oktober 2016 – November 2018

Studium zum „Master of Science Meeresbiologie“

Universität Rostock, Mecklenburg-Vorpommern, Deutschland; Student

Thema der Masterarbeit:

„Confocal Laser Scanning Microscopy (CLSM) a new tool for the visualization of marine microendoliths“

Senckenberg am Meer, Wilhelmshaven, Niedersachsen, Deutschland

Oktober 2012 – März 2016

Studium zum „Bachelor of Science Biowissenschaften“

Universität Rostock, Mecklenburg-Vorpommern, Deutschland; Student

Thema der Bachelorarbeit:

„Transport von Plastikpartikeln durch *Arenicola marina*“

Universität Rostock, Mecklenburg-Vorpommern, Deutschland

Akademische Dezember 2022

Zusatzqualifikation Ausbildungshelfer der Forschungstaucherausbildung an der Uni Rostock

Anerkennung als „Ausbildungshelfer für die Ausbildung von Forschungstauchern“ durch die BG Bau/DGUV Berlin

August 2022

Zertifizierung des „Hochschulzertifikats der Hochschuldidaktik“ an der Uni Rostock im Rahmen der „Kompetenzentwicklung Lehre und Lernen“

August 2022

Qualifizierung als lizenzierter „Taucheinsatzleiter für Forschungstaucher“ durch die KFT Kommission Forschungstauchen Deutschland, Helgoland

Oktober 2020

Zertifizierung als „Forschungstaucher mit Nitrox-Qualifikation“ durch die KFT Kommission Forschungstauchen Deutschland, Helgoland

Februar 2016 – Juli 2016

Ausbildung als „geprüfter Forschungstaucher“ an der Uni Rostock, Prüfung vor der Prüfungskommission für Forschungstauchen, DGUV, Berlin

Interdisziplinärer Austausch:

Juli – August 2023

Interdisziplinärer Austausch im Projekt EXPLO
„Exploring the dynamics and causes of prehistoric land use change in the cradle of European farming“
Unterwasser Ausgrabungsarbeiten im Ohrid-See, Albanien
Träger: Universitäten Bern, Oxford und Thessaloniki

Juni – Juli 2022

Interdisziplinärer Austausch im Projekt EXPLO
„Exploring the dynamics and causes of prehistoric land use change in the cradle of European farming“
Unterwasser Ausgrabungsarbeiten im Ohrid-See, Nordmazedonien
Träger: Universitäten Bern, Oxford und Thessaloniki

August 2019

Kurs „Dokumentationstechniken für Forschungstaucher“
Sven Lovén Centre der Kristineberg Meeresforschungsstation, Schweden
Träger: Universität Göteborg, Schweden

Publikationen:

Schätzle, P. K., Schubert, H., Kesy, K., Bengtsson, M., Koziorowska-Makuch, K., & Kuliński, K. (2023). The decay of *Zostera marina*, representative for beach wrack, at the micro-tidal southwestern Baltic Sea coast on the island of Poel in Germany (No. EGU23-5467). Copernicus Meetings.

Schätzle, P. K., & Schubert, H. (2022, May). Evaluating beach wrack decay through the seasons under wet (underwater) and changing (wet/dry) conditions at the Baltic Sea coast. In EGU General Assembly Conference Abstracts (pp. EGU22-7567).

Möller, T., Woelfel, J., Beldowski, J., Busk, T., Gorbunova, J., Hogland, W., .. & Torn, K. (2021). Ecological aspects of sustainable beach wrack management. *Rostocker Meeresbiologische Beiträge*, (31), 56-107.

Schätzle, P. K., Wisshak, M., Bick, A., Freiwald, A., & Kieneke, A. (2021). Exploring confocal laser scanning microscopy (CLSM) and fluorescence staining as a tool for imaging and quantifying traces of marine microbioerosion and their trace-making microendoliths. *Journal of Microscopy*, 284(2), 118-131.

Konferenzen:

Juni 2023

EcoSummit2023 internationale Konferenz in Gold Coast, QLD, Australien

Mündliche Präsentation: „*The fate of Zostera marina as part of beach wrack at the micro-tidal Baltic Sea coast in Poel, Germany*”

April 2023

EGU 2023 internationale Konferenz in Wien, Österreich

Mündliche Präsentation: „*The decay of Zostera marina, representative for beach wrack, at the micro-tidal southwestern Baltic Sea coast on the island of Poel in Germany*”

Mai 2022

EGU 2022 internationale Konferenz in Wien, Österreich

Mündliche Präsentation: „*Evaluating beach wrack decay through the seasons under wet (underwater) and changing (wet/dry) conditions at the Baltic Sea coast*”

Oktober 2021

Youmares 12 internationale Konferenz in Hamburg, Deutschland

Session Host der Session 8: „*Socio-economic factors & sustainable, ecosystem-based management*”; Präsentation: „*Baltic beach wrack baseline assessment*”